공학석사 학위논문

Determination of Optimal Width of Breakwater Caisson by Reliability Based Design Optimization

신뢰도 기반 설계 최적화를 활용한 방파제 케이슨의 최적 폭 산정

2017 년 2 월

서울대학교 대학원

건설환경공학부

김 택 상

ABSTRACT

This research uses the FORM (First Order Reliability Method) approximation which is one of the system reliability methods, to calculate the failure probability of the vertical caisson of a composite breakwater and determines the optimal width of the caisson by reliability based design optimization. Five different breakwater cross-sections (one fictitious breakwater in a textbook and four different sections of the breakwater in Shibushi, Japan) and four wave conditions (one wave condition in a textbook and three wave conditions of the Shibushi breakwater) are used in this research. In order to express the limit state function, six different random variables are used. The limit state function is approximated by a normal distribution and the failure probability considering both sliding failure and tilting failure is obtained from the FORM approximation. After calculating the failure probability, the function of expected total lifetime cost is formulated by incorporating the results of system reliability analysis in the economic analysis. Finally, the optimal width of the vertical caisson of the breakwater is obtained by minimizing the expected total lifetime cost using the harmony search algorithm.

Keywords: vertical caisson, system reliability, FORM approximation, minimization of expected total lifetime cost, harmony search

Student Number: 2015-21285

Table of Contents

List of Table

List of Figures

List of Symbols

Latin Uppercase

B	Caisson width of the bottom of the upright section
B_M	Berm width
C_T	Total lifetime cost
C_I	Initial construction cost
C_F	Damage cost due to failure
C	Increment of construction cost to enforce the stability of structure
C_0	Initial construction cost unrelated to the width of vertical caisson
D	Thickness of rubble mound
$EQCF$	Expected damage cost when time is 0
$H_{1/3}$	Significant wave height
$I(\mathbf{x})$	Index function
J	Jacobian

M_P Moment around the bottom of an upright section

M_U Moment around the heel of the upright section

M_e Net moment around the heel of the upright section

N The number of decision variables

P Total horizontal wave force exerted upon the upright section

P_f Failure probability

$\mathbf{R}$ Correlation matrix

S Sum of squares

$T_{1/3}$ Significant wave period

T_R Serviced time

U Total uplift pressure

W^* Weight of upright section in still water

W_e Net weight of upright section in still water

$\mathbf{Z}$ Standard normal random variables with zero means and unit variances

Latin Lowercase

bw Arbitrary distance bandwidth

d Water depth above the armor layer of the rubble foundation

$f(\mathbf{x})$ Objective function

$g_m(\mathbf{x})$ Safety margin

$g_s(\mathbf{x})$ Limit state function for sliding failure

$g_t(\mathbf{x})$ Limit state function for tilting failure

h Water depth

h_c Crest elevation of the breakwater above the design water level

h_{fm} Mobilizing forces, strengths and stresses, etc.

h_{sm} Stabilizing forces, strengths and stresses, etc.

$h(\mathbf{x})$ New sampling density function

h' Distance from the design water level to the bottom of the upright section

i Net annual discount rate

j Annual discount rate

k Iteration number

p_1
p_2 Pressure intensities
p_3

p_e Largest bearing pressure at the heel

p_u Toe pressure

r Interest rate

r_i Residuals

t Height of the foot protection

$\mathbf{u}^*$ Joint design points

$\mathbf{u}_k^*$ Minimum-distance points from the origin

$\mathbf{x}$ Set of each decision variable

$\mathbf{x}'$ Harmony vector

Greek Uppercase

Φ_m m-variate standard normal CDF

Greek Lowercase

α_k Unit normal to the hyperplane

$\boldsymbol{\beta}$ Reliability indices or Curve parameters

β Angle between the direction of approach and a line normal to the breakwater

β_k Distance from the origin to the hyperplane

η^* Wave pressure according to elevation

γ_c Density of the upright section for the cap concrete

γ_s Density of the upright section for the submerged portion

γ_u Density of the upright section for the portion of the caisson above the still water level

λ_1

λ_2 Correlation factor that depends on the structural type of

λ_3

breakwaters

μ Friction coefficient between the upright section and the rubble stone foundation

θ Angle of the sea bottom

CHAPTER 1. INTRODUCTION

1.1 Background

Harbor structures have been generally designed by the deterministic design method. The safety factor is calculated with the force acting on the structure and the resistance of the structure. The calculated safety factor is then compared against the required safety factor to judge the safety of the structure. It is assumed that the uncertainty of the load on and resistance of the structure can be determined by using the safety factor as an evaluation index. However, it poses a possibility of over- or under-estimation of structure dimension since the quantitative and comparative evaluations of a structure displacement are not easy.

In order to overcome the shortcomings of the deterministic design method, a probabilistic design method has been used since 1970's, which now is known as a reliability design method. The reliability design methods for coastal structures have been studied since the mid 1980's. In place of the safety factor of the deterministic design method, reliability design method considers the probabilistic uncertainty of the design variables affecting the failure of the structure. This method is such that the probability of failure is within an allowable limit to satisfy stability, functionality, and economic feasibility of the structure.

However, there is a problem to restrict the applicability of the reliability design methods. The problem is how we assign the allowable (or target) failure probability. In order to solve it, the economic analysis is used to establish the target failure

probability. In this research, the minimization of expected total lifetime cost suggested by Lee (2002) is used.

The reliability design of caisson breakwater based on economic analysis has been performed for a long time. However, most of the researches focused on the sliding failure and overturning failure. In this research, the reliability design is performed considering the sliding failure and tilting failure, except for the overturning failure. It is because overturning failure will never occur without some bearing capacity failure. These facts imply that the tilting failure caused by bearing capacity failure is more important than overturning failure.

1.2 Previous Studies

Several authors (CUR-TAW 1990; Burcharth 1997) discussed the application of reliability theory in the design of coastal structures. Over the last few decades, design methods have been improved by using optimization techniques. The main advantage is that the values of the design variables are provided by the optimization procedure and are not fixed by the engineer. The constraints to be imposed on the problem and the objective function to be optimized are only considered to designer concerns.

Some authors consider the construction cost (Castillo et al., 2006) or the total cost (construction, maintenance and repairs) as the design criteria (Lee, 2002). Lee (2002) proposed an optimal design method incorporating sliding failure probability, and he applied it to the vertical caisson of a composite breakwater. In order to eliminate the complex numerical integration involved in the evaluation of probability of failure, he used the First-Order Reliability Method (FORM). A minimization of expected total lifetime cost is formulated by incorporating the results of FORM in the economic analysis. Applying the minimization of expected total lifetime cost to the fictitious composite breakwaters, the optimal design variable was determined. This method is significant because it combined the reliability design with economic analysis. However, it has limitations that considered only one failure mode, i.e. sliding failure and only one design variable, i.e. caisson width.

Castillo et al. (2006) also suggested the optimal design method of the vertical caisson of a composite breakwater. They used similar methodology like Lee (2002), whereas the design variables were multi-variables and four failure modes were

used: sliding failure, foundation failure, overtopping failure, and berm instability failure. However, design variables were designed independently for each failure mode. And, when using the economic analysis, they considered only the initial construction cost without consideration of the maintenance and operation cost.

Takagi and Esteban (2013) suggested a new method that considering tilting failure which was not considered in previous researches. When the caisson are installed in deep waters they can suffer from tilting failure at the shore-heel side of the caisson, in addition to the possibility of sliding failure. Takayama and Higashira (2002) investigated the patterns of damage in 56 breakwaters in Japan and concluded that 66% of these were associated with sliding failure, 27% were related to complex failure patterns that include both sliding and tilting failure, 5% with tilting failure, and 2% with overturning failure.

Methodology in this research is similar to the research of Lee (2002). However, the tilting failure is considered in addition to the sliding failure and the optimal caisson width is calculated considering both failures, not independently. Although there is only one random variable, the harmony search algorithm, which can be applied to the multi-variable function, was used in order to obtain the optimal caisson width. Therefore, this method can be applied to the problem of multi-variable function.

1.3 Objectives

The ultimate objective of the research is to determine the optimal width of a vertical caisson which can minimize the expected total lifetime cost by using the reliability based design optimization. In order to express the expected total lifetime cost related to the failure probability, sliding and tilting failure probabilities are considered simultaneously. In the previous researches, each of the failure modes was considered separately or only a dominant failure mode was considered. But, in the present research, failure modes were considered at the same time, thus it is possible to obtain more reliable results.

The first sub-objective is to calculate the failure probability, the FORM approximation is used to calculate failure probability because limit state functions of this research are simple. If the limit state functions are too complex and have a large curvature, it would be difficult to apply the FORM approximation because there is a possibility to make huge errors.

The second sub-objective is to find a suitable function which can well express the relation between caisson width and failure probability. Nonlinear least square is used to obtain the function. However, the nonlinear least square can calculate the parameters of the function, not calculating the form of the function. So, it is assumed that the function form is Gaussian function. And, the best suitable function is found by changing the number of Gaussian functions.

The third sub-objective is to determine the optimal width of the caisson. In this research, the expected total lifetime cost is an objective function for optimization and it is expressed as one variable function, thus optimal caisson width is calculated by differential. However, in order to apply this research to multi-

variables function, to calculate the optimal caisson width by using optimization method such as the harmony search algorithm is an additional objective of the research.

An additional sub-objective is to suggest the overall safety factor of the reliability based design optimization. Because most engineers are not familiar with the reliability based design optimization, it is hard to understand the total process. So, in order to use the result of reliability based design optimization easily, the overall safety factor is provided. Therefore, although the engineers do not understand the total process of the reliability based design optimization, they can easily apply the reliability design to the structure design by using the overall safety factor.

CHAPTER 2. THEORETICAL BACKGROUDS

2.1 Goda Formulas of Wave Pressure

The wave pressure formulas proposed by Goda (2010) for the design of vertical breakwaters assume the trapezoidal pressure distribution along a vertical wall, as shown in Fig. 2.1, regardless of whether the waves are breaking or nonbreaking.

In this figure, h denotes the water depth in front of the breakwater, d the depth above the armor layer of the rubble foundation, h' the distance from the design water level to the bottom of the upright section, and h_c the crest elevation of the breakwater above the design water level.

The wave pressure is assumed to act to the elevation below:

$$\eta^* = 0.75(1+\lambda_1 \cos\beta)H_{\max} \tag{2.1}$$

in which β denotes the angle between the direction of wave approach and a line normal to the breakwater. The factor λ_1 has been introduced to deal with breakwaters of special configurations other than breakwaters made of simple upright sections. For the latter, the factor is set as $\lambda_1 = 1$.

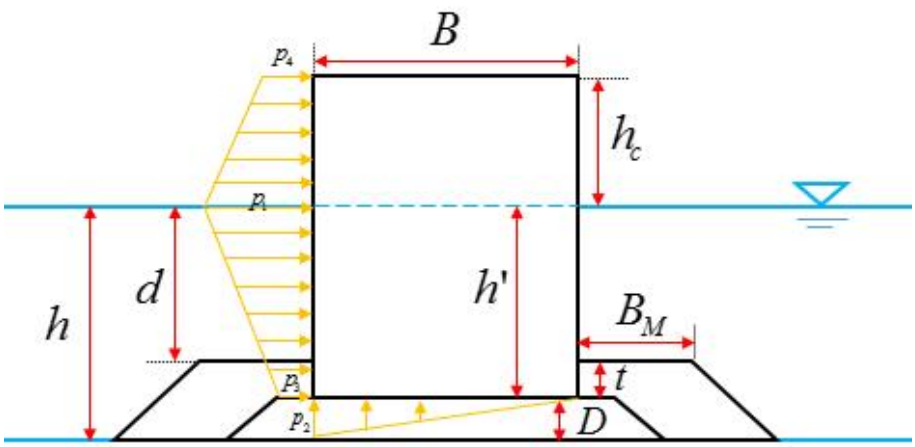

Figure 2.1 Distribution of wave pressure for a vertical breakwater

The pressure intensities are to be estimated as below:

$$p_1 = \frac{1}{2}(1+\cos\beta)(\alpha_1\lambda_1 + \alpha_2\lambda_2\cos^2\beta)\rho g H_{\max} \tag{2.2a}$$

$$p_2 = \frac{p_1}{\cosh(2\pi h / L)} \tag{2.2b}$$

$$p_3 = \alpha_3 p_1 \tag{2.2c}$$

in which

$$\alpha_1 = 0.6 + \frac{1}{2}\left[\frac{4\pi h / L}{\sinh(4\pi h / L)}\right]^2 \tag{2.3a}$$

$$\alpha_2 = \min\left\{\frac{h_b - d}{3h_b}\left(\frac{H_{\max}}{d}\right)^2, \frac{2d}{H_{\max}}\right\} \tag{2.3b}$$

$$\alpha_3 = 1 - \frac{h'}{h}\left[1 - \frac{1}{\cosh(2\pi h / L)}\right] \tag{2.3c}$$

The symbol λ_2 denotes a correction factor that depends on the structural type of breakwaters, and it is set at $\lambda_2 = 1$ for the standard breakwaters with simple upright sections.

The uplift pressure acting on the bottom of the upright section is assumed to have a triangular distribution with toe pressure p_u given by Eq. (2.4) below:

$$p_u = \frac{1}{2}(1+\cos\beta)\alpha_1\alpha_3\lambda_3\rho g H_{\max} \tag{2.4}$$

where the symbol λ_3 denotes a correction factor that depends on the structure type of breakwaters, and it is set at $\lambda_3 = 1$ for the standard breakwaters with simple upright sections.

The total wave pressure and its moment around the bottom of an upright section

can be calculated with the following equations:

$$P = \frac{1}{2}(p_1 + p_3)h' + \frac{1}{2}(p_1 + p_4)h_c^* \tag{2.5}$$

$$M_P = \frac{1}{6}(2p_1 + p_3)h'^2 + \frac{1}{2}(p_1 + p_4)h'h_c^* + \frac{1}{6}(p_1 + p_4)h_c^{*2} \tag{2.6}$$

in which

$$p_4 = \begin{cases} p_1(1 - h_c / \eta^*) : \eta^* > h_c \\ 0 \qquad\qquad\quad : \eta^* \le h_c \end{cases} \tag{2.7}$$

$$h_c^* = \min\left\{\eta^*, h_c\right\} \tag{2.8}$$

The total uplift pressure and its moment around the heel of the upright section are calculated with

$$U = \frac{1}{2} p_u B \tag{2.9}$$

$$M_U = \frac{2}{3} UB \tag{2.10}$$

where B denotes the width of the bottom of the upright section.

The largest bearing pressure at the heel p_e is calculated as

$$p_e = \begin{cases} \dfrac{2W_e}{3t_e} & : t_e \le \dfrac{1}{3}B \\ \dfrac{2W_e}{B}\left(2 - 3\dfrac{t_e}{B}\right) & : t_e > \dfrac{1}{3}B \end{cases} \tag{2.11}$$

in which

$$t_e = \frac{M_e}{W_e} \tag{2.12}$$

$$M_e = Mg\frac{B}{2} - M_U - M_P \tag{2.13}$$

$$W_e = Mg - U \tag{2.14}$$

where M_e denotes the net moment around the heel of the upright section and W_e denotes the net weight of the upright section in still water.

2.2 Failure Modes of Caisson Breakwater

Failure modes of caisson breakwaters are sliding, overturning, and geotechnical failure of rubble mound foundation. Each mode of failure is defined by a corresponding limit state equation as, for example:

$$g_m(x_1, x_2, \cdots, x_n) = h_{sm}(x_1, x_2, \cdots, x_n) - h_{fm}(x_1, x_2, \cdots, x_n);\ m \in M \tag{2.15}$$

where $(x_1, x_2, \cdots, x_n)$ refer to the values of the variables involved, $g_m(x_1, x_2, \cdots, x_n)$ is the safety margin and $h_{sm}(x_1, x_2, \cdots, x_n)$ and $h_{fm}(x_1, x_2, \cdots, x_n)$ are two opposing magnitudes (such as stabilizing and mobilizing forces, strengths and stresses, etc.) that tend to prevent and produce the associated mode of failure, respectively, and M is the set of all failure modes.

Failure of caisson breakwater is dominated by sliding and tilting as mentioned in the introduction. Therefore, the failure modes of sliding and tilting will be considered in this research.

2.2.1 Sliding Failure

Sliding failure occurs when the caisson of the breakwater suffers horizontal displacement. It can occur as a slip either at the interface between the caisson concrete base and the rubble material, or entirely in the rubble material. The

upright section of the breakwater must be designed to be safe against sliding. In order to analyze the stability against the sliding, the limit state function of sliding must be established correctly. The limit state function for sliding can be written as

$$g_s(x_1, x_2, \cdots, x_n) = \mu(W^* - U) - P \tag{2.16}$$

where W^* is the weight of the upright section in still water, μ is the friction coefficient between the upright section and the rubble stone foundation. U is the total uplift pressure force, and P is the horizontal wave force exerted upon the upright section. Figure 2.2 illustrates the vertical caisson when the sliding failure occurs.

2.2.2 Tilting Failure

Tilting failure occurs when the bearing pressure at the shore-heel side is above a certain, e.g. $500\ kN/m^2$. Especially, tilting failure usually occurs in deeper water because the weight of the caisson increases with water depth. In deeper water, the limitation of wave heights due to breaking is relieved, with the increasing possibility of larger wave thrusts exerted upon a breakwater. The limit state function for tilting can be written as

$$g_t(x_1, x_2, \cdots, x_n) = 500 - p_e \tag{2.17}$$

where p_e is the largest bearing pressure at the heel. As you can see the section 2.1, the largest bearing pressure is the function of the net moment, M_e and net weight, W_e. Figure 2.3 illustrates the vertical caisson when the tilting failure occurs.

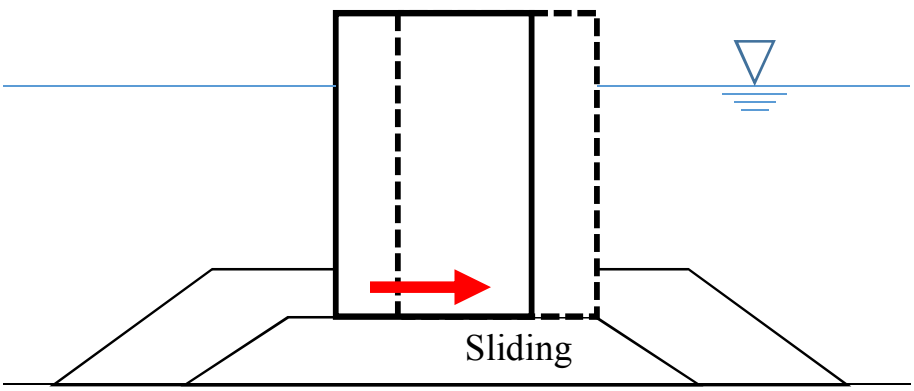

Figure 2.2 Vertical caisson when the sliding failure occurs

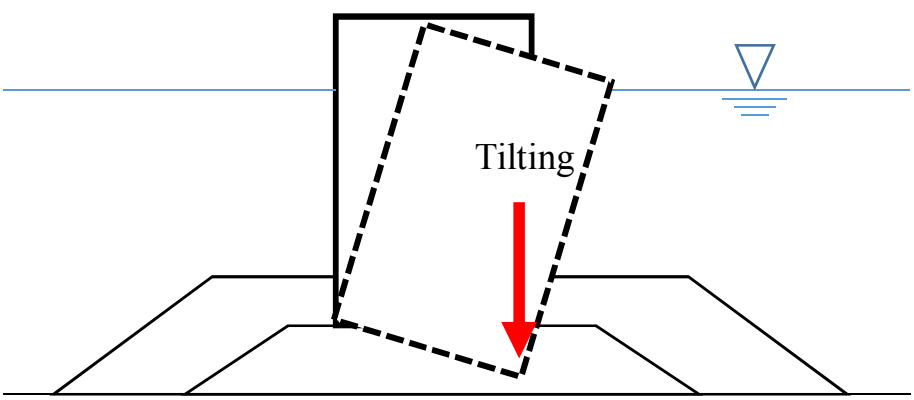

Figure 2.3 Vertical caisson when the tilting failure occurs

2.3 System Reliability

System reliability is the reliability of whole structure, not reliability of each components of structure. The systems are classified into 3 types. The first one is a series system. The series system fails if any of its component events occur and it is defined as

$$E_{\text{system}} = \bigcup_{i=1}^{n} E_i \tag{2.18}$$

There is no redundant part in the series system. The statically determinate structure and electrical substation with single-transmission-line belong to series system. The second one is a parallel system. The parallel system fails only if every component event occurs and it is defined as

$$E_{\text{system}} = \bigcap_{i=1}^{n} E_i \tag{2.19}$$

Because the system has a lot of redundant part in the parallel system, some components failure does not affect to the system failure. The examples of parallel system are a bunch of wires or cables and electrical substation with equipment items in parallel. The last one is a general system. The general system that is neither series nor parallel system. There are two kinds of general system; cut-set system and link-set system. The cut-set system is a series system of sub-parallel systems and the link-set system is a parallel system of sub-series systems. They are defined as

$$\text{Cut-set system: } E_{\text{system}} = \bigcup_{k=1}^{K} \bigcap_{i \in C_k} E_i \tag{2.20a}$$

Link-set system: $E_{\text{system}} = \bigcap_{l=1}^{L} \bigcup_{i \in L_l} E_i$ (2.20b)

Most structures belong to the general system. A structure with multiple failure paths and general electrical substations belongs to them. Figure 2.4 ~ 2.6 represent the example of structure and failure domain of series, parallel, and general system.

The analysis of system reliability is difficult because of its complexity, dependence between failure modes, and lack of information. In order to eliminate the complex numerical integration involved in the evaluation of failure probability of system reliability, four different methods are usually used to calculate the failure probability; inculsion-exculsion formula, simulations, bounding formulas, and FORM approximation. In this research, simulations and FORM approximation are used. The better results between simulations and FORM approximation will be used to further research.

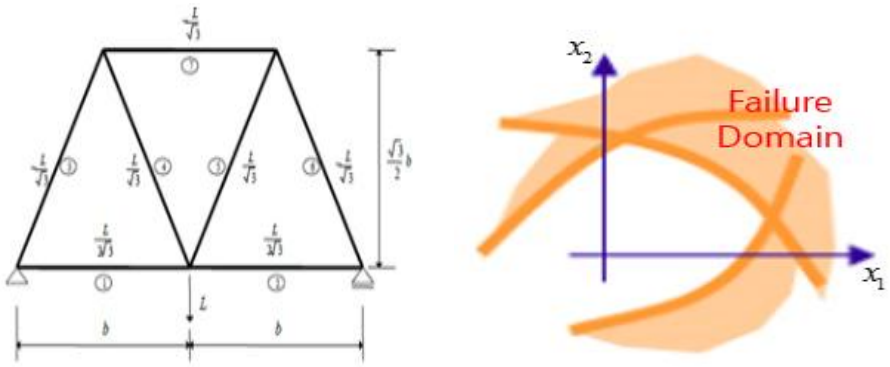

Figure 2.4 Statically determinate truss (series system) and failure domain

Modified from Song, J., and A. Der Kiureghian (2003, JEM ASCE)

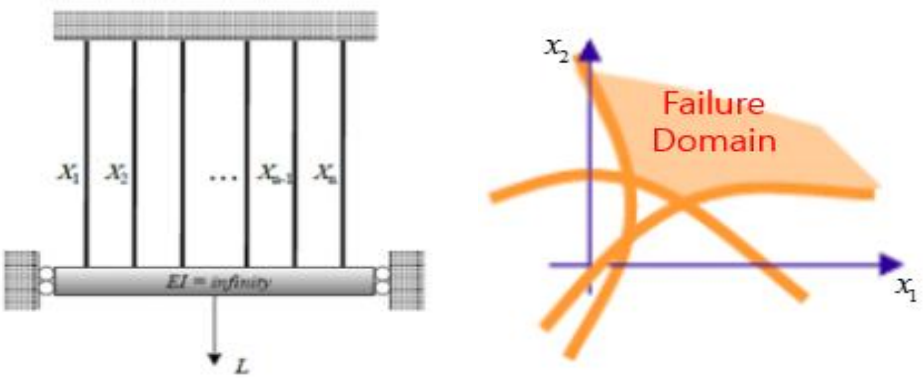

Figure 2.5 Bunch of cables (parallel system) and failure domain

Modified from Song, J., and A. Der Kiureghian (2003, JEM ASCE)

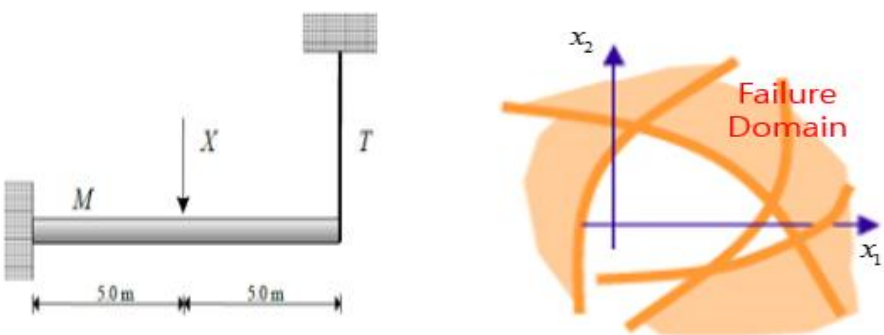

Figure 2.6 Cantilever beam – bar (general system) and failure domain

Modified from Song, J., and A. Der Kiureghian (2003, JEM ASCE)

2.3.1 Simulations

Simulations are the methods that count the number of samples in the system failure domain and estimate the ratio. Simulations are defined as

$$P(E_{\text{system}}) = \int_D f_{\mathbf{X}}(\mathbf{x})d\mathbf{x} \cong \frac{\#(\mathbf{x} \in D)}{\#(\mathbf{x})} \tag{2.21}$$

In this research, Monte Carlo Simulation (MCS) is used. MCS uses index function, $I(\mathbf{x})$ to calculate the failure probability. The index function is defined as

$$I(\mathbf{x}) = \begin{cases} 1 & g(\mathbf{x}) \le 0 \\ 0 & \text{otherwise} \end{cases} \tag{2.22}$$

If the random variables are included in the failure domain, the value of index function is 1, otherwise the value is 0. The detailed calculation process is as below:

$$P_f = \int_{(\cup\cap)g(\mathbf{x})\le 0} f_{\mathbf{X}}(\mathbf{x})d\mathbf{x} = \int_{\mathbf{x}} I(\mathbf{x}) f_{\mathbf{X}}(\mathbf{x})d\mathbf{x} = E_g\left[I(\mathbf{x})\right] \tag{2.23}$$

where $E_g\left[I(\mathbf{x})\right]$ is the average of index function value. Simulate $\mathbf{x}_i$, $i = 1, \cdots, N$ according to $f_{\mathbf{X}}(\mathbf{x})$ and assume that $q_i = I(\mathbf{x}_i)$. Then, the failure probability can be rewritten as

$$P_f = \lim_{N\to\infty} \frac{\sum_{i=1}^{N} q_i}{N} \tag{2.24}$$

The estimation of failure probability using *N* sample is

$$\hat{P}_f \cong \frac{\sum_{i=1}^{N} q_i}{N} \tag{2.25}$$

Therefore, it is very important to select the number of sample because it effects the accuracy of simulation. Figure 2.7 represents the schematic diagram of MCS.

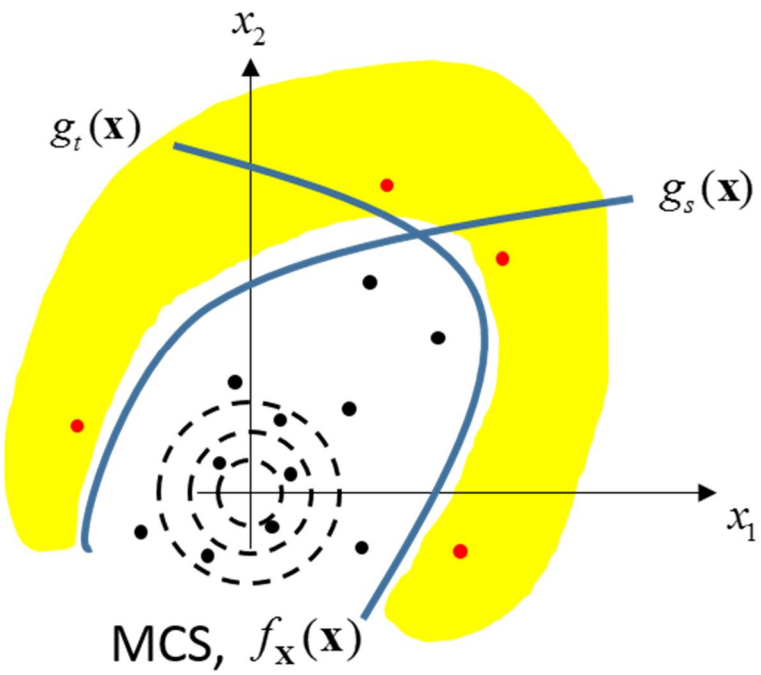

Figure 2.7 Schematic diagram of MCS

2.3.2 FORM Approximation

Consider the series system reliability problem defined by a set of limit state functions $g_k(\mathbf{x}),\ k=1,2,\cdots,m$. Let $G_k(\mathbf{u}),\ k=1,2,\cdots,m$, denote the corresponding limit state functions in the standard normal space. FORM approximation to the system failure probability is obtained by linearizing each limit state function $G_k(\mathbf{u})$ at a point $\mathbf{u}_k^*$, such that the surface is approximated by the tangent hyperplane

$$\beta_k - \alpha_k \mathbf{u} = 0 \tag{2.26}$$

where $\alpha_k = -\nabla G_k(\mathbf{u}_k^*) / \left\| \nabla G_k(\mathbf{u}_k^*) \right\|$ is the unit normal to the hyperplane and $\beta_k = \alpha_k \mathbf{u}_k^*$ is the distance from the origin to the hyperplane. The linearization points $\mathbf{u}_k^*$ is the minimum-distance points from the origin, and it is defined as

$$\mathbf{u}^* = \arg\min \left\{ \|\mathbf{u}\| \,|\, G_k(\mathbf{u}) = 0,\ k=1,2,\cdots,m \right\} \tag{2.27}$$

The above is an optimization problem with multiple inequality constraints. Figure 2.8 illustrates the linearization points for series and parallel systems. If the failure probability of parallel system is calculated by the minimum-distance points, big discrepancy with actual failure probability may occur. Therefore, using the joint design points, $\mathbf{u}^*$, is a better choice for parallel systems.

$$\mathbf{u}^* = \arg\min \left\{ \|\mathbf{u}\| \,|\, G_k(\mathbf{u}) \le 0,\ k=1,2,\cdots,m \right\} \tag{2.28}$$

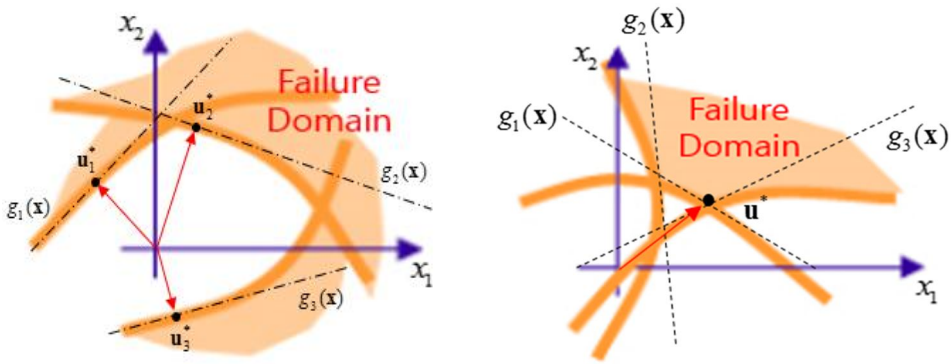

Figure 2.8 Linearization points for series(←) and parallel(→) systems

Modified from Song, J., and A. Der Kiureghian (2003, JEM ASCE)

With the limit state surfaces linearized, the system failure domain is approximated by a hyper-polygon. The corresponding approximates of the failure probability are derived as follows: Let $Z_k = \alpha_k \mathbf{u}$. The mean, variance, and correlation coefficients are

$$E[Z_k] = 0 \quad (\because E[\mathbf{u}] = 0) \tag{2.29a}$$

$$Var[Z_k] = \|\alpha_k\|^2 = 1 \tag{2.29b}$$

$$\begin{aligned} \rho_{Z_k Z_l} &= \frac{\mathrm{cov}[Z_k, Z_l]}{\sigma_{Z_k}\sigma_{Z_l}} = E[Z_k Z_l] - E[Z_k]E[Z_l] = E[Z_k \cdot Z_l^{\mathrm{T}}] \\ &= E[\alpha_k \mathbf{u}\mathbf{u}^{\mathrm{T}}\alpha_l^{\mathrm{T}}] = \alpha_k E[\mathbf{u}\mathbf{u}^{\mathrm{T}}]\alpha_l^{\mathrm{T}} = \alpha_k \mathrm{I}\alpha_l^{\mathrm{T}} = \alpha_k \alpha_l^{\mathrm{T}} \end{aligned} \tag{2.29c}$$

$\mathbf{Z}$ is standard normal random variables because it has zero means and unit variances. For a series system, the failure probability can be expressed as

$$P(E_{sys}) \overset{FORM}{\cong} P(\bigcup_{k=1}^{m} \beta_k - Z_k \le 0) = 1 - P(\bigcap_{k=1}^{m} Z_k \le \beta_k) = 1 - \Phi_m(\boldsymbol{\beta}; \mathbf{R}) \tag{2.30a}$$

where $\Phi_m(\boldsymbol{\beta}; \mathbf{R})$ is the *m*-variate standard normal CDF with correlation matrix $\mathbf{R} = \left[\rho_{Z_k Z_l} \right]$ and evaluated at the thresholds $\boldsymbol{\beta} = (\beta_1, \cdots, \beta_m)$. For a parallel system, the failure probability can be expressed as

$$P(E_{sys}) \overset{FORM}{\cong} P(\bigcap_{k=1}^{m} \beta_k - Z_k \le 0) = P(\bigcap_{k=1}^{m} Z_k \le -\beta_k) = \Phi_m(-\boldsymbol{\beta}; \mathbf{R}) \tag{2.30b}$$

The FORM approximation is an easy way to calculate failure probability, however it may have huge errors due to the curvature of the limit state function.

Ditlevsen & Madsen (1996) proposed the calculating method of bivariate normal integrals and it can be expressed as

$$\Phi_1(b_1, b_2; \rho_{12}) = \Phi(b_1)\Phi(b_2) + \int_0^{\rho_{12}} \varphi_2(b_1, b_2; \rho) d\rho \tag{2.31}$$

2.4 Nonlinear Least Squares

Nonlinear least squares is the form of least squares analysis used to fit a set of *m* observations with a model that is non-linear in *n* unknown parameters ($m \geq n$). It is used in some forms of nonlinear regression. The basis of the method is to approximate the model by a linear one and to refine the parameters by successive iterations.

Consider a set of *m* data points, $(x_1, y_1),\ (x_2, y_2),\ \cdots,\ (x_m, y_m)$, and a curve (model function) $\mathbf{y} = f(\mathbf{x}, \boldsymbol{\beta})$, that in addition to the variable *x* also depends on *n* parameters, $\boldsymbol{\beta} = (\beta_1,\ \beta_2,\ \cdots, \beta_n)$, with $m \geq n$. It is desired to find the vector $\boldsymbol{\beta}$ of parameters such that the curve fits best the given data in the least squares sense, that is, the sum of squares is minimized

$$S = \sum_{i=1}^{m} r_i^2 \tag{2.32}$$

where the residuals r_i are given by

$$r_i = y_i - f(x_i, \boldsymbol{\beta}) \quad \text{for} \quad i = 1,\ 2,\ \cdots,\ m \tag{2.33}$$

The minimum value of *S* occurs when the gradient is zero. Since the model contains *n* parameters there are *n* gradient equations:

$$\frac{\partial S}{\partial \beta_j} = 2 \sum_i r_i \frac{\partial r_i}{\partial \beta_j} = 0 \quad \text{for} \quad j = 1,\ 2,\ \cdots,\ n \tag{2.34}$$

In a nonlinear system, the derivatives $\partial r_i / \partial \beta_j$ are functions of both the independent variable and the parameters, so these gradient equations do not have a closed solution. Instead, initial values must be chosen for the parameters. Then, the

parameters are refined iteratively, that is, the values are obtained by successive approximation,

$$\beta_j \approx \beta_j^{k+1} = \beta_j^k + \Delta\beta_j \tag{2.35}$$

where k is the iteration number and the vector of increments, $\Delta\beta$ is known as the shift vector. At each iteration the model is linearized by approximation to a first-order Taylor series expansion about β^k

$$f(x_i, \boldsymbol{\beta}) \approx f(x_i, \boldsymbol{\beta}^k) + \sum_j \frac{\partial f(x_i, \boldsymbol{\beta}^k)}{\partial \beta_j}(\beta_j - \beta_j^k) \approx f(x_i, \boldsymbol{\beta}^k) + \sum_j J_{ij}\Delta\beta_j \tag{2.36}$$

The Jacobian, J, is a function of constants, the independent variable and the parameters, so it changes from one iteration to the next. Thus, in terms of the linearized model, $\partial r_i / \partial \beta_j = -J_{ij}$ and the residuals are given by

$$\Delta y_i = y_i - f(x_i, \boldsymbol{\beta}^k) \tag{2.37a}$$

$$r_i = y_i - f(x_i, \boldsymbol{\beta}) = \left(y_i - f(x_i, \boldsymbol{\beta}^k)\right) + \left(f(x_i, \boldsymbol{\beta}^k) - f(x_i, \boldsymbol{\beta})\right) = \Delta y_i - \sum_{s=1}^{n} J_{is}\Delta\beta_s \tag{2.37b}$$

Substituting these expressions into the gradient equations, they become

$$-2\sum_{i=1}^{m} J_{ij}\left(\Delta y_i - \sum_{s=1}^{n} J_{is}\Delta\beta_s\right) = 0 \tag{2.38}$$

which, on rearrangement, become n simultaneous linear equations, the normal equations

$$\sum_{i=1}^{m}\sum_{s=1}^{n} J_{ij}J_{is}\Delta\beta_s = \sum_{i=1}^{m} J_{ij}\Delta y_i \quad \text{for} \quad j = 1,\ 2,\ \cdots,\ n \tag{2.39a}$$

The normal equations are written in matrix notation as

$$(\mathbf{J}^{\mathrm{T}}\mathbf{J})\Delta\boldsymbol{\beta} = \mathbf{J}^{\mathrm{T}}\Delta\mathbf{y} \tag{2.39b}$$

2.5 Minimization of Expected Total Lifetime Cost

Following Lee (2002), minimization of expected total lifetime cost can be formulated by incorporating the results of reliability analysis in the economic analysis. To minimize the expected total lifetime cost consisted of the expected initial construction cost and the expected damage cost due to sliding failure, all of the expected cost in economic analysis should be defined as a function of design variable, the width of vertical caisson of composite breakwaters.

$$E[C_T(B)] = E[C_I(B)] + E[C_F(B)] \tag{2.40a}$$

$$E[C_I(B)] = C_0 - C\ln(P_f(B)) \tag{2.40b}$$

$$E[C_F(B)] = (EQCF)(P_f(B))\frac{1-e^{-iT_R}}{i} \tag{2.40c}$$

where $E[C_T(B)]$ is the expected total lifetime cost, $E[C_I(B)]$ is the expected initial construction cost, $E[C_F(B)]$ is the expected damage cost, C_0 is the initial construction cost unrelated to the width of vertical caisson, C is the increment of construction cost to enforce the stability of structure, $P_f(B)$ is the failure probability through system reliability, $EQCF$ is the expected damage cost when $t = 0$, i is the net annual discount rate, j is the annual discount rate, r is the interest rate, and T_R is the serviced time.

Assume that the expected total lifetime cost uses the summation of Gaussian functions so that the probability of sliding failure only resulting from the reliability analysis can be related to the width of vertical caisson directly.

$$P_f(B) = \sum_{i=1}^{n} a_i e^{-\left(\frac{B-c_i}{b_i}\right)^2} \tag{2.41}$$

in which a,b,c are constants to be determined through nonlinear least squares method and n is the number of summations

If the value of a,b,c are determined, the optimal width of vertical caisson can be calculated by using the harmony search method.

$$\frac{\partial E[C_T(B)]}{\partial P_f} = 0$$

$$\frac{-C}{P_f(B)} + (EQCF)\frac{1-e^{-iT_R}}{i} = 0$$

Therefore, the optimal width of vertical caisson is given by

$$P_f(B)_{opt} = \frac{Ci}{EQCF(1-e^{-iT_R})} = \sum_{i=1}^{n} a_i e^{-\left(\frac{B-c_i}{b_i}\right)^2} \tag{2.42}$$

2.6 Harmony Search Algorithm

The harmony search algorithm was first developed by Geem et al (2001), and it has been applied to many optimization problems. The harmony search algorithm is composed of three components: usage of harmony memory, pitch adjusting, and randomization. The usage of harmony memory (HM) is important because it ensures that good harmonies are considered as elements of new solution vectors. In order to use this memory effectively, the HS algorithm adopts a parameter, called Harmony Memory Considering Rate (HMCR). If this rate is too low, only few elite harmonies are selected and it may converge too slowly. If this rate is extremely high, the pitches in the harmony memory are mostly used, and other ones are not

explored well, leading not into good solutions.

The second component is the pitch adjustment which has parameter such as Pitch Adjusting Rate (PAR). PAR can be used to control the degree of the adjustment. A low pitch adjusting rate can slow down the convergence of HS because of the limitation in the exploration of only a small subspace of the whole search space. On the other hand, a very high pitch-adjusting may cause the solution to scatter around some potential optima as in a random search.

The third component is the randomization, which is to increase the diversity of the solutions. Although the pitch adjustment has a similar role, it is limited to certain area and thus corresponds to a local search. The use of randomization can drive the system further to explore various diverse solutions so as to attain the global optimality.

The steps in the procedure of Harmony Search are shown in Figure 2.9, and they are as follows:

Step 1. Initialize the problem and algorithm parameters.

Step 2. Initialize the Harmony Memory (HM).

Step 3. Improvise a new harmony

Step 4. Update Harmony Memory

Step 5. Check the stopping criteria. If criteria are not satisfied, go to Step 3.

These steps are described in the next five subsections.

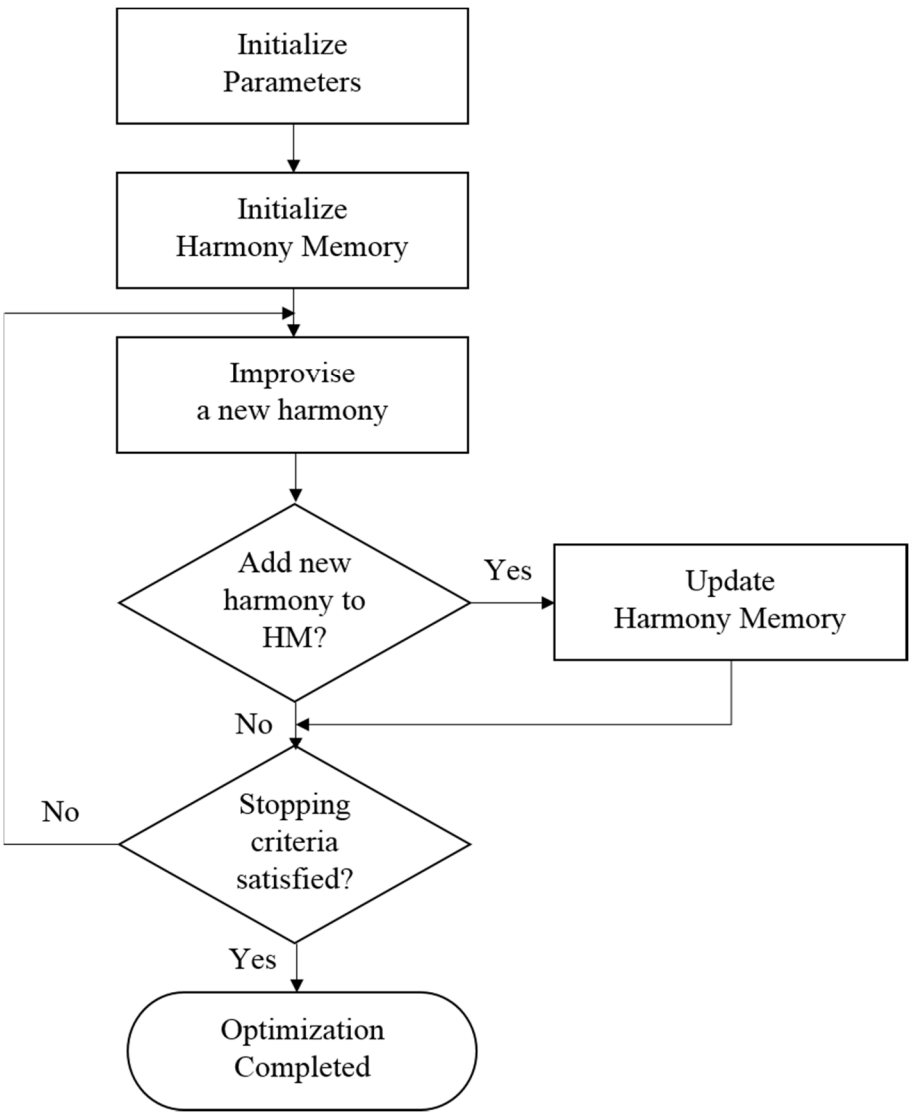

Figure 2.9 Optimization procedure of Harmony Search algorithm.

2.6.1 Initialize the Problem and Algorithm Parameters

In Step 1, the optimization problem is specified as follows:

$$\begin{aligned} &\min f(x) \\ &\text{s.t} \quad x_i \in X_i \quad (i = 1,2,\cdots,N) \end{aligned}$$

where $f(x)$ is an objective function; $\mathbf{x}$ is the set of each decision variable x_i; N is the number of decision variables, X_i is the set of the possible range of values for each decision variable, that is ${}_L x_i \le X_i \le {}_U x_i$. ${}_L x_i$ and ${}_U x_i$ are the lower and upper bounds for each decision variable.

The HS algorithm parameters are determined in this step. These are the Harmony Memory Size (HMS); Harmony Memory Considering Rate (HMCR); Pitch Adjusting Rate (PAR); and stopping criteria.

2.6.2 Initialize the Harmony Memory

In step 2, the HM matrix is filled with as many randomly generated solution vectors.

$$\mathrm{HM} = \begin{bmatrix} x_1^1 & x_2^1 & \cdots & x_{N-1}^1 & x_N^1 \\ x_1^2 & x_2^2 & \cdots & x_{N-1}^2 & x_N^2 \\ \vdots & \vdots & \ddots & \vdots & \vdots \\ x_1^{HMS-1} & x_2^{HMS-1} & \cdots & x_{N-1}^{HMS-1} & x_N^{HMS-1} \\ x_1^{HMS} & x_2^{HMS} & \cdots & x_{N-1}^{HMS} & x_N^{HMS} \end{bmatrix}$$

2.6.3 Improvise a new harmony

In Step 3, a new harmony vector, $x' = (x_1', x_2', \cdots, x_N')$, is generated based on three rules: (1) memory consideration, (2) pitch adjustment and (3) random

selection. Generating a new harmony is called 'improvisation'.

In the memory consideration, the value of the first decision variable ($x_1^{'}$) for the new vector is chosen from any of the values in the specified HM range ($x_1^{'1} \sim x_1^{'HMS}$). Values of other decision variables ($x_2^{'},\cdots,x_N^{'}$) are chosen in the same way. The HMCR, which varies between 0 and 1, is the rate of choosing one value from the historical values stored in the HM, while (1-HMCR) is the rate of randomly selecting one value from the possible range of values.

$$x_i^{'} \leftarrow \begin{cases} x_i^{'} \in \left\{x_i^1, x_i^2, \cdots, x_i^{HMS}\right\} & \text{with probability} \quad \text{HMCR} \\ x_i^{'} \in X_i & \text{with probability} \quad 1-\text{HMCR} \end{cases}$$

Every component obtained by the memory consideration is examined to determine whether it should be pitch-adjusted. This operation uses the PAR parameter. The PAR, which varies between 0 and 1, is the rate of replacing decision variable as $x_i^{'} \pm \text{rand}(\cdot) \times bw$, while (1-PAR) is the rate of doing nothing.

$$x_i^{'} \leftarrow \begin{cases} x_i^{'} \pm \text{rand}(\cdot) \times bw & \text{with probability} \quad \text{PAR} \\ x_i^{'} & \text{with probability} \quad 1-\text{PAR} \end{cases}$$

where *bw* is an arbitrary distance bandwidth and $\text{rand}(\cdot)$ is a random number between 0 and 1.

2.6.4 Update Harmony Memory

If the new harmony vector, $x' = (x_1^{'}, x_2^{'}, \cdots, x_N^{'})$ is better than the worst harmony in the HM, the new harmony is included in the HM and the existing worst harmony is excluded from the HM.

2.6.5 Check stopping criteria

If the stopping criteria (maximum number of improvisations) is satisfied, computation is terminated. Otherwise, Steps 3 and 4 are repeated.

CHAPTER 3. SYSTEM RELIABILITY

Above mentioned earlier, the system reliability is the reliability of whole structure, not the reliability of each component of structure. The first step to calculate the system reliability is to obtain the random variables. Random numbers are generated following the normal distribution with the mean and the standard deviation. The limit state function for sliding employs the random variables of the friction coefficient (μ), the weight of upright section in still water (W^*), the uplift pressure (U), and the horizontal wave force (P), and the limit state function for tilting employs the random variables of net moment at the heel (M_e) and net weight (W_e).

Second, the failure probability is calculated by using system reliability. Among system reliability, the FORM approximation is used to obtain the failure probability. The sliding failure probability and tilting failure probability are calculated while changing the breakwater cross-sections and wave conditions. Then, the failure probability which considers both failure is calculated.

Lastly, the suitable function is determined which can express to the relation between failure probability and the width of vertical caisson. The function form is assumed as Gaussian function and the number of summation of Gaussian function is found which can well express the relation between caisson width and failure probability. After obtaining the suitable function, nonlinear least square method is used to find the parameters.

3.1 Generation of Random Variables

Generation of random variables are firstly needed for the reliability design. The number of random variables in this research is 6: (1) the friction coefficient (μ); (2) the weight of upright section in still water (W^*); (3) the uplift pressure force (U); (4) the horizontal wave force (P); (5) the net moment at the heel (M_e); and (6) the net weight (W_e). These random variables can be expressed as the linear combination of the fixed deterministic value of breakwater and the wave condition by using the formula given in section 2.1.

Two different breakwaters were used in this research: (1) Goda's fictitious composite breakwater; and (2) Shibushi breakwater in Japan. Goda's fictitious composite breakwater has been used in the previous research and sliding failure is dominant. On the other hand, Shibushi breakwater in Japan is located in deeper water than Goda's fictitious composite breakwater, so the tilting failure may be dominant.

3.1.1 Goda's Fictitious Composite Breakwater

Goda's fictitious composite breakwater is the breakwater suggested by Goda (2010) in his book "Random Seas and Design of Maritime Structures." The fixed deterministic values of the breakwater are shown in Table 3.1, the figure of the upright section of the breakwater is the same as Figure 2.1, and the wave conditions at the breakwater are shown in Table 3.2.

Table 3.1. Fixed deterministic values of Goda's fictitious composite breakwater

Deterministic Values	Definition	Value	Units
h	Water depth in front of the breakwater	10.1	m
h'	Distance from the design water level to the bottom of the upright section	7.1	m
h_c	Crest elevation of the breakwater	3.4	m
d	Water depth above the armor layer of the rubble foundation	5.6	m
B_M	Berm width	8.0	m
D	Constant thickness of the rubble mound	3.0	m
t	Height of the foot protection	1.5	m
$\tan\theta$	Mean angle tangent of the sea bottom	0.01	-
β	Angle between the direction of wave approach and a line normal to the breakwater	15	degree
γ_s	Density of the upright section for the submerged portion (Concrete caisson filled with sand)	1.1	$\mathrm{ton/m^3}$
γ_u	Density of the upright section for the portion of the caisson above the still water level	2.1	$\mathrm{ton/m^3}$
γ_c	Density of the upright section for the cap concrete	2.3	$\mathrm{ton/m^3}$

Table 3.2 Wave conditions at the Goda's fictitious composite breakwater

Wave condition	Mean	c.o.v	Distribution	Reference
$H_{1/3}$ Significant wave height	5.8 m	0.1 m	Normal	Goda (2010)
$T_{1/3}$ Significant wave period	11.4 s	-	Fixed Value	Goda (2010)

3.1.2 Shibushi Breakwater

The Shibushi breakwater was built to protect Shibushi Port in Japan. The Shibushi Breakwater is composed of seven sections like Figure 3.1, but in this research, section 2, 4, 5, 7 were used. The fixed deterministic values of the sections of Shibushi breakwater are similar to the values of Goda's fictitious composite breakwater. Comparing with the values of Goda's fictitious composite breakwater, only the different values are shown in Table 3.3.

As shown in Table 3.3, one of the features of Shibushi breakwater is that the distance from the design water level to the bottom of the upright section (h') does not increase although water depth increases. The value of h' only changes 8.5 m to 9.0 m from section 2 to section 4. Instead, the thickness of rubble mound, D, increases as water depth increases.

The wave conditions at the Shibushi breakwater are shown in Table 3.4. Typhoon 1 ~ Typhoon 3 are typhoons that actually arrived at Shibushi breakwater in 2003 ~ 2005. Significant wave height and significant wave period of typhoons are shown in Table 3.4.

Figure 3.1 Shibushi port in Japan

Received from Takagi, H., Esteban, M., and Shibayama, T. (2015)

Table 3.3. Fixed deterministic values of Shibushi breakwater

Deterministic Values	Section 2	Section 4	Section 5	Section 7
h	11.5 m	12.4 m	13.2 m	15.0 m
h'	8.5 m	9.0 m	9.0 m	9.0 m
h_c	7.0 m	7.0 m	7.0 m	7.0 m
d	7.2 m	7.7 m	7.7 m	7.7 m
D	3.0 m	3.4 m	4.2 m	6.0 m
t	1.3 m	1.3 m	1.3 m	1.3 m

Table 3.4 Wave conditions at Shibushi breakwater

Typhoon	Wave condition	Mean	c.o.v	Distribution	Reference
Typhoon 1	$H_{1/3}$	7.97 m	0.1 m	Normal	Takagi et al. (2015)
	$T_{1/3}$	13.7 s	-	Fixed Value	
Typhoon 2	$H_{1/3}$	9.03 m	0.1 m	Normal	
	$T_{1/3}$	12.8 s	-	Fixed Value	
Typhoon 3	$H_{1/3}$	9.62 m	0.1 m	Normal	
	$T_{1/3}$	15.2 s	-	Fixed Value	

3.1.3 Generation of Random Variable

Through the linear combination of above wave conditions and fixed deterministic values of breakwater, six random variables which are used to system reliability can be expressed. Because the linear combination of normal distribution follows the normal distribution, random variables also follow the normal distribution.

The mean and coefficient of variation of random variables which were obtained from the linear combination are different depending on the wave condition and the deterministic value of breakwater. For example, Table 3.5 represents the characteristics of random variables when using deterministic values of Goda's fictitious composite breakwater and wave conditions which were shown in Table 3.1 and Table 3.2. If we use the condition of Shibushi breakwater, the characteristics of random variables will be changed.

When the design variable, caisson width, is changed, the mean and standard deviation of some random variables are also changed. The value of caisson width varies from 10 m to 50 m at the interval of 0.1 m. 15,000 random numbers following the normal distribution with the mean and standard deviation will be generated in case of every caisson width. Box & Muller (1958) method was used for generating random numbers. Because MATLAB function "mvnrnd" is based on the Box & Muller method, it is very easy to use.

Table 3.5. Random variables when using the conditions of Goda's breakwater

Random Variable	Mean	c.o.v	Distribution	Units
μ Friction coefficient	0.65	0.1	Normal	
W^* Weight of upright section of caisson	-	0.05		kN/m
U Uplift pressure force	-	0.02		kN/m
P Horizontal wave force	1740	0.02		kN/m
M_e Net moment at the heel	-	0.08		kN · m/m
W_e Net weight	-	0.07		kN/m

- : Values depend on the design variable, caisson width.

After obtaining all random numbers, chi-square test was performed for checking if each distribution follows the normal distribution. For example, Figure 3.2 shows the relative histogram and probability density function of normal distribution of random variables when the caisson width is 20 m. It seems that all random variables follow the normal distribution. In order to check quantitatively, one of the goodness-of-fit test, the chi-square test was performed. The null hypothesis (H_0) is that random variables follow the normal distribution. The p-values of chi-square test are presented in Table 3.6. Because the p-value of all random variables are larger than significance level, 0.01, all design variables follow the normal distribution.

Table 3.6. Results of chi-square test of random variables

Random variables	μ	W	U	P	M_e	W_e
p-value	0.269	0.068	0.459	0.313	0.396	0.126

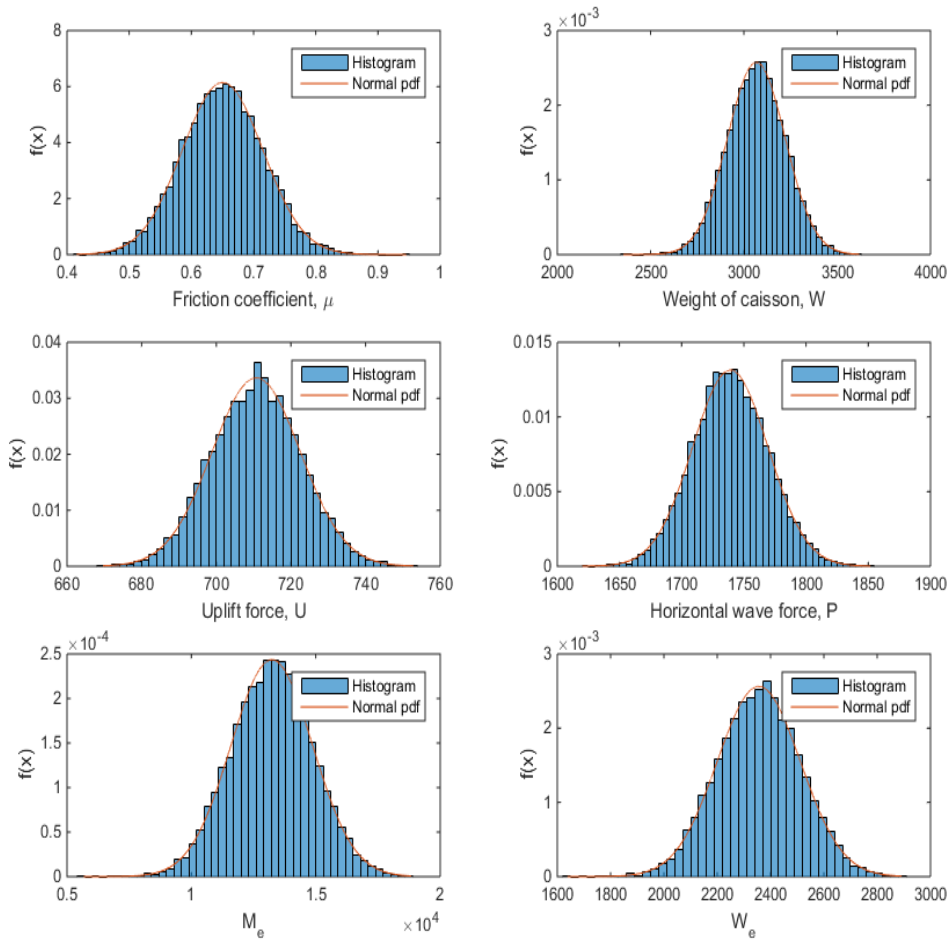

Figure 3.2 Relative histogram and pdf of normal distribution of random variables when the caisson width is 20 m

3.2 Calculation of Failure Probability

It is assumed that the vertical caisson of each breakwaters follows series system, meaning that the vertical caisson fails if either sliding failure or tilting failure occurs. The failure probability that considers both sliding and tilting simultaneously can be calculated through the system reliability by simulations and FORM approximation. However, in case of simulations, millions of data generation is required to obtain the accurate failure probability and it requires tremendous the calculation time. Therefore, the FORM approximation is used to calculate the failure probability in this research. The failure probability varies depending on the design variable, caisson width. As mentioned in the background theory, the form of failure function against to caisson width is assumed as summation of Gaussian functions. However, there is no previous research about the Gaussian function that can express both failure probabilities against to caisson width. So, the reason why the Gaussian function is chosen will be explained later.

3.2.1 Simulations and its limitation

The failure probability against the caisson width obtained by Monte Carlo Simulation is shown in Figure 3.3. It changes with the caisson width. But, as mentioned above, in order to obtain the accurate failure probability, more sampling number is needed. For example, Figure 3.4 represents the failure probability and coefficient of variation of Goda's fictitious breakwater against the sampling number when the caisson width is 25 m. Because the failure probability is not converged, it is dangerous to apply the failure probability from MCS to the

optimization later.

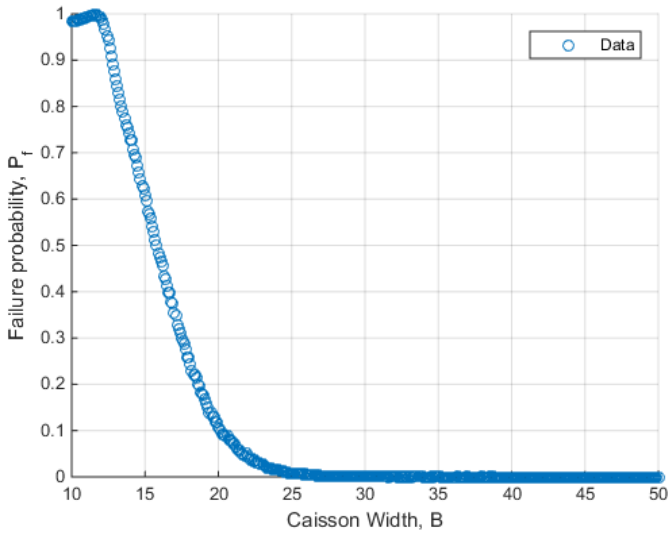

Figure 3.3 Failure probability versus caisson width calculated by Monte Carlo Simulation

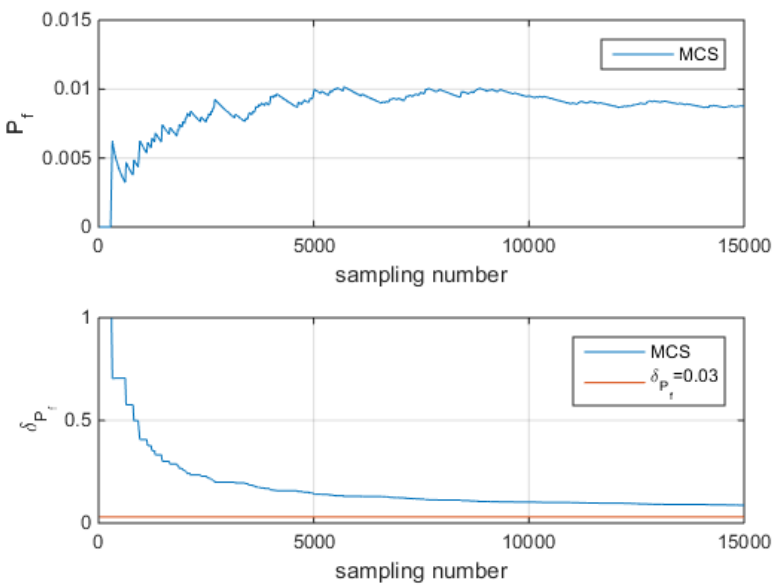

Figure 3.4 Failure probability and c.o.v with the sampling number when the caisson width is 25 m

3.2.2 FORM Approximation

The FORM approximation finds the design point at which is distance from the origin to limit state function becomes minimum and the failure probability is calculated using the tangential line at the design point. Therefore, if the curvature of the limit state function is large, there can be a huge error between the actual value and model value. However, sliding failure function and tilting failure function which are limit state functions in this study are simple functions and when comparing the failure probability from the FORM approximation with the failure probability from Monte Carlo Simulation, there is no big difference between two failure probabilities. Therefore, it is all right to apply the FORM approximation in this study. The FORM approximation does not need the data generation unlike Monte Carlo Simulation and calculation time is fast.

The failure probability against the caisson width is calculated for Goda's fictitious composite breakwater and four different sections of Shibushi breakwater by using the FORM approximation. Three different wave conditions are applied in the case of Shibushi breakwater. Therefore, the total number of design case is 13, (Goda: 1(breakwater cross-section)×1(wave condition) = 1, Shibushi breakwater: 4(breakwater cross-sections) × 3(wave conditions) = 12) and each design case is repeated five times for reliability design based optimization later.

(1) Goda's fictitious composite breakwater

The failure probability against the caisson width was calculated for Goda's fictitious composite breakwater by using the FORM approximation. As shown in Table 3.2, significant wave height and significant wave period are 5.8 m and 11.4 s, respectively. The results are shown in Figure 3.5 and 3.6. Figure 3.5 represents the sliding failure probability and tilting failure probability respectively in order to determine which failure is dominant, and Figure 3.6 represents the final failure probability considering both failures. We can easily find that the sliding failure is dominant failure over the whole interval of caisson width for Goda's fictitious composite breakwater from Figure 3.5. Therefore, the shape of final failure probability against caisson width in Figure 3.6 is similar to the shape of sliding failure probability against caisson width in Figure 3.5.

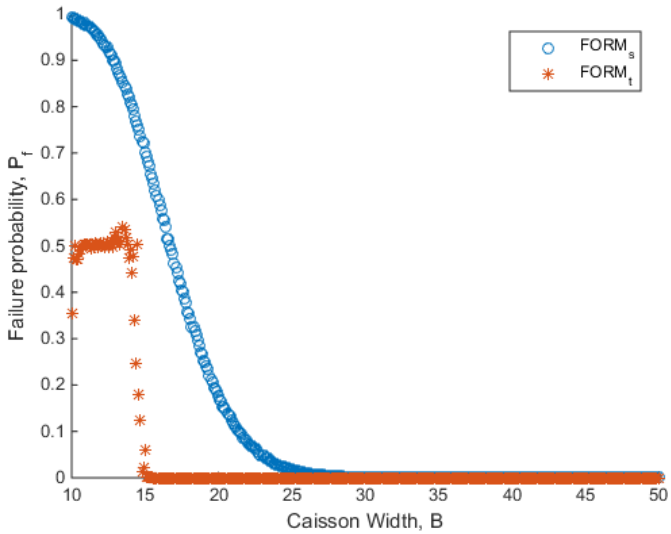

Figure 3.5 Sliding and tilting failure probability against caisson width for Goda's fictitious composite breakwater

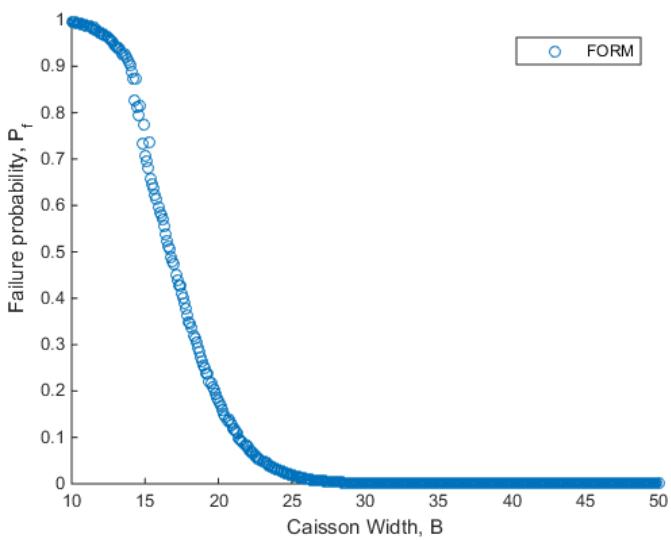

Figure 3.6 Final failure probability against caisson width for Goda's fictitious composite breakwater

(2) Shibushi breakwater

The failure probability against the caisson width was calculated for the Shibushi breakwater by using the FORM approximation. Because there are four different breakwater type and three different wave conditions, a total of 12 failure probabilities were calculated. All the results are presented in Appendix A. Only show some important results are presented here.

First, Figure 3.7 and 3.8 show the failure probability against the caisson width when Typhoon 1 wave condition (significant wave = 7.97 m, significant wave period = 13.7 s) is applied to the section 2 of Shibushi breakwater. Unlike Goda's fictitious composite breakwater, tilting failure is dominant in a certain range of caisson width. Therefore, the shape of final failure probability against the caisson width in Figure 3.8 shows both sliding failure probability and tilting failure probability.

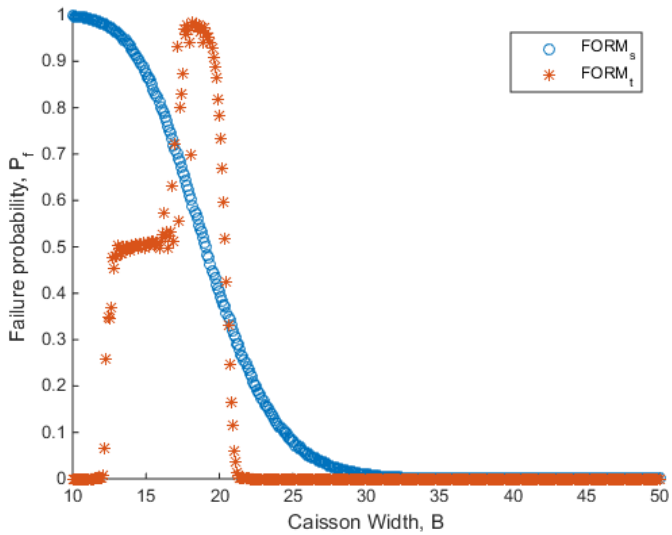

Figure 3.7 Sliding and tilting failure probability against caisson width at section 2 of Shibushi breakwater (Typhoon 1 wave condition)

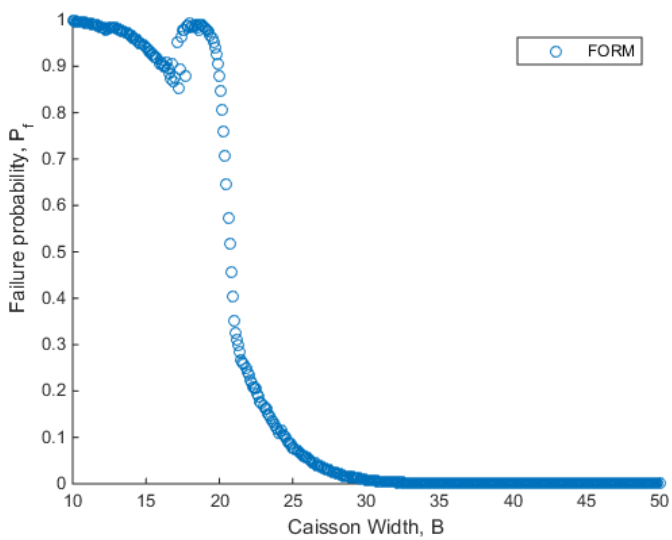

Figure 3.8 Final failure probability against caisson width at section 2 of Shibushi breakwater (Typhoon 1 wave condition)

Second, Figure 3.9 and 3.10 show the failure probability against the caisson width when Typhoon 3 wave condition (significant wave height = 9.62 m, significant wave period = 15.2 s) is applied to the section 2 of Shibushi breakwater. Significant wave height and period of Typhoon 3 wave condition are greater than those of Typhoon 1 wave condition. Comparing Figure 3.9 with Figure 3.7, we can confirm that sliding failure becomes dominant failure in the entire range of caisson width when significant wave height and period increase for the same breakwater. Therefore, like Figure 3.6, the shape of final failure probability against the caisson width in Figure 3.10 is similar to the shape of sliding failure probability in Figure 3.9.

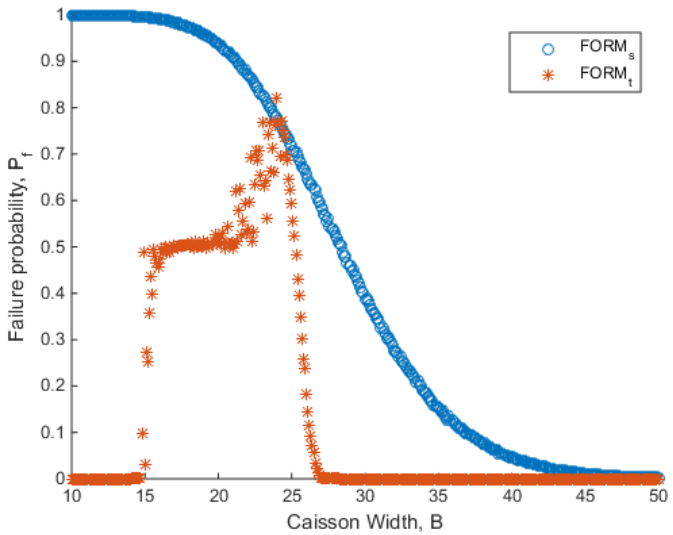

Figure 3.9 Sliding and tilting failure probability against caisson width at section 2 of Shibushi breakwater (Typhoon 3 wave condition)

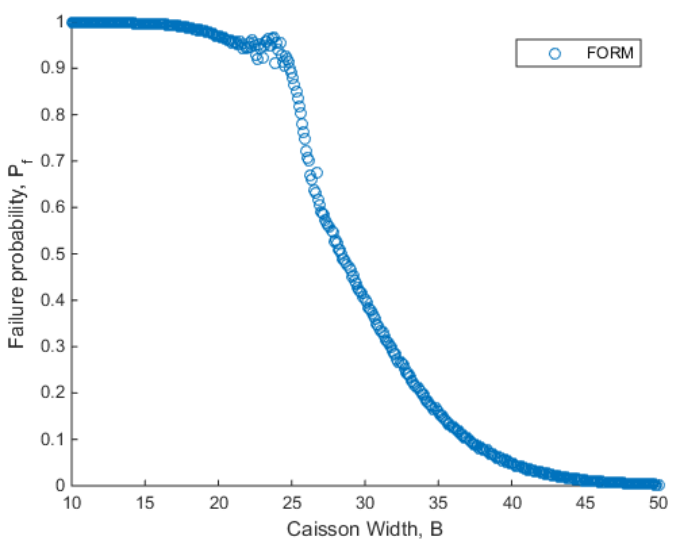

Figure 3.10 Final failure probability against caisson width at section 2 of Shibushi breakwater (Typhoon 3 wave condition)

Third, Figure 3.11 and 3.12 show the failure probability against the caisson width when Typhoon 1 wave condition (significant wave height = 7.97 m, significant wave period = 13.7 s) is applied to the section 7 of Shibushi breakwater. Generally, tilting failure becomes dominant as the water depth increases. However, when comparing the tilting failure probability of the section 7 with that of the section 2 (Figure 3.7) where the water depth is smaller than section 7, these two values are quite similar. Therefore, it is hard to say that the tilting failure becomes dominant when water depth increases at least in the present research. The important factor that makes the tilting failure become dominant may not be the water depth but the distance from the design water level to the bottom of the upright section.

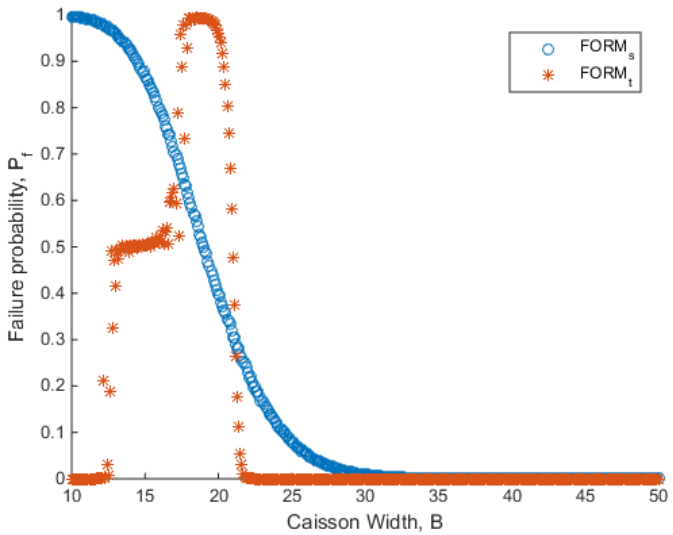

Figure 3.11 Sliding and tilting failure probability against caisson width at section 7 of Shibushi breakwater (Typhoon 1 wave condition)

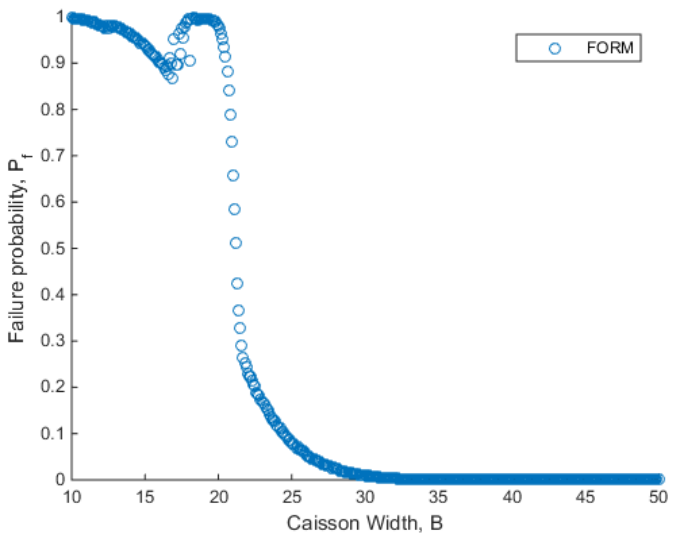

Figure 3.12 Final failure probability against caisson width at section 7 of Shibushi breakwater (Typhoon 1 wave condition)

To check how much the distance from the design water level to the bottom of the upright section affects the tilting and final failure probabilities quantitatively, the failure probability against caisson width was calculated for a hypothetical case. Basically, the fixed deterministic value of Section 7 shown in Table 3.3 was used, but the distance from the design water level to the bottom of the upright section was changed from 9 m to 12 m and the thickness of rubble mound was changed from 6 m to 3 m. Typhoon 1 wave condition was used. Figure 3.13 and 3.14 shows the failure probability against caisson width for the hypothetical case.

As shown in Figure 3.13, the tilting failure probability is dominant in a wider range than that of tilting failure probability in Figure 3.7. Therefore, the shape of tilting failure probability is well expressed in the final failure probability shown in Figure 3.14. In short, the important factor that makes the tilting failure become dominant is the distance from the design water level to the bottom of the upright section, not the water depth. Although the water depth increases, the tilting failure is not dominant unless the distance from the design water level to the bottom of the upright section changes.

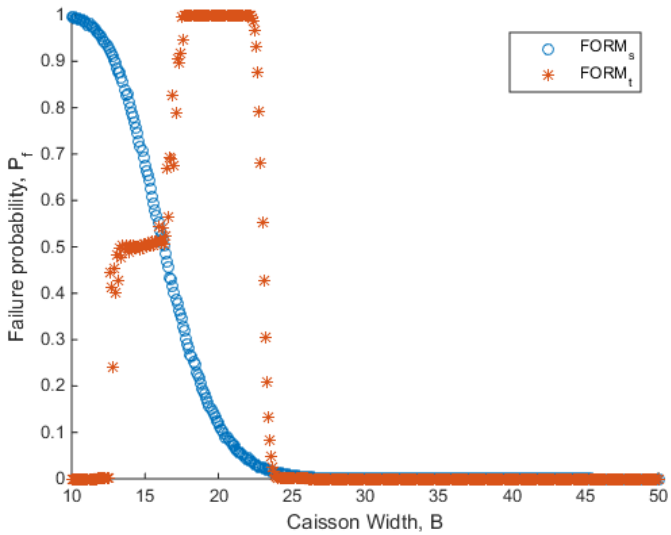

Figure 3.13 Sliding and tilting failure probability against caisson width for hypothetical case (Typhoon 1 wave condition)

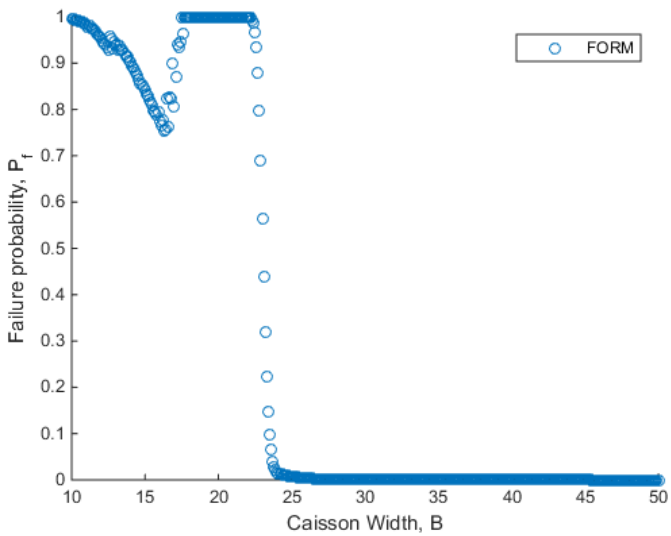

Figure 3.14 Final failure probability against caisson width for hypothetical case (Typhoon 1 wave condition)

3.3 Selection of Suitable Function

After calculating the failure probability against caisson width using the FORM approximation, the suitable function which can well express the relation between caisson width and failure probability must be obtained. In order to obtain the suitable function, nonlinear least squares method was used, which is one of the curve fitting method.

Curve fitting finds the parameters of a certain function, but it cannot find the optimum function. Therefore, the form of function must be assumed firstly. In this research, Gaussian function is assumed to express the relation between caisson width and failure probability for two reasons. First reason is that there is a previous research in which the sliding failure probability against caisson width was expressed as an exponential function. Second reason is that the curve of tilting failure probability against the caisson width is similar to the bell-shaped curve. Therefore, the Gaussian function can be considered to be suitable when either sliding failure is dominant or tilting failure is dominant. Even when both failure probabilities are combined, Gaussian function can be used.

There are two concerns for curve fitting. First one is the range of caisson width which can be applied to the function, and second one is the number of summation of Gaussian function. These two concerns will be explained in detail.

3.3.1 Selection of Range of Caisson Width

The first concern is the range of caisson width which can be applied to the function. It is wanted to find the function which expresses the relation between

caisson width and failure probability in the entire range, but it is almost impossible. Therefore, two methods are suggested to reduce the range of caisson width.

Because the failure of the structure occurs at a low failure probability, the caisson width of high failure probability is out of interest. On the other hand, there is a wide range of caisson width in which the failure probabilities are almost zero. If this range is included, the final form of function can be significantly distorted. Therefore, in this research, the curve fitting was made using the data of the failure probability between 0.5 and 0.001, and the results was compared with that obtained using the entire data to find the better result.

(1) Curve fitting using the entire data

Figure 3.15 ~ 3.17 shows the fitted-curve by using the entire data for three different failure cases. Figure 3.15 shows the fitted curve when sliding failure is dominant, Figure 3.16 shows the fitted curve when tilting failure is dominant, and Figure 3.17 shows the fitted curve when both failures are dominant. The form of fitted curve was used as the summation of four Gaussian functions.

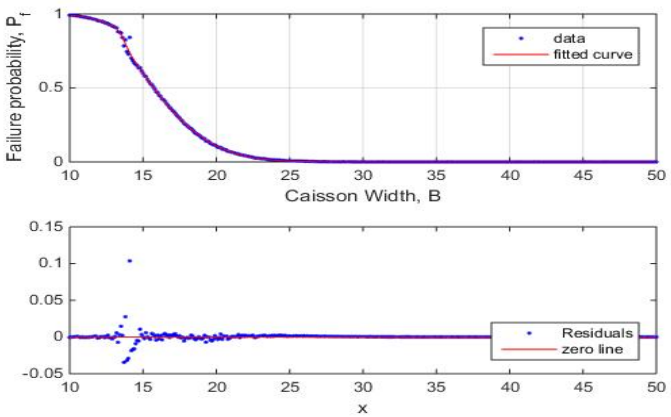

Figure 3.15 Fitted curve determined by using entire data when sliding failure is dominant

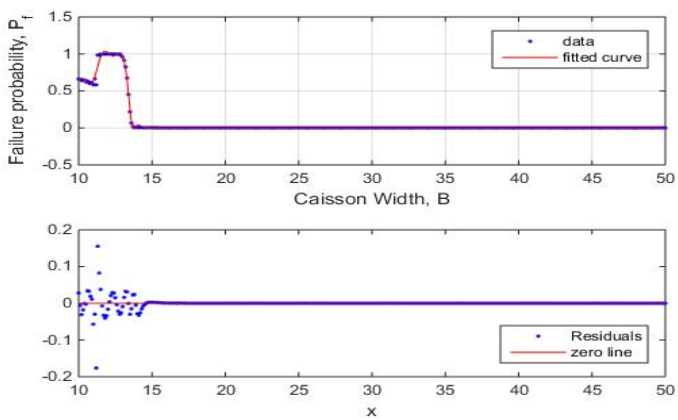

Figure 3.16 Fitted curve when tilting failure is dominant

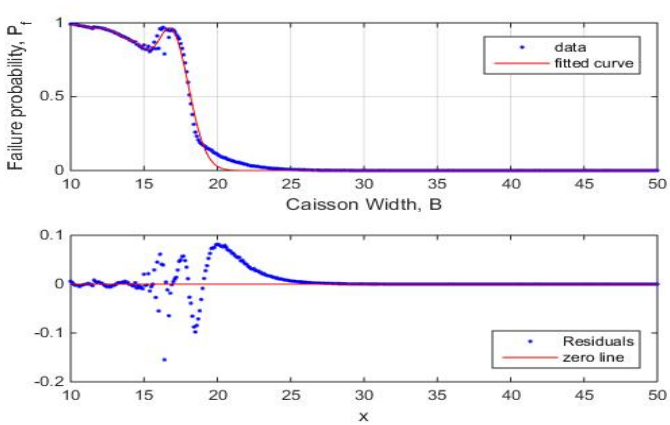

Figure 3.17 Fitted curve when both failures are dominant

Two problems were found when the entire range was used for curve fitting. First, as shown in Figure 3.16, when the tilting failure is dominant, there are some points where the failure probability is bigger than 1. Second, as shown in Figure 3.17, when both the sliding failure and tilting failure are dominant, the maximum discrepancy of failure probability between actual value and function value is about 0.1. Therefore, when we use the data in entire range, the function cannot represent the actual data and other method is needed. Additionally, the value of RMSE was 0.0066 when sliding failure is dominant, 0.0189 when tilting failure is dominant, and 0.0245 when both failures are dominant.

(2) Curve fitting obtained by using the data of failure probability between 0.001 and 0.5

Figure 3.18 ~ 3.20 shows the fitted-curve for the same cases as above. Figure 3.18 shows the fitted curve when sliding failure is dominant, Figure 3.19 shows the fitted curve when tilting failure is dominant, and Figure 3.20 shows the fitted curve when both failures are dominant.

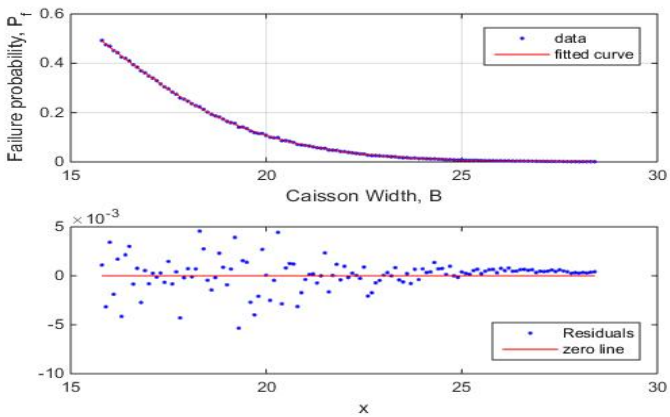

Figure 3.18 Fitted curve determined by using the data of failure probability between 0.001 and 0.5 when sliding failure is dominant

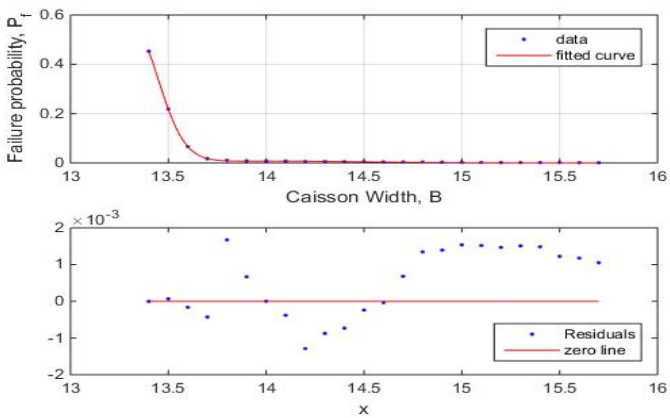

Figure 3.19 Fitted curve when tilting failure is dominant

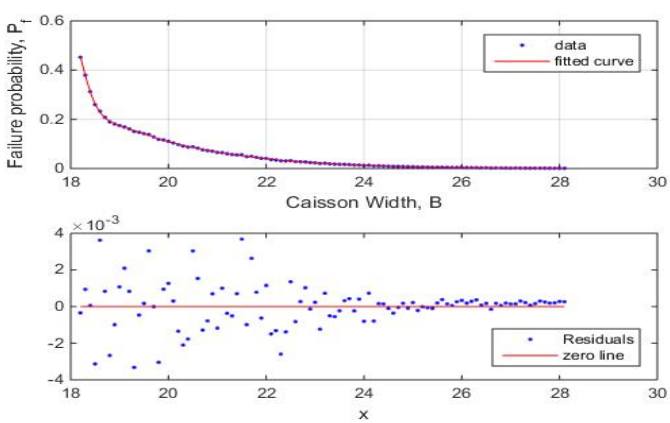

Figure 3.20 Fitted curve when both failures are dominant

If the width range is reduced, the curve fitting problems that occurred in the entire width range disappeared. In other words, the failure probability is always less than one for all cases and there is no big discrepancy between actual value and function value as shown in the residual diagram in Figure 3.18 ~ 3.20. Therefore, the fitted curve in a certain width range can well represent the actual data. The value of RMSE is also reduced. When sliding failure is dominant, the RMSE is 0.0016. When tilting failure is dominant, the RMSE is 0.0016, and when both failures are dominant, the RMSE is 0.0013. When comparing RMSE in certain width range with RMSE in entire width range, the value of RMSE is reduced to about 1/10 times ~ 1/40 times. Therefore, curve fitting in certain width range (failure probability: 0.001 ~ 0.5) will be used in the remaining of the research.

3.3.2 Selection of the Number of Gaussian Functions

The second concern is the number of Gaussian Functions. The number of parameters is three for one Gaussian function. Curve fitting was performed while increasing the number of Gaussian functions and the optimum number of Gaussian functions were determined which can well represent the actual data.

Figure 3.21 shows the fitted curve when using five Gaussian functions. Overfitting occurs when five Gaussian functions are used, due to too many parameters relative to the number of observations. In order to avoid this overfitting problem, the number of parameters must be reduced, therefore, the number of Gaussian functions increases up to 4.

Figure 3.22 and 3.23 show the fitted curve when using 3 and 4 Gaussian functions, respectively. The shape of fitted-curve is quite similar and the RMSE is

also similar. When using 3 Gaussian functions, RMSE is 0.0014, and when using 4 Gaussian functions, RMSE is 0.0013. Although the difference is small between the results of three or four Gaussian functions, the summation of four Gaussian functions will be used in further research. It's because it has smaller RMSE and the upper and lower residuals are smaller than those in the summation of 3 Gaussian functions.

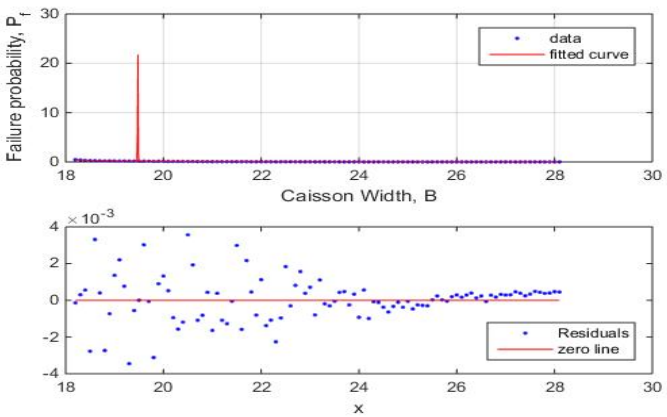

Figure 3.21 Fitted curve when using 5 Gaussian functions

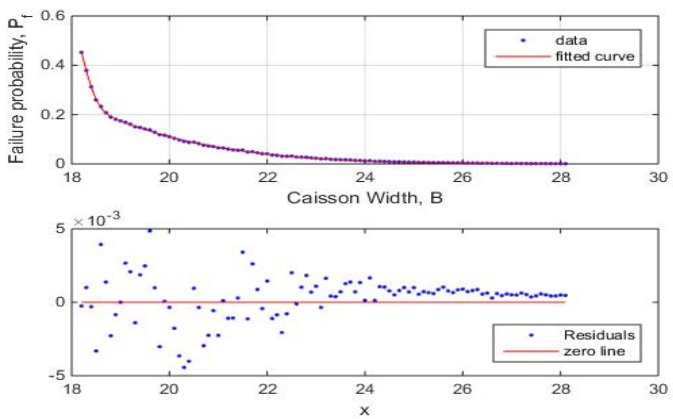

Figure 3.22 Fitted curve when using 3 Gaussian functions

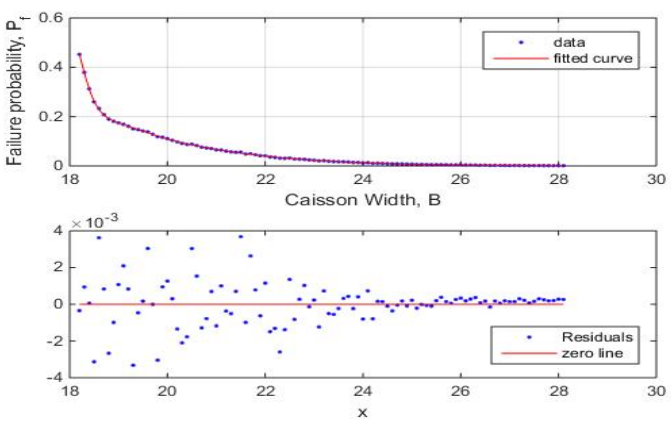

Figure 3.23 Fitted curve when using 4 Gaussian functions

3.3.3 Application of Summation of 4 Gaussian Functions

The summation of 4 Gaussian functions was applied to the data of failure probability between 0.001 and 0.5, and the parameters of the Gaussian functions were obtained by the nonlinear least squares method. Above mentioned earlier, the number of total design cases is 13 and each case was repeated five times. All the results are given in Appendix B. Here, 2 cases (one for Goda's fictitious composite breakwater and another for Shibushi breakwater) are explained

(1) Goda's fictitious composite breakwater

Figure 3.24 shows the fitted curve related to the caisson width and failure probability for Goda's fictitious composite breakwater by using the summation of 4 Gaussian functions in certain width range. The upper part in Figure 3.24 represents the fitted curve and lower part represents the residual diagram. R-square is almost one and root-mean-square-error (rmse) is almost zero. The curve can be expressed as the summation of 4 Gaussian functions as follows:

$$P_f(B) = \sum_{i=1}^{4} a_i e^{-\left(\frac{B-c_i}{b_i}\right)^2}$$

	$i=1$	$i=2$	$i=3$	$i=4$
a_i	0.022	0.008	0.004	1.232
b_i	-1.672	-1.495	-1.306	-3.545
c_i	0.011	0.069	0.074	1.908

(2) Shibushi breakwater

Figure 3.25 shows the fitted curve related to the caisson width and failure probability at section 7 of Shibushi breakwater by using the summation of 4 Gaussian functions in certain width range. R-square is also almost one and root-mean-square-error (rmse) is almost zero. The curve can be expressed as the summation of 4 Gaussian functions as follows:

$$P_f(B) = \sum_{i=1}^{4} a_i e^{-\left(\frac{B-c_i}{b_i}\right)^2}$$

	$i=1$	$i=2$	$i=3$	$i=4$
a_i	0.516	-0.003	0.988	0.137
b_i	-1.844	-0.937	-5.065	-2.419
c_i	0.0140	0.321	2.583	1.266

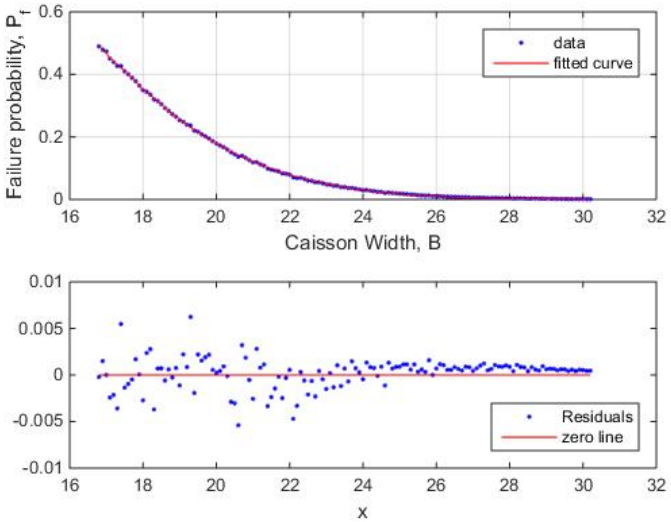

Figure 3.24 Fitted curve and residual diagram at Goda's breakwater

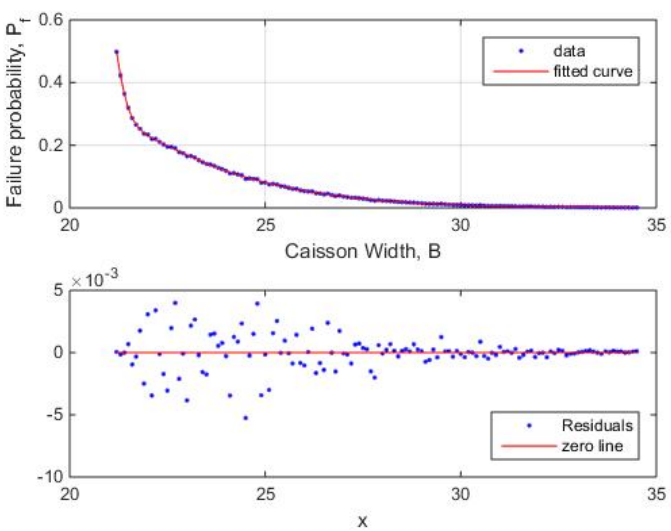

Figure 3.25 Fitted curve and residual diagram at section 7 of Shibushi breakwater

CHAPTER 4. Reliability Based Design Optimization

In this chapter, the reliability based design optimization is performed by using the failure probability function against the caisson width. The objective function is the expected total lifetime cost function suggested by Lee (2002) and the constraint is the caisson width.

To express the expected total lifetime cost function as a function of caisson width, the initial conditions such as expected initial construction cost and failure probability by deterministic design method have to be expressed as a function of the caisson width. Expected initial construction cost can be expressed as a function of the caisson width by multiplying the costs by volume of materials like concrete, gravel, sand. The failure probability using deterministic design method is also required and it can be obtained from the FORM approximation.

After expressing the expected total lifetime cost function as a function of the caisson width, the expected total lifetime cost function against the caisson width was applied to the 13 design cases of the research. The optimal width and minimal expected total lifetime cost was obtained from the harmony search algorithm. Overall safety factors from the reliability based design optimization were presented to use the result of reliability design easily.

4.1 Setting Initial Condition

The expected total lifetime cost function which is the objective function of the research can be expressed as in equation (2.40). Although the failure probability was expressed as a function of caisson width, other initial condition also can be expressed as a function of caisson width to express the objective function as a function of caisson width. Table 4.1 shows the initial condition value of the expected total lifetime cost function.

Table 4.1. Initial condition value of expected total lifetime cost function

Initial Condition	Definition	Value
C_0	Initial construction cost unrelated to the width of vertical caisson	$0.35E[C_I(B)]$
C	Increment of construction cost to enforce the stability of structure	$\frac{0.65E[C_I(B)]}{\ln {}^*P_a(B)}$
$EQCF$	Expected damage cost when $t=0$	$0.7E[C_I(B)]$
i	Net annual discount rate	0.08
T_R	Serviced time. (year)	50

${}^*P_a(B)$: Failure probability of deterministically designed caisson

As shown in Table 4.1, various initial conditions are the function of initial construction cost, and the initial construction cost must be expressed as a function of caisson width for optimization later. Additionally, the failure probability of deterministically designed caisson is required. First, how to express the initial construction cost as a function of caisson width will be explained and then the failure probability of deterministically designed caisson will be calculated.

4.1.1 Expected Initial Construction Cost

Goda's fictitious composite breakwater and Shibushi breakwater are composed of caisson, rubble mound, and foot protection. Those are constructed by using sand, gravel, and concrete. Therefore, in order to calculate the initial construction cost, the price of materials like sand, gravel, and concrete is needed. Table 4.2 shows the price of materials.

Table 4.2 Price of materials

	Sand	Gravel	Concrete
Price	20 \$ / m^3	70 \$ / m^3	250 \$ / m^3

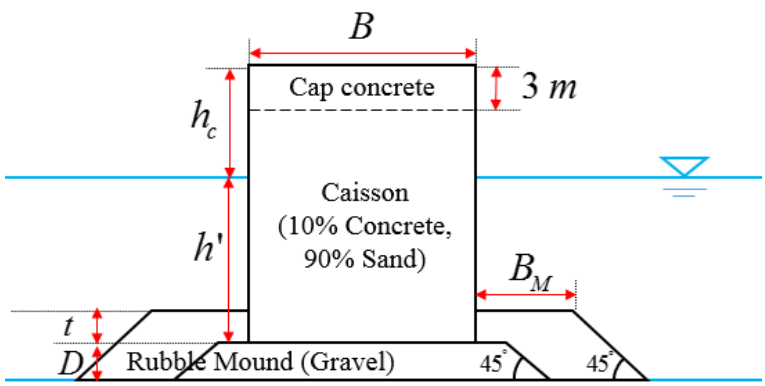

Figure 4.1 Components of breakwater in the research

Figure 4.1 shows the components of the breakwater in the research. Concrete is used for cap concrete, 10% concrete and 90% sand are used for caisson, and gravel is used for rubble mound and foot protection. Based on the components as above, the volumes for materials can be expressed as the equations below:

(1) Concrete: $3B + \frac{1}{10} \times (h_c + h' - 3)B = \left(3 + \frac{(h_c + h' - 3)}{10} \right) B$

(2) Gravel: $\left(4B_M + 2B + 2(D+t) \right) \times \frac{D+t}{2} - (D-t)B = 2tB + (D+t)^2 + 2B_M(D+t)$

(3) Sand: $\frac{9}{10} \times (h_c + h' - 3)B = \frac{9(h_c + h' - 3)}{10} B$

As shown in the above equations, the volume of materials are expressed as a function of caisson width. Now, the expected initial construction cost is expressed as a function of caisson width by multiplying these volume by the price shown in Table 4.2, like the equation below:

$$
\begin{aligned}
&E[C_I(B)] \\
&= 250\left(3 + \frac{(h_c + h' - 3)}{10} \right) B + 70\left(2tB + (D+t)^2 + 2B_M(D+t) \right) + 20\left(\frac{9(h_c + h' - 3)}{10} B \right) \\
&= \left(750 + 43(h_c + h' - 3) + 140t \right) B + 70\left((D+t)^2 + 2B_M(D+t) \right)
\end{aligned}
$$

4.1.2 Failure Probability of Deterministically Designed Caisson

In the deterministic design method, the safety factor for sliding failure of caisson breakwater is 1.5. However, there is no previous research about the safety factor for tilting failure. Therefore, the safety factor for tilting failure was assumed to be the same as that for sliding failure, i.e. 1.5. First, caisson width is determined such that the safety factor becomes 1.5 and then the failure probability of deterministically designed caisson can be calculated by substituting caisson width into the summation of 4 Gaussian functions which was obtained the from FORM approximation.

4.2 Expected Total Lifetime Cost

The expected total lifetime cost can be expressed as function of failure probability.

$$E[C_T(B)] = C_0 - C\ln(P_f(B)) + (EQCF)(P_f(B))\frac{1-e^{-iT_R}}{i}$$

Using the function obtained from FORM approximation, the expected total lifetime cost can be rewritten as

$$E[C_T(B)] = C_0 - C\ln(\sum_{i=1}^{4} a_i e^{-\left(\frac{B-c_i}{b_i}\right)^2}) + (EQCF)(\sum_{i=1}^{4} a_i e^{-\left(\frac{B-c_i}{b_i}\right)^2})\frac{1-e^{-iT_R}}{i}$$

By substituting the initial condition against caisson width into the above equation, the expected total lifetime cost function is changed into the function of caisson width and it can be expressed as the equation below:

$$E[C_T(B)]$$
$$= 0.35E[C_I(B)] - \frac{0.65E[C_I(B)]}{\ln P_a(B)}\ln(\sum_{i=1}^{4} a_i e^{-\left(\frac{B-c_i}{b_i}\right)^2}) + 0.7E[C_I(B)](\sum_{i=1}^{4} a_i e^{-\left(\frac{B-c_i}{b_i}\right)^2})\frac{1-e^{-iT_R}}{i}$$

where $E[C_I(B)]$ is the initial construction cost against caisson width which was obtained from section 4.1.1, and $P_a(B)$ is the failure probability of deterministically designed caisson which was obtained from section 4.1.2.

The expected total lifetime cost function against caisson width was applied to the 13 design cases of the research. For the consistency of the research, the same breakwater types and wave conditions as section 3.1.2 were used here.

(1) Goda's fictitious composite breakwater

Figure 4.2 shows the initial cost, expected cost of failure, and the expected total lifetime cost of Goda's fictitious composite breakwater. As the caisson width increases, initial construction cost increases and the expected cost of failure decreases. On the other hand, the expected total lifetime cost has minimal cost in a certain caisson width as shown in Figure 4.2. The optimal width is about 24 m and will be obtained later by performing the optimization.

(2) Shibushi breakwater

Figure 4.3 shows the initial cost, expected cost of failure, and the expected total lifetime cost at section 2 of Shibushi breakwater when Typhoon 1 was applied. The overall shape of function is similar to the shape of function at Goda's fictitious composite breakwater, but the optimal width and the minimal expected total lifetime cost slightly increased. Considering that the caisson height of Shibushi breakwater is larger than that of Goda's fictitious composite breakwater and the significant wave height at Shibushi breakwater is higher than that at Goda's fictitious composite breakwater, this result looks reasonable.

Figure 4.4 shows the initial cost, expected cost of failure, and the expected total lifetime cost at section 2 of Shibushi breakwater when Typhoon 3 was applied. Considering that the significant wave height of Typhoon 3 is higher than that of Typhoon 1, the results that optimal width and the minimal expected total lifetime cost increase also look reasonable.

Figure 4.5 shows the initial cost, expected cost of failure, and the expected total lifetime cost at section 7 of Shibushi breakwater when Typhoon 1 was applied. As shown in Figure 4.5, the optimal width is similar to the optimal width at section 2 of Shibushi breakwater when Typhoon 1 was applied. But, the minimal expected total lifetime cost is higher. Recalling that the big difference between the two sections is the thickness of rubble mound, the optimal width is not affected by the thickness of rubble mound, and the minimal expected total lifetime cost increase when the thickness of rubble mound increases.

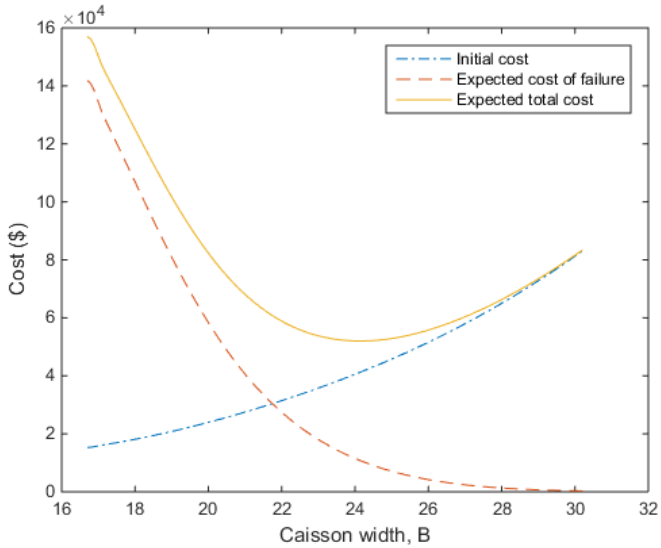

Figure 4.2 Initial cost, expected cost of failure, and expected total lifetime cost at Goda's fictitious composite breakwater

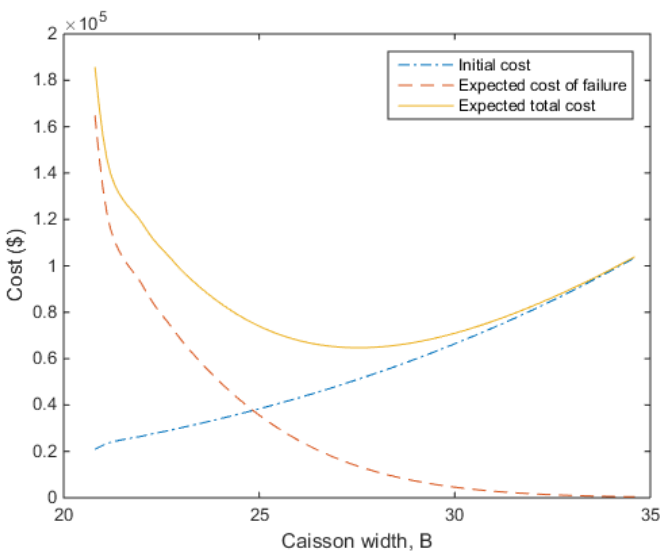

Figure 4.3 Initial cost, expected cost of failure, and expected total lifetime cost at

section 2 of Shibushi breakwater when Typhoon 1 was applied.

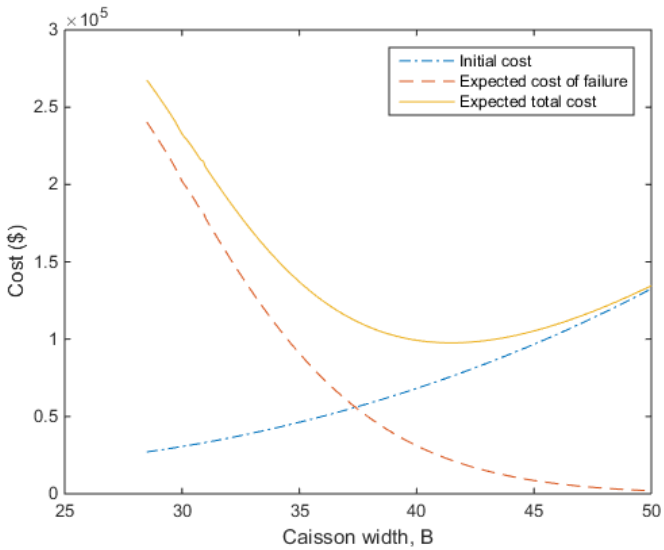

Figure 4.4 Initial cost, expected cost of failure, and expected total lifetime cost at section 2 of Shibushi breakwater when Typhoon 3 was applied.

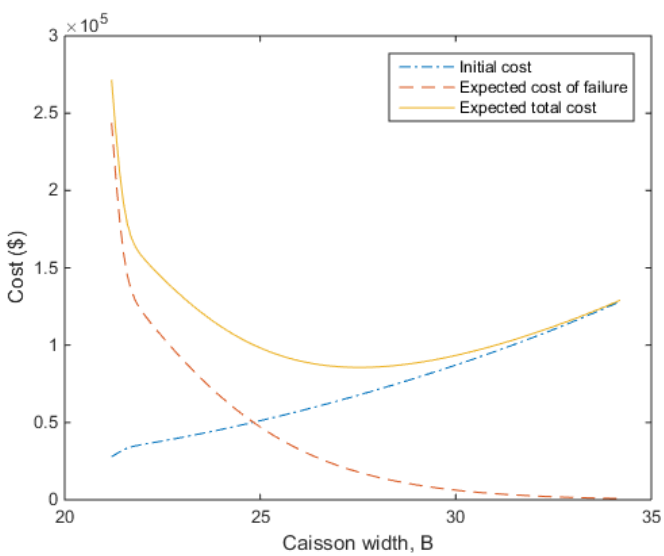

Figure 4.5 Initial cost, expected cost of failure, and expected total lifetime cost at section 7 of Shibushi breakwater when Typhoon 1 was applied.

4.3 Optimal Width Determined by Harmony Search Algorithm

When the objective function is complex, it is easier to use the optimization method like harmony search algorithm than to use a direct differential method. The objective function is the expected total lifetime cost and the constraint is that the caisson width is greater than zero. Therefore, the optimization problem can be expressed as

$$\begin{aligned} &\min \ E[C_T(B)] \\ &\text{s.t} \quad B > 0 \end{aligned}$$

The parameters are set as follows: Harmony Memory Size (HMS) is 5 because it usually 5 times the number of variable, and the caisson width is the only variable in this research. HMCR is 0.95 and PAR is 0.1 in this research, which is the typical value in most applications. The optimal width and minimal expected total lifetime cost were calculated by using harmony search algorithm and its parameters. All the results are presented in the Appendix C.

(1) Goda's fictitious composite breakwater

Figure 4.6 shows the functions of Figure 4.2, and additionally shows the optimal width and the minimal expected total lifetime cost obtained by harmony search. Optimization process by using harmony search was repeated 5 times and the

optimal width and the minimal expected total lifetime cost were calculated respectively. When the optimal width was calculated through optimization, overall safety factor can be calculated. Optimal width, minimal expected total lifetime cost, and overall safety factor according to the trial were shown in Table 4.3.

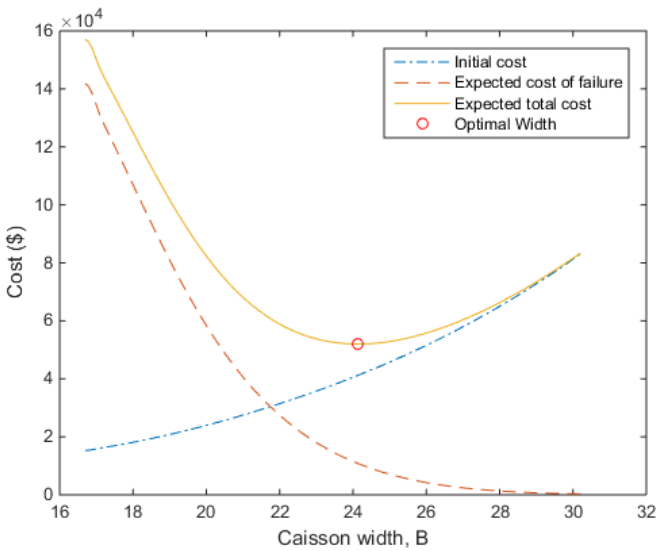

Figure 4.6 Optimal width and minimal expected total lifetime cost at Goda's fictitious composite breakwater

Table 4.3 Optimal width, minimal expected total lifetime cost and overall safety factor at Goda's fictitious composite breakwater

Trial	1	2	3	4	5
Optimal Width	24.2 m	24.1 m	24.1 m	24.1 m	24.1 m
Minimal Cost	5.23×10^4 $	5.21×10^4 $	5.26×10^4 $	5.23×10^4 $	5.22×10^4 $
Overall Safety Factor	1.45	1.44	1.44	1.44	1.44

The optimal width obtained by Harmony Search was about 24.1 m, and the minimal expected total lifetime cost is about 52,300 $. Overall safety factor was about 1.44. If using this overall safety factor when breakwater caisson designs, the expected total lifetime cost would be minimized.

(2) Shibushi breakwater

Figure 4.7 shows the functions of Figure 4.3 (breakwater type: Section 2, wave condition: Typhoon 1), and additionally shows the optimal width and the minimal expected total lifetime cost obtained by Harmony Search. Optimal width, minimal expected total lifetime cost, and overall safety factor according to the trial were shown in Table 4.4. The optimal width obtained by Harmony Search was about 27.4 m, and the minimal expected total lifetime cost is about 64,400 $. Overall safety factor was about 1.44.

Figure 4.8 shows the functions of Figure 4.4 (breakwater type: Section 2, wave condition: Typhoon 3), and additionally shows the optimal width and the minimal expected total lifetime cost obtained by Harmony Search. Optimal width, minimal expected total lifetime cost, and overall safety factor according to the trial were shown in Table 4.5. The optimal width obtained by Harmony Search was about

41.5 m, and the minimal expected total lifetime cost is about 98,000 $. Overall safety factor was about 1.46.

Figure 4.9 shows the functions of Figure 4.5 (breakwater type: Section 2, wave condition: Typhoon 3), and additionally shows the optimal width and the minimal expected total lifetime cost obtained by Harmony Search. Optimal width, minimal expected total lifetime cost, and overall safety factor according to the trial were shown in Table 4.6. The optimal width obtained by Harmony Search was about 27.6 m, and the minimal expected total lifetime cost is about 86,000 $. Overall safety factor was about 1.45.

The value of overall safety factor is quite similar regardless of design case in the research, and the value was about 1.44 ~ 1.47. However, overall safety factor must have more conservative value because the number of design case of the study is too small. Therefore, the overall safety factor which consider sliding and tilting failure was 1.5 in the research.

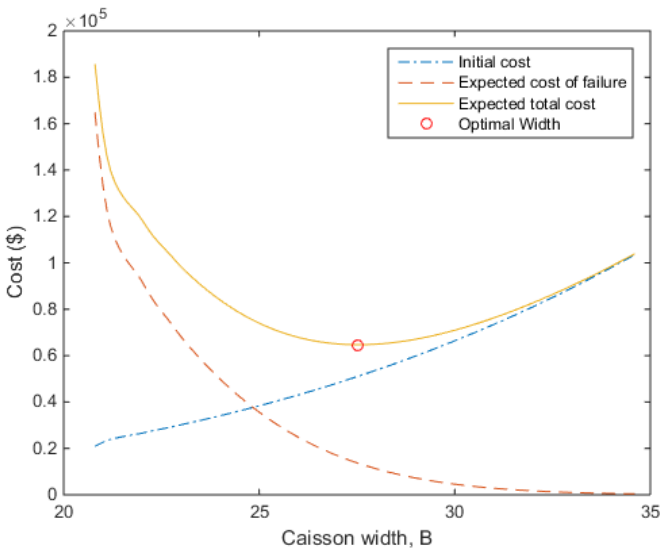

Figure 4.7 Expected total lifetime cost at section 2 of Shibushi breakwater when Typhoon 1 condition was applied

Table 4.4 Optimal width, minimal expected total lifetime cost and overall safety factor at section 2 of Shibushi breakwater (Typhoon 1)

Trial	1	2	3	4	5
Optimal Width	27.4 m	27.5 m	27.4 m	27.5 m	27.4 m
Minimal Cost	6.44×10^4 $	6.42×10^4 $	6.38×10^4 $	6.49×10^4 $	6.36×10^4 $
Overall Safety Factor	1.43	1.44	1.44	1.44	1.43

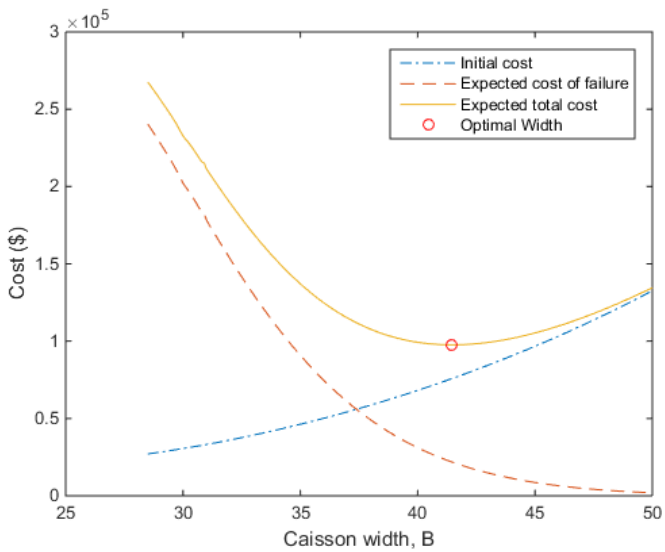

Figure 4.8 Expected total lifetime cost at section 2 of Shibushi breakwater when Typhoon 3 condition was applied

Table 4.5 Optimal width, minimal expected total lifetime cost and overall safety factor at section 2 of Shibushi breakwater (Typhoon 3)

Trial	1	2	3	4	5
Optimal Width	41.6 m	41.5 m	41.4 m	41.5 m	41.3 m
Minimal Cost	9.87×10^4 $	9.77×10^4 $	9.82×10^4 $	9.81×10^4 $	9.75×10^4 $
Overall Safety Factor	1.47	1.46	1.46	1.46	1.46

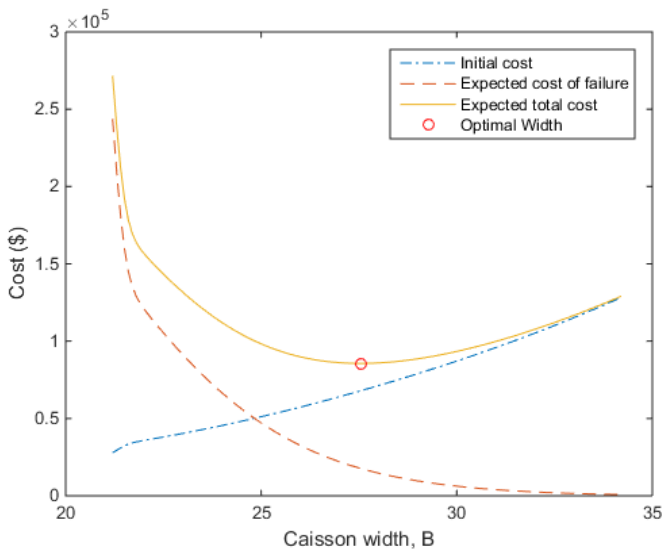

Figure 4.9 Expected total lifetime cost at section 7 of Shibushi breakwater when Typhoon 1 condition was applied

Table 4.6 Optimal width, minimal expected total lifetime cost and overall safety factor at section 7 of Shibushi breakwater (Typhoon 1)

Trial	1	2	3	4	5
Optimal Width	27.6 m	27.6 m	27.6 m	27.7 m	27.8 m
Minimal Cost	8.60×10^4 $	8.62×10^4 $	8.52×10^4 $	8.53×10^4 $	8.63×10^4 $
Overall Safety Factor	1.45	1.44	1.45	1.45	1.45

CHAPTER 5. CONCLUSIONS

5.1 Research Summary

In this research, the optimal width of vertical caisson and the minimal expected total lifetime cost were calculated by using system reliability and Reliability Based Design Optimization. Five different breakwater cross-sections, one for Goda's fictitious composite breakwater and four for different sections of Shibushi breakwater, and four different wave conditions were used in the research.

First Order Reliability Method approximation was used to calculate the failure probability against the caisson width of the breakwater caisson. Summation of 4 Gaussian functions was used to represent the relation between caisson width and failure probability and the parameters of the function were estimated by non-linear least squares.

Next, reliability based design optimization was used to determine the optimal width of vertical caisson and the minimal expected total lifetime cost. By using the function of failure probability in terms of caisson width obtained from FORM approximation and initial conditions, the expected total lifetime cost function was formulated as a function of caisson width which is the design variable in the

research. Optimization process was performed by using harmony search algorithm.

The optimal width of vertical caisson and minimal expected total lifetime cost had a different value according to wave condition and breakwater type. The optimal width at Goda's breakwater is about 24.1 m, and the minimal cost is about 52,300 $. On the other hand, the optimal width at Shibushi breakwater had a different value according to the each design case. It's because the wave conditions and the fixed deterministic values of caisson were all different depending on the design cases. In other words, when significant wave height or thickness of rubble mound increased, the expected total lifetime cost increased as well. The overall safety factor was determined 1.5 in the research, irrespective of breakwater types and wave conditions. Engineers who are not familiar with the reliability design can also design the caisson width by using this overall safety factor.

There are several important implications in the research as follows:

(1) This research applied the tilting failure for the first time when designing the width of breakwater caisson.

(2) This research confirmed that the distance from the design water level to the bottom of the upright section affects the tilting failure, and when the distance increased, the tilting failure became dominant in broad range of caisson width.

(3) This research suggested the summation of 4 Gaussian functions to represent the relation between caisson width and failure probability.

(4) This research applied harmony search algorithm for the first time in Korea when performing optimization process of breakwater construction.

5.2 Research Limitations and Future Study

There are several limitations in this research. If someone designs the optimal width of breakwater caisson as by improving the limitations, the better results would be obtained. The limitations and future study are as below:

1. Random variable generation
   (1) When generating the random variable, it was assumed that the significant wave height follows the normal distribution to apply the FORM approximation easily. However, in reality, significant wave height follows the Weibull distribution rather than normal distribution. It should be considered in the future study.
   (2) When generating the random variable, it was assumed that many material properties such as density and significant wave period have a constant value. However, in reality, they are not constant values and they are also random variables which have uncertainty. Therefore, the uncertainty of more material properties should be considered in the future study.

2. System reliability
   (1) When calculating the failure probability, only two failure modes were considered. However, in reality, many type of failure such as overturning failure and other failures can occur. Therefore, other failure modes must be considered in the future

study.

(2) The FORM approximation was used among different system reliability methods. However, there is a possibility that it can make some errors because of curvature of limit state function. In order to reduce this error, the Importance Sampling which is one of the other system reliability methods can be used and it can obtain the accurate failure probability.

(3) The summation of 4 Gaussian functions was used as a suitable function which can represent the relation between caisson width and failure probability. However, it may be necessary to find the suitable function form in the future. One suggestion is to use Genetic Programing. Genetic Programming can determine the parameters and formula structure. If Genetic Programming will be applied to the future study, the function obtained from Genetic Programming represents the relation between caisson width and failure probability more than this research.

3. Reliability Based Design Optimization

(1) The design variable in this research was only one variable, i.e. the caisson width. However, in reality, the height of caisson, the width of berm, and the thickness of rubble mound must be designed as well. So, these factors must be considered in the future.

(2) The objective function in this research considered the failure probability in terms of caisson width only. In other words, it cannot consider the failure probability if caisson height or other design factors are changed. Therefore, when applying this research to the research which have multiple design variables, it is necessary to find a new objective function.

REFERENCES

Box, G. E., Muller, M. E. (1958). "A note on the generation of random normal deviates." *The annals of mathematical statistics*, Vol. 29(2), pp 610-611.

Burchart, H.F. (1997). "Reliability based design of coastal structures." *Advances in coastal and ocean engineering*, Vol. 3, pp 145-196.

Castillo, C., Minguez, R., Castillo, E., Losada, M. (2006). "An optimal engineering design method with failure rate constraints and sensitivity analysis: Application to composite breakwaters." *Coastal Eng.*, Vol. 53(1), pp 1-25.

CUR-TAW. (1990). "Probabilistic design of flood defenses." *Rep. No. 141*.

Geem, Z.W., Kim, J.H., Loganathan, G.V. (2001). "A new heuristic optimization algorithm: Harmony search." *Simulation,* Vol.76, pp 60-68.

Goda, Y. (2010). *Random seas and design of maritime structures*. 3rd ed., World Scientific, Singapore.

Goda, Y., Takagi, H. (2000). "A reliability design method of caisson breakwaters with optimal wave heights." *Coastal Engineering Journal*, Vol. 42, pp 357-387.

Hussarts, M., Vrijling, J.K., Van Gelder, P., de Looff, H., Blonk, C. (2000). “The probabilistic optimization of revetment on the dikes along Frisian coast.” *Proc. Of Coast. Struc. ’99*, ASCE, pp 325-329.

Hoby, P.M., Sajikumar, N., Sumam, K.S. (2015). “Probabilistic Optimal Design of Rubble-Mound Breakwater.” *J. Waterway, Port, Coastal, Ocean Eng*. Vol. 141(4), 06015002.

Lee, C.W. (2002). "Optimal Design of the Monolithic Vertical Caisson of Composite Breakwaters by the Minimization of Expected Total Lifetime Cost." *KSCE Journal of Civil Engineering*, Vol. 22, pp 819–831.

Mahdavi, M., Fesanghary, M., Damangir, E. (2007). “An improved harmony search algorithm for solving optimization problems.” *Applied mathematics and computation*, Vol. 188(2), pp 1567-1579.

Nikolaidis, E., Ghiocel, D.M., Singhal. S. (2004). *Engineering design reliability handbook*, CRC Press.

Takagi, H., Shibayama, T., Esteban, M. (2007). “An expansion of the reliability design method for caisson-type breakwaters towards deep water using the fourth order approximation of standing waves.” *Proc. Of Asian and Pacific Coasts 2007 (APAC)*, pp. 1723-1735.

Takagi, H., Esteban, M., Shibayama, T. (2008). “Proposed methodology for evaluating the potential failure risk for existing caisson-breakwaters in a storm event using a level Ⅲ reliability-based approach.”

Proc.31st Int. Conf. on Coastal Engineering, ASCE, pp. 3655-3667.

Takagi, H., Kashihara, H., Esteban, M. Shibayama, T. (2011). "Assessment of Future Stability of Breakwaters under Climate Change." *Coastal Engineering Journal*, Vol. 53, pp. 21-39.

Takagi, H., Esteban, M. (2013). "Practical Methods of Estimating Tilting Failure of Caisson Breakwaters using a Monte-Carlo Simulation." *Coastal Engineering Journal*, Vol. 55, pp. 1-22.

Takagi, H., Esteban, M., Shibayama, T. (2015) "Stochastic Design of Caisson Breakwaters: Lessons from Past Failures and Coping with Climate Change." *Handbook of Coastal Disaster Mitigation for Engineers and Planners,* pp. 635-673.

Takayama, T., Suzuki, Y., Kawai, H., Fujisaku, H. (1994). "Approach to probabilistic design for a breakwater. *Report of the port and harbour research institute*, Vol. 30, pp. 35-64.

Takayama, T., Higashira. K. (2002). "Statistical analysis on damage characteristics of breakwaters." *Proc. of Ocean Development Conf.* Vol. 18.

Voortman, H.G., Kujiper, H.K.T., Vrijling, J.K. (1998). "Economic Optimal Design of Vertical Breakwaters." *Coastal Engineering*, Vol. 26.

APPENDIX A – Failure Probability

(1) Goda's fictitious composite breakwater

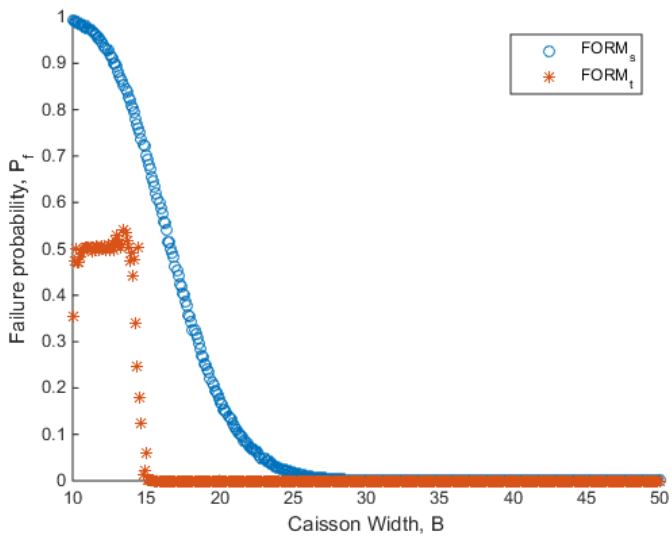

Figure A.1 Sliding and tilting failure probabilities for Goda's fictitious composite breakwater

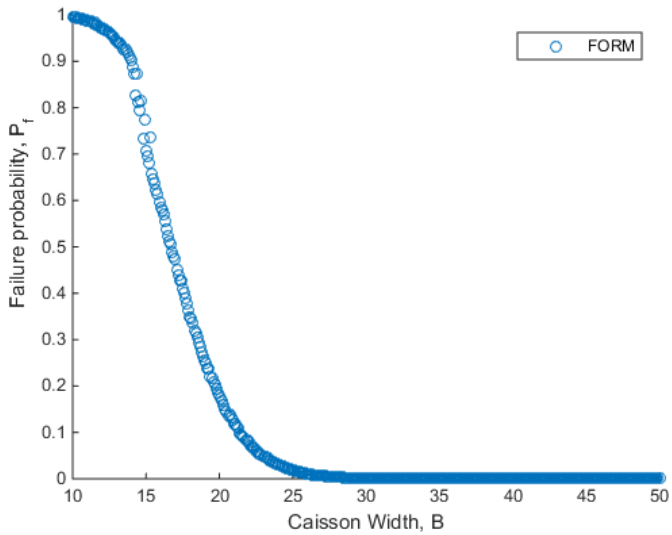

Figure A.2 Final failure probabilities for Goda's fictitious composite breakwater

(2) Section 2 of Shibushi breakwater (Wave Condition: Typhoon 1)

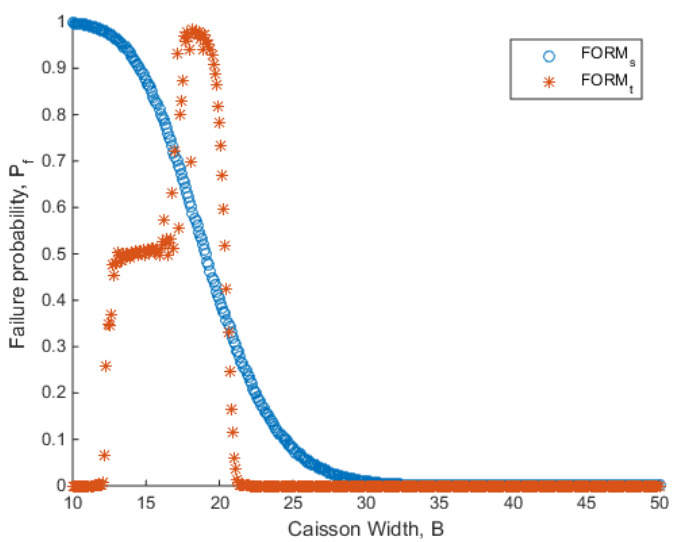

Figure A.3 Sliding and tilting failure probabilities at section 2 of Shibushi breakwater when Typhoon 1 wave condition is used

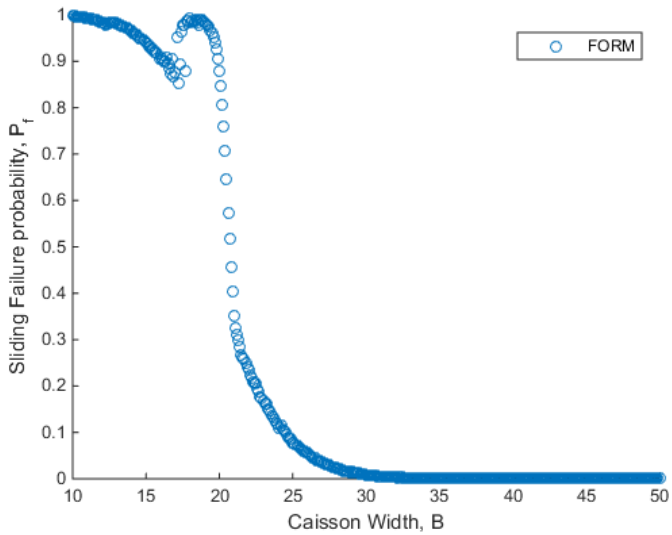

Figure A.4 Final failure probabilities at section 2 of Shibushi breakwater when Typhoon 1 wave condition is used

(3) Section 2 of Shibushi breakwater (Wave Condition: Typhoon 2)

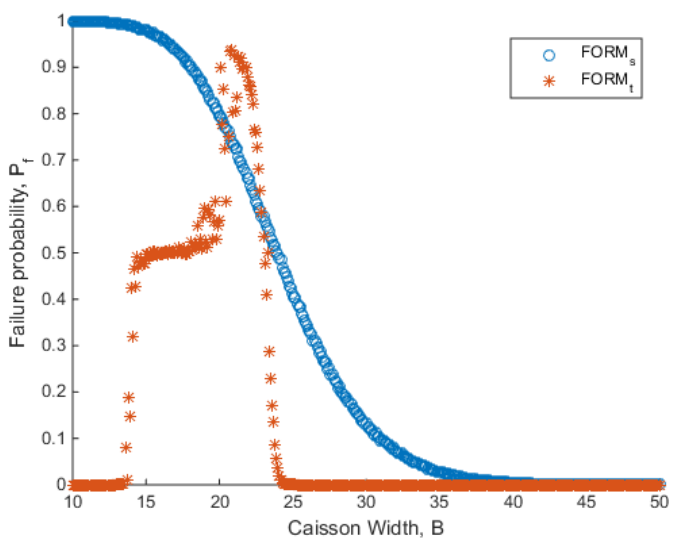

Figure A.5 Sliding and tilting failure probabilities at section 2 of Shibushi breakwater when Typhoon 2 wave condition is used

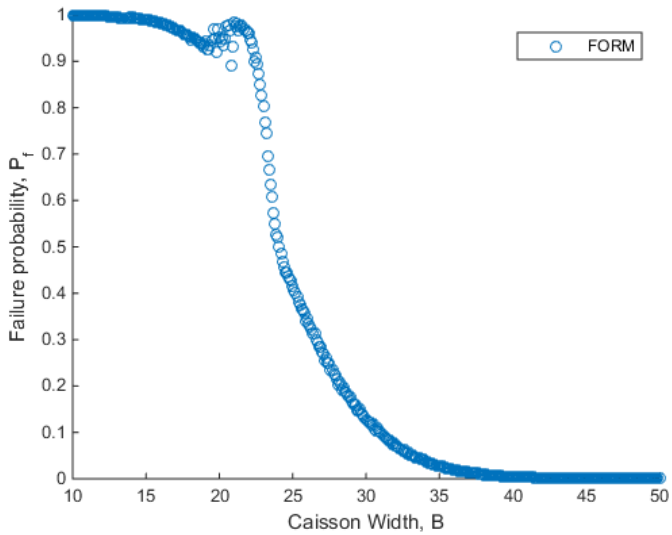

Figure A.6 Final failure probabilities at section 2 of Shibushi breakwater when Typhoon 2 wave condition is used

(4) Section 2 of Shibushi breakwater (Wave Condition: Typhoon 3)

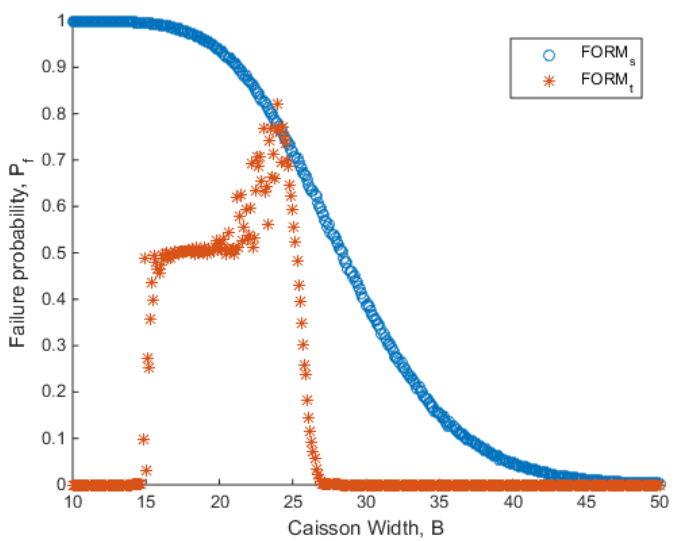

Figure A.7 Sliding and tilting failure probabilities at section 2 of Shibushi breakwater when Typhoon 3 wave condition is used

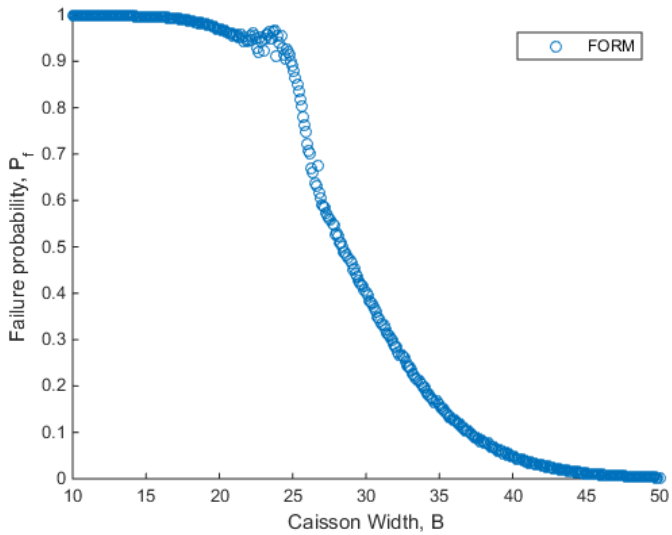

Figure A.8 Final failure probabilities at section 2 of Shibushi breakwater when Typhoon 3 wave condition is used

(5) Section 4 of Shibushi breakwater (Wave Condition: Typhoon 1)

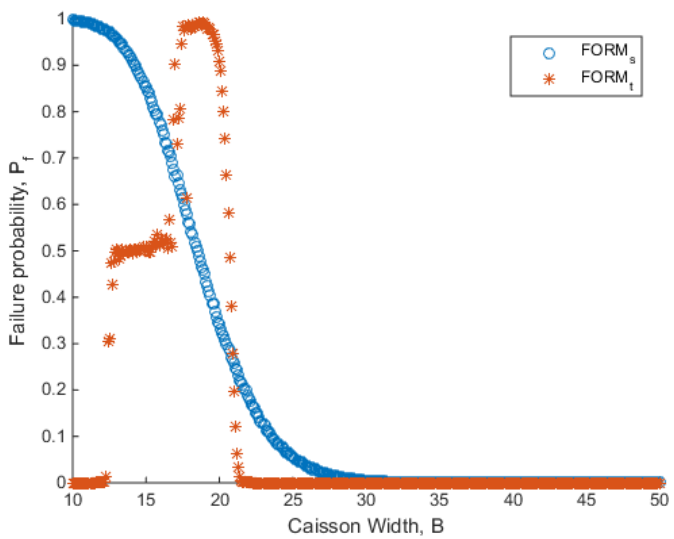

Figure A.9 Sliding and tilting failure probabilities at section 4 of Shibushi breakwater when Typhoon 1 wave condition is used

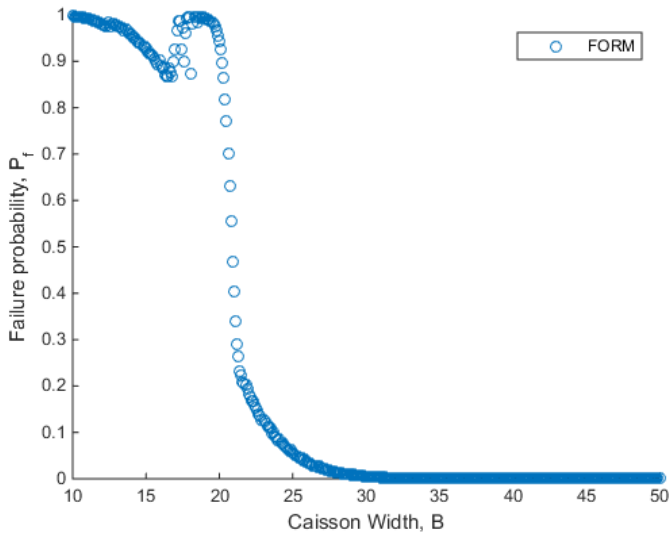

Figure A.10 Final failure probabilities at section 4 of Shibushi breakwater when Typhoon 1 wave condition is used

(6) Section 4 of Shibushi breakwater (Wave Condition: Typhoon 2)

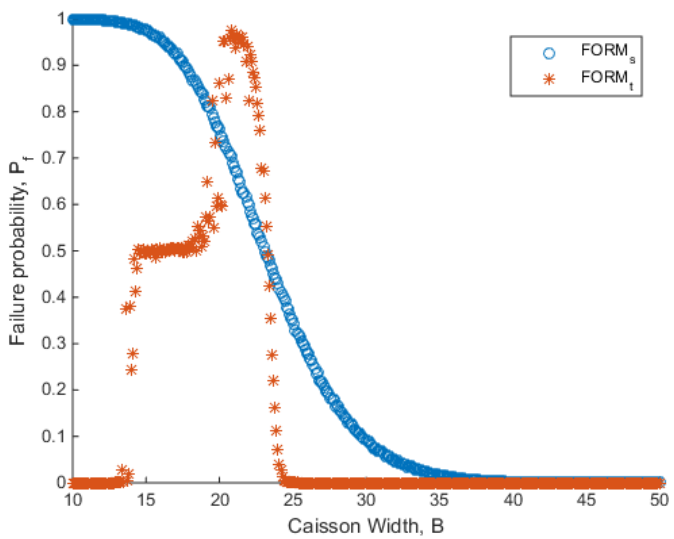

Figure A.11 Sliding and tilting failure probabilities at section 4 of Shibushi breakwater when Typhoon 2 wave condition is used

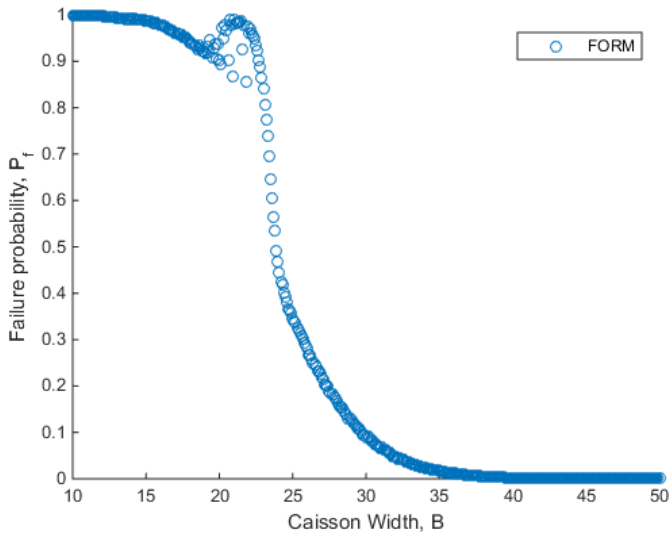

Figure A.12 Final failure probabilities at section 4 of Shibushi breakwater when Typhoon 2 wave condition is used

(7) Section 4 of Shibushi breakwater (Wave Condition: Typhoon 3)

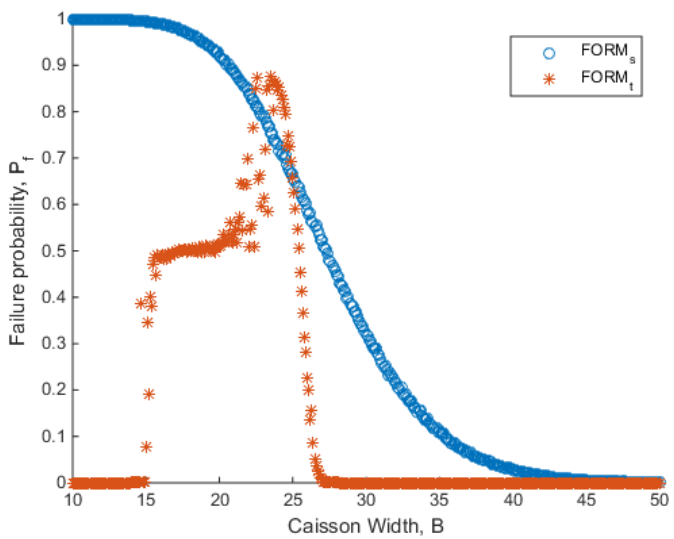

Figure A.13 Sliding and tilting failure probabilities at section 4 of Shibushi breakwater when Typhoon 3 wave condition is used

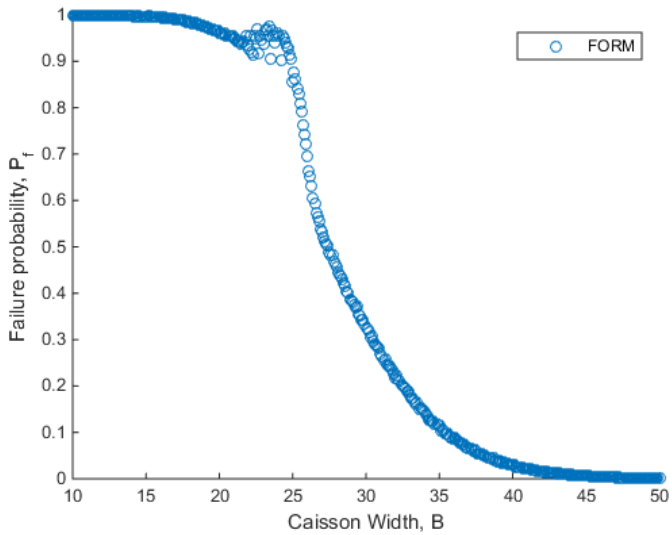

Figure A.14 Final failure probabilities at section 4 of Shibushi breakwater when Typhoon 3 wave condition is used

(8) Section 5 of Shibushi breakwater (Wave Condition: Typhoon 1)

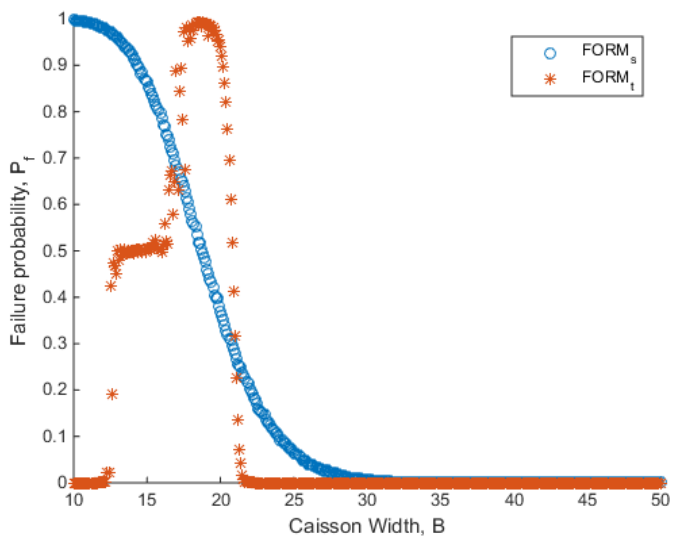

Figure A.15 Sliding and tilting failure probabilities at section 5 of Shibushi breakwater when Typhoon 1 wave condition is used

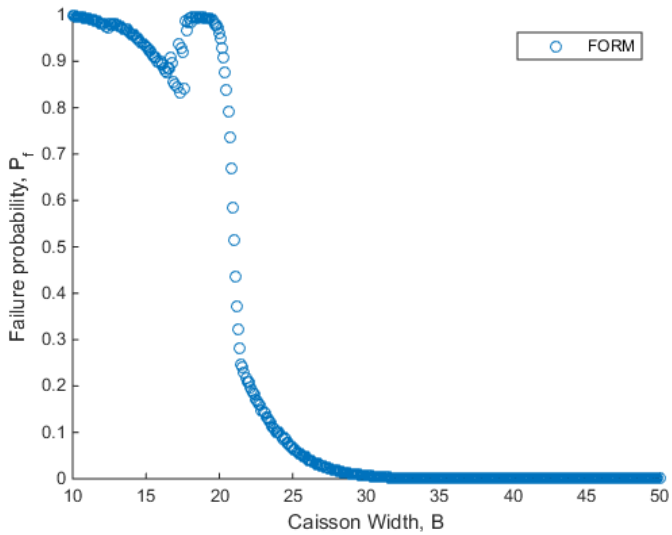

Figure A.16 Final failure probabilities at section 5 of Shibushi breakwater when Typhoon 1 wave condition is used

(9) Section 5 of Shibushi breakwater (Wave Condition: Typhoon 2)

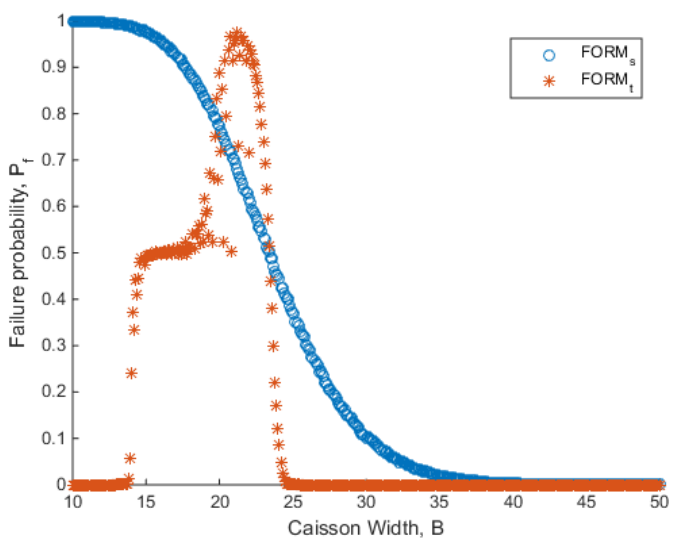

Figure A.17 Sliding and tilting failure probabilities at section 5 of Shibushi breakwater when Typhoon 2 wave condition is used

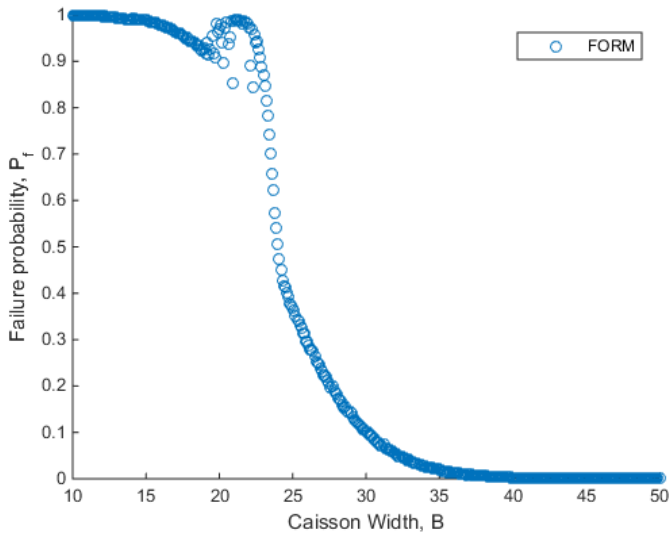

Figure A.18 Final failure probabilities at section 5 of Shibushi breakwater when Typhoon 2 wave condition is used

(10) Section 5 of Shibushi breakwater (Wave Condition: Typhoon 3)

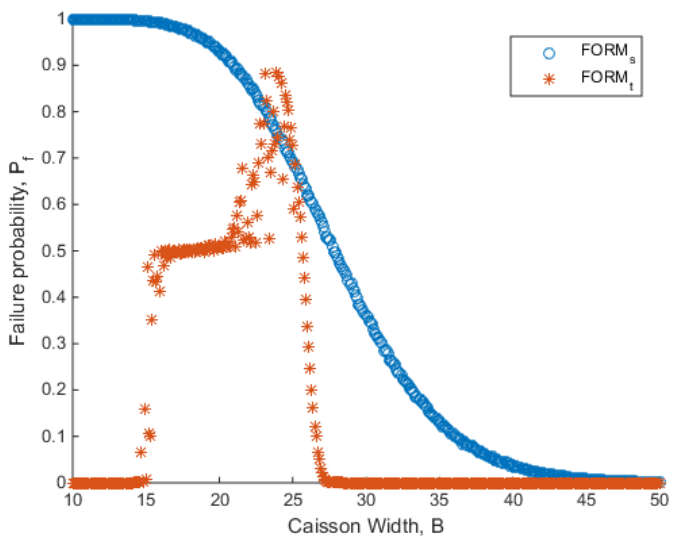

Figure A.19 Sliding and tilting failure probabilities at section 5 of Shibushi breakwater when Typhoon 3 wave condition is used

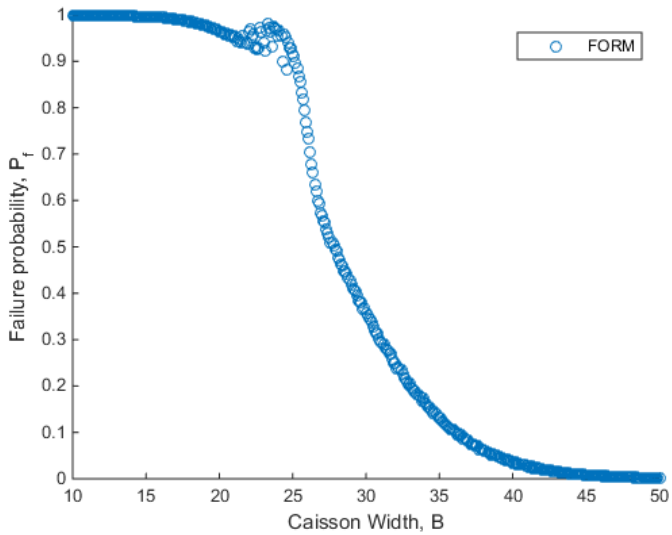

Figure A.20 Final failure probabilities at section 5 of Shibushi breakwater when Typhoon 3 wave condition is used

(11) Section 7 of Shibushi breakwater (Wave Condition: Typhoon 1)

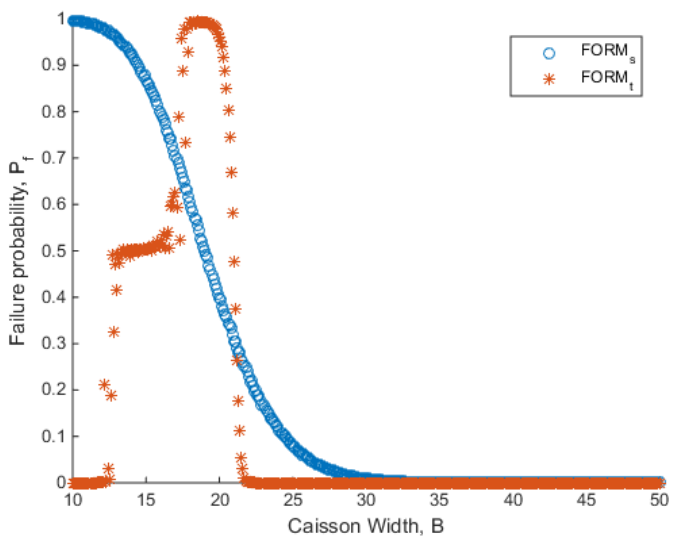

Figure A.21 Sliding and tilting failure probabilities at section 7 of Shibushi breakwater when Typhoon 1 wave condition is used

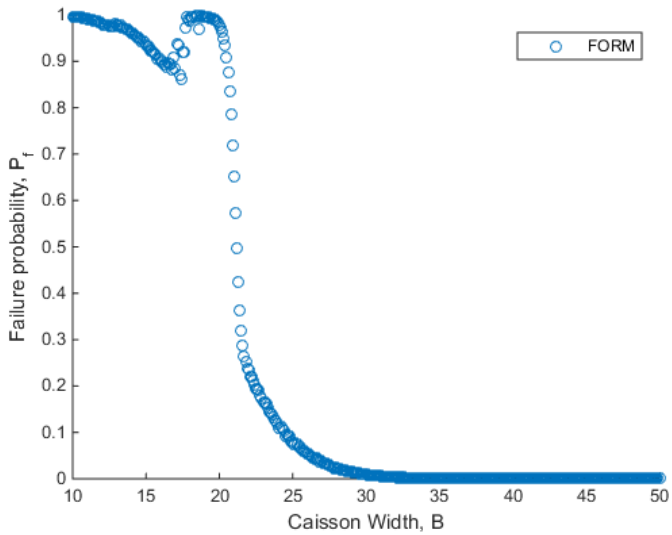

Figure A.22 Final failure probabilities at section 7 of Shibushi breakwater when Typhoon 1 wave condition is used

(12) Section 7 of Shibushi breakwater (Wave Condition: Typhoon 2)

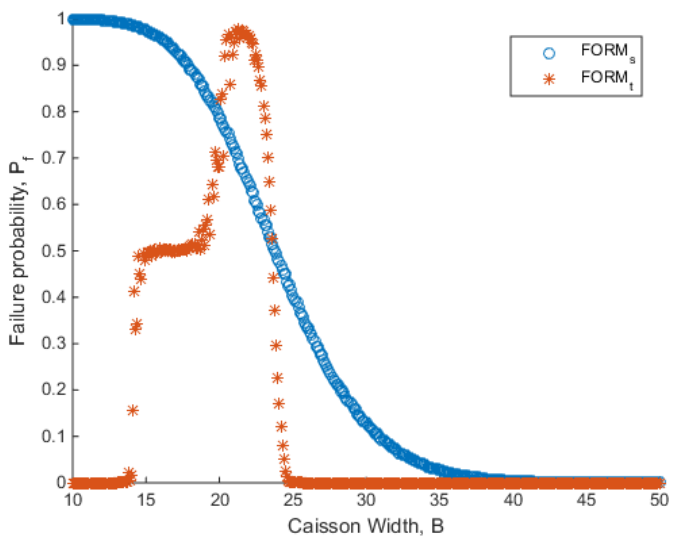

Figure A.23 Sliding and tilting failure probabilities at section 7 of Shibushi breakwater when Typhoon 2 wave condition is used

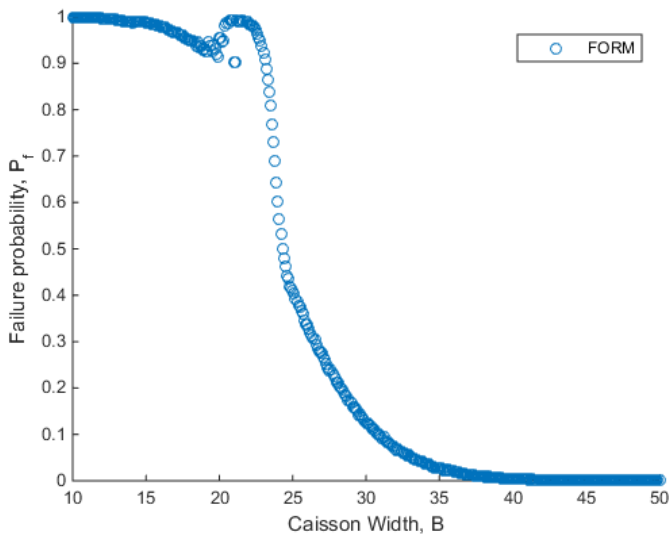

Figure A.24 Final failure probabilities at section 7 of Shibushi breakwater when Typhoon 2 wave condition is used

(13) Section 7 of Shibushi breakwater (Wave Condition: Typhoon 3)

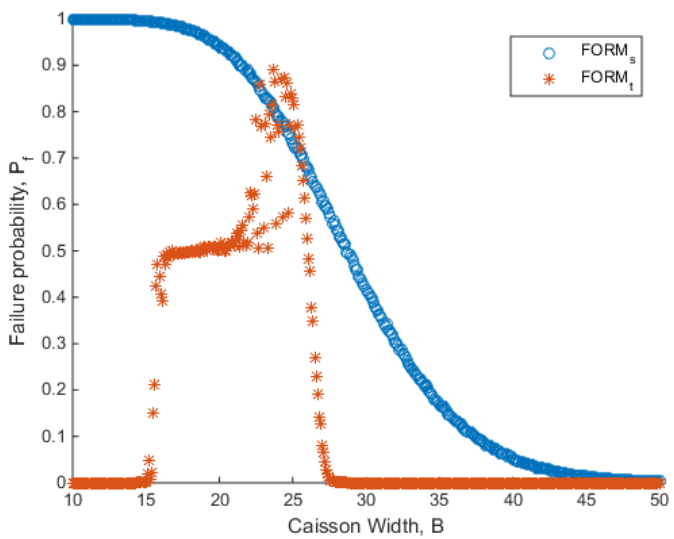

Figure A.25 Sliding and tilting failure probabilities at section 7 of Shibushi breakwater when Typhoon 3 wave condition is used

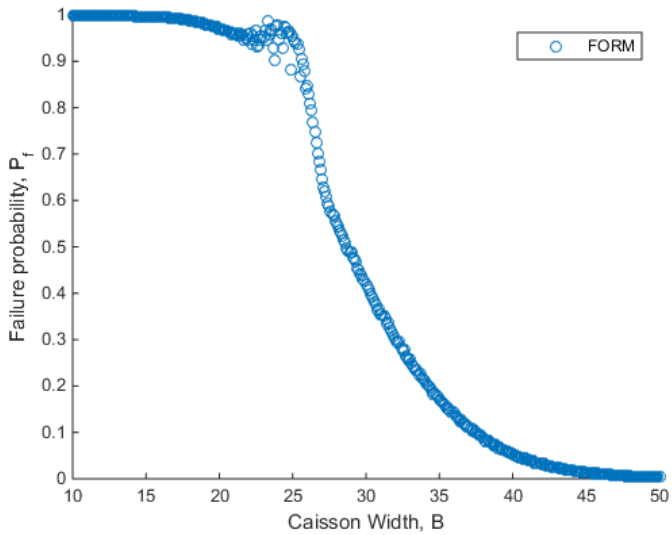

Figure A.26 Final failure probabilities at section 7 of Shibushi breakwater when Typhoon 3 wave condition is used

APPENDIX B – Fitted Curve

(1) Goda's fictitious composite breakwater

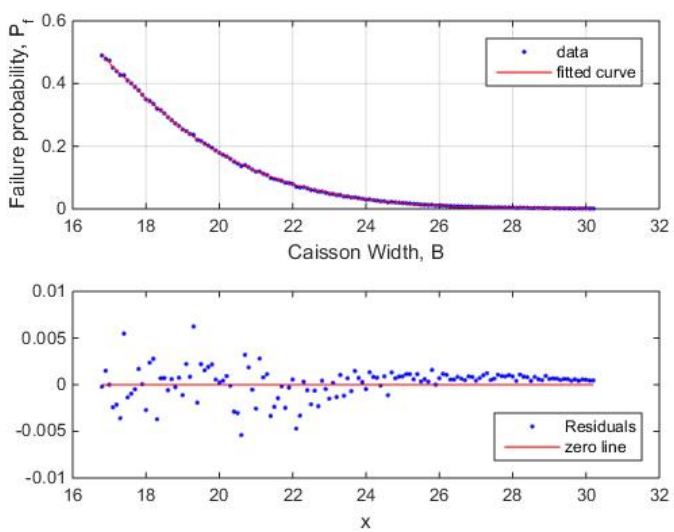

Figure B.1 Fitted curve and residual diagram at Goda's fictitious composite breakwater

Curve can be expressed to summation of 4 Gaussian functions like below equation:

$$P_f(B) = \sum_{i=1}^{4} a_i e^{-\left(\frac{B-c_i}{b_i}\right)^2}$$

	$i=1$	$i=2$	$i=3$	$i=4$
a_i	0.022	0.008	0.004	1.232
b_i	-1.672	-1.495	-1.306	-3.545
c_i	0.011	0.069	0.074	1.908

(2) Section 2 of Shibushi breakwater (Wave Condition: Typhoon 1)

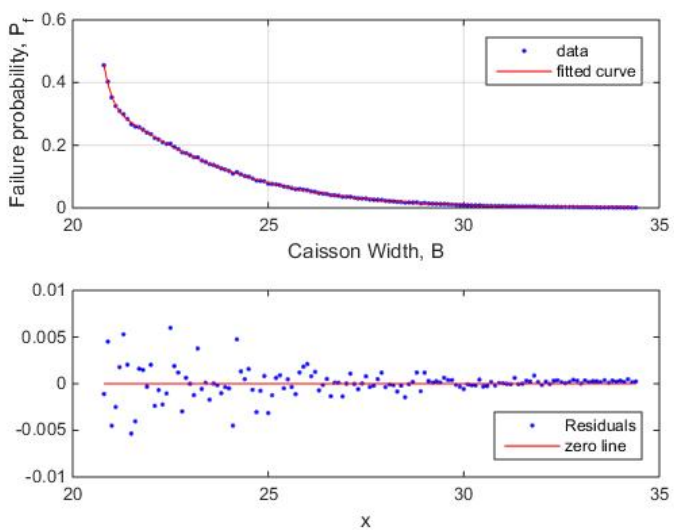

Figure B.2 Fitted curve and residual diagram at section 2 of Shibushi breakwater when Typhoon 1 condition is used

Curve can be expressed to summation of 4 Gaussian functions like below equation:

$$P_f(B) = \sum_{i=1}^{4} a_i e^{-\left(\frac{B-c_i}{b_i}\right)^2}$$

	$i=1$	$i=2$	$i=3$	$i=4$
a_i	0.694	0.013	1.03E+12	0.042
b_i	-1.908	-1.547	-44.88	-1.371
c_i	0.155	0.186	8.022	0.683

(3) Section 2 of Shibushi breakwater (Wave Condition: Typhoon 2)

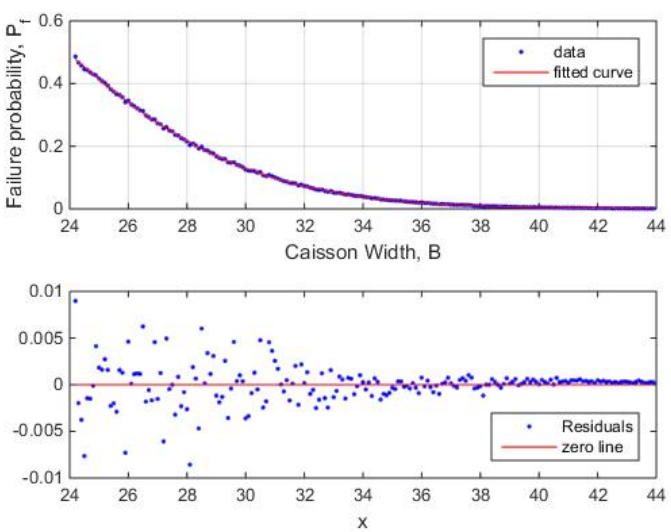

Figure B.3 Fitted curve and residual diagram at section 2 of Shibushi breakwater when Typhoon 2 condition is used

Curve can be expressed to summation of 4 Gaussian functions like below equation:

$$P_f(B) = \sum_{i=1}^{4} a_i e^{-\left(\frac{B-c_i}{b_i}\right)^2}$$

	$i=1$	$i=2$	$i=3$	$i=4$
a_i	0	0.075	0.002	1.031
b_i	-3.66	-2.224	-1.159	-3.591
c_i	0.220	1	0.023	1.974

(4) Section 2 of Shibushi breakwater (Wave Condition: Typhoon 3)

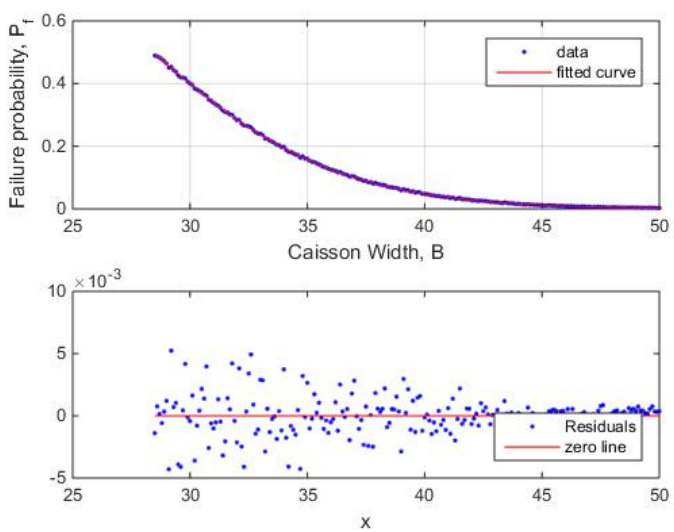

Figure B.4 Fitted curve and residual diagram at section 2 of Shibushi breakwater when Typhoon 3 condition is used

Curve can be expressed to summation of 4 Gaussian functions like below equation:

$$P_f(B) = \sum_{i=1}^{4} a_i e^{-\left(\frac{B-c_i}{b_i}\right)^2}$$

	$i=1$	$i=2$	$i=3$	$i=4$
a_i	0.007	0.003	0.098	0.921
b_i	-1.669	-1.502	-2.173	-3.743
c_i	0.034	0.149	1.106	2.238

(5) Section 4 of Shibushi breakwater (Wave Condition: Typhoon 1)

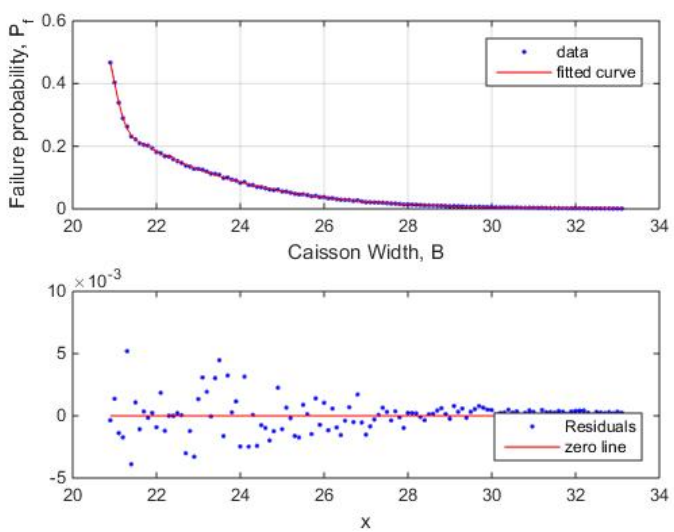

Figure B.5 Fitted curve and residual diagram at section 4 of Shibushi breakwater when Typhoon 1 condition is used

Curve can be expressed to summation of 4 Gaussian functions like below equation:

$$P_f(B) = \sum_{i=1}^{4} a_i e^{-\left(\frac{B-c_i}{b_i}\right)^2}$$

	$i=1$	$i=2$	$i=3$	$i=4$
a_i	0.270	0.007	0.009	2.368
b_i	-1.771	-1.451	-1.307	-5.479
c_i	0.112	0.028	0.011	2.545

(6) Section 4 of Shibushi breakwater (Wave Condition: Typhoon 2)

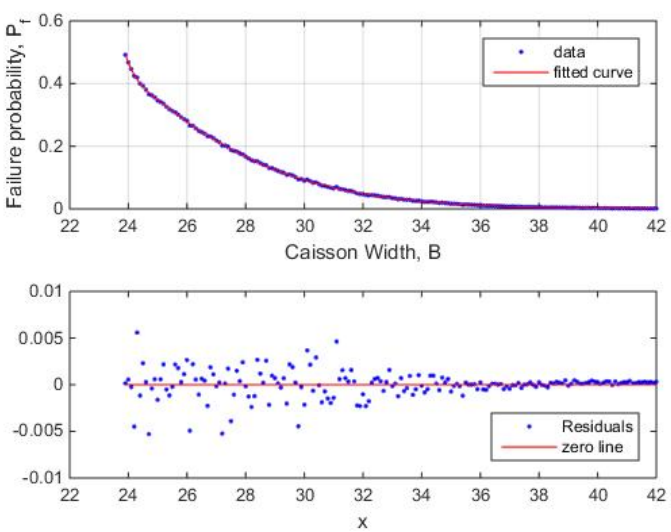

Figure B.6 Fitted curve and residual diagram at section 4 of Shibushi breakwater when Typhoon 2 condition is used

Curve can be expressed to summation of 4 Gaussian functions like below equation:

$$P_f(B) = \sum_{i=1}^{4} a_i e^{-\left(\frac{B-c_i}{b_i}\right)^2}$$

	$i=1$	$i=2$	$i=3$	$i=4$
a_i	3.813	0.097	-0.004	0.724
b_i	-2.217	-2.011	-1.25	-3.454
c_i	0.249	0.886	0.062	1.981

(7) Section 4 of Shibushi breakwater (Wave Condition: Typhoon 3)

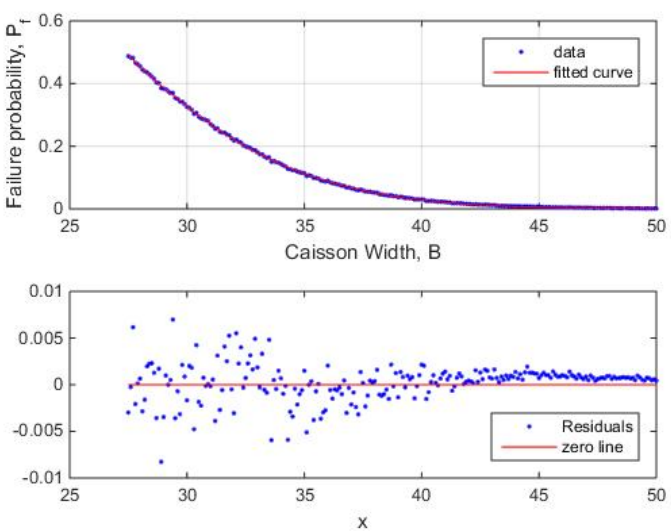

Figure B.7 Fitted curve and residual diagram at section 4 of Shibushi breakwater when Typhoon 3 condition is used

Curve can be expressed to summation of 4 Gaussian functions like below equation:

$$P_f(B) = \sum_{i=1}^{4} a_i e^{-\left(\frac{B-c_i}{b_i}\right)^2}$$

	$i=1$	$i=2$	$i=3$	$i=4$
a_i	0.003	0.003	0.007	1.181
b_i	-1.583	-1.385	-1.204	-3.527
c_i	0.001	0.072	0.014	1.926

(8) Section 5 of Shibushi breakwater (Wave Condition: Typhoon 1)

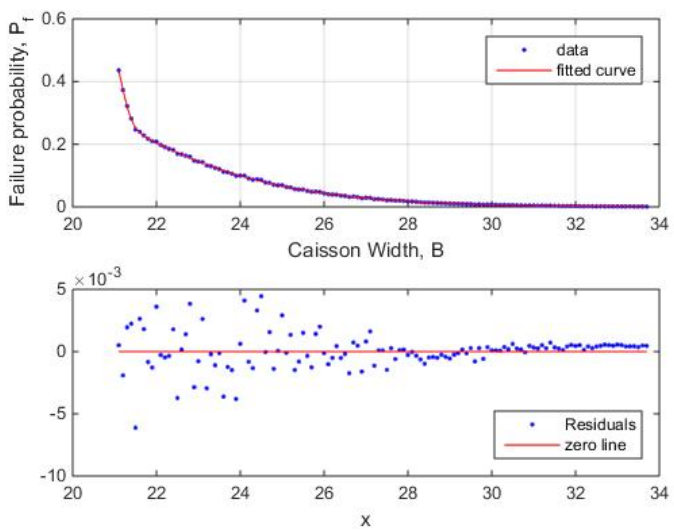

Figure B.8 Fitted curve and residual diagram at section 5 of Shibushi breakwater when Typhoon 1 condition is used

Curve can be expressed to summation of 4 Gaussian functions like below equation:

$$P_f(B) = \sum_{i=1}^{4} a_i e^{-\left(\frac{B-c_i}{b_i}\right)^2}$$

	$i=1$	$i=2$	$i=3$	$i=4$
a_i	0.233	0.280	0	0.129
b_i	-1.768	-2.602	-1.347	-2.383
c_i	0.010	1.147	2.29E-4	1.792

(9) Section 5 of Shibushi breakwater (Wave Condition: Typhoon 2)

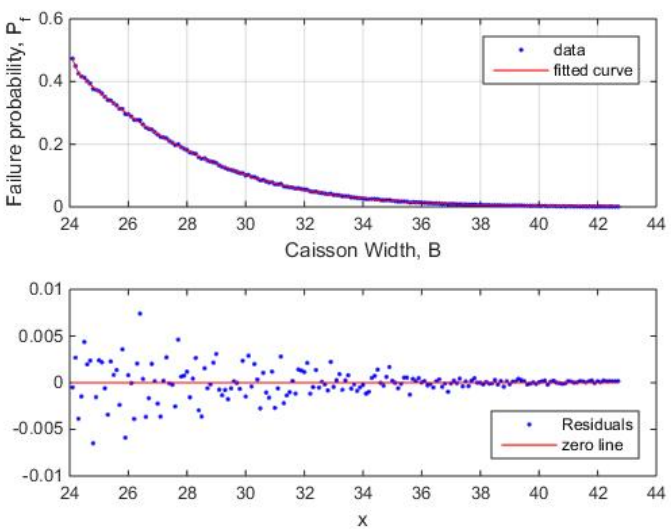

Figure B.9 Fitted curve and residual diagram at section 5 of Shibushi breakwater when Typhoon 2 condition is used

Curve can be expressed to summation of 4 Gaussian functions like below equation:

$$P_f(B) = \sum_{i=1}^{4} a_i e^{-\left(\frac{B-c_i}{b_i}\right)^2}$$

	$i=1$	$i=2$	$i=3$	$i=4$
a_i	12.45	-7.1E-4	-0.009	1.381
b_i	-2.007	-1.392	-0.744	-3.94
c_i	0.119	0.079	1.014	2.086

(10) Section 5 of Shibushi breakwater (Wave Condition: Typhoon 3)

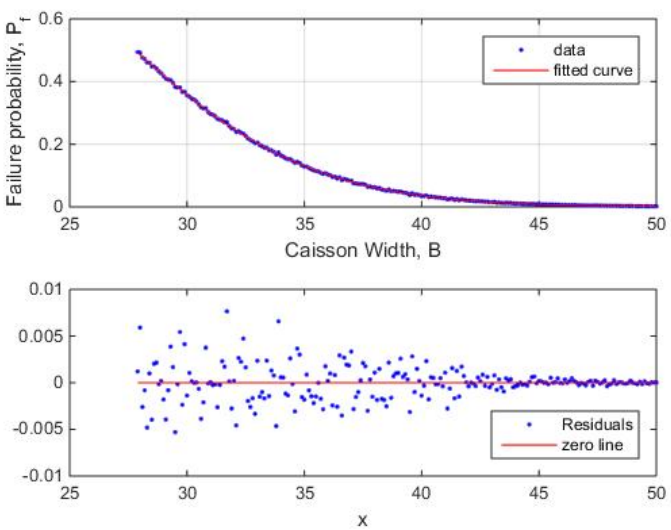

Figure B.10 Fitted curve and residual diagram at section 5 of Shibushi breakwater when Typhoon 3 condition is used

Curve can be expressed to summation of 4 Gaussian functions like below equation:

$$P_f(B) = \sum_{i=1}^{4} a_i e^{-\left(\frac{B-c_i}{b_i}\right)^2}$$

	$i=1$	$i=2$	$i=3$	$i=4$
a_i	0.107	0.005	-0.012	1.631
b_i	-2.094	-1.34	-1.245	-4.568
c_i	1.209	0.010	0.007	2.393

(11) Section 7 of Shibushi breakwater (Wave Condition: Typhoon 1)

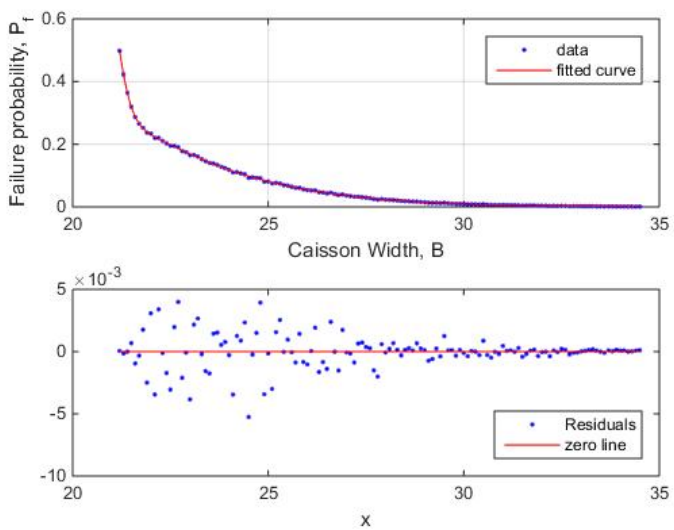

Figure B.11 Fitted curve and residual diagram at section 7 of Shibushi breakwater when Typhoon 1 condition is used

Curve can be expressed to summation of 4 Gaussian functions like below equation:

$$P_f(B) = \sum_{i=1}^{4} a_i e^{-\left(\frac{B-c_i}{b_i}\right)^2}$$

	$i=1$	$i=2$	$i=3$	$i=4$
a_i	0.516	-0.003	0.988	0.137
b_i	-1.844	-0.937	-5.065	-2.419
c_i	0.140	0.321	2.583	1.266

(12) Section 7 of Shibushi breakwater (Wave Condition: Typhoon 2)

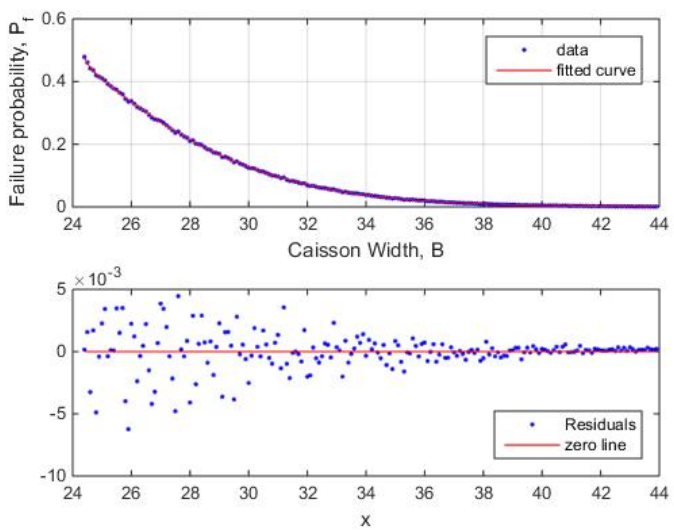

Figure B.12 Fitted curve and residual diagram at section 7 of Shibushi breakwater when Typhoon 2 condition is used

Curve can be expressed to summation of 4 Gaussian functions like below equation:

$$P_f(B) = \sum_{i=1}^{4} a_i e^{-\left(\frac{B-c_i}{b_i}\right)^2}$$

	$i=1$	$i=2$	$i=3$	$i=4$
a_i	1.08E+11	0.004	0	1.297
b_i	-3.249	-1.493	-11.16	-3.758
c_i	0.283	0.360	0.003	1.988

(13) Section 7 of Shibushi breakwater (Wave Condition: Typhoon 3)

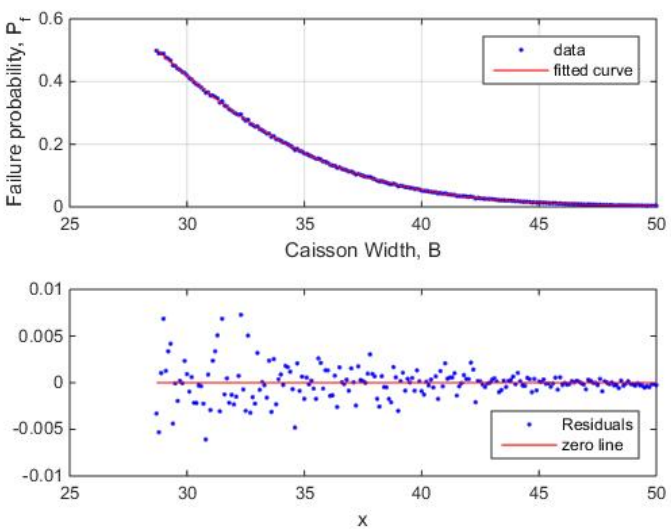

Figure B.13 Fitted curve and residual diagram at section 7 of Shibushi breakwater when Typhoon 3 condition is used

Curve can be expressed to summation of 4 Gaussian functions like below equation:

$$P_f(B) = \sum_{i=1}^{4} a_i e^{-\left(\frac{B-c_i}{b_i}\right)^2}$$

	$i=1$	$i=2$	$i=3$	$i=4$
a_i	1.204	0.003	0.008	-0.014
b_i	-3.75	-1.522	-1.14	-2.791
c_i	2.201	0.016	0.011	2.053

APPENDIX C – Optimal Width and Cost

(1) Goda's fictitious composite breakwater

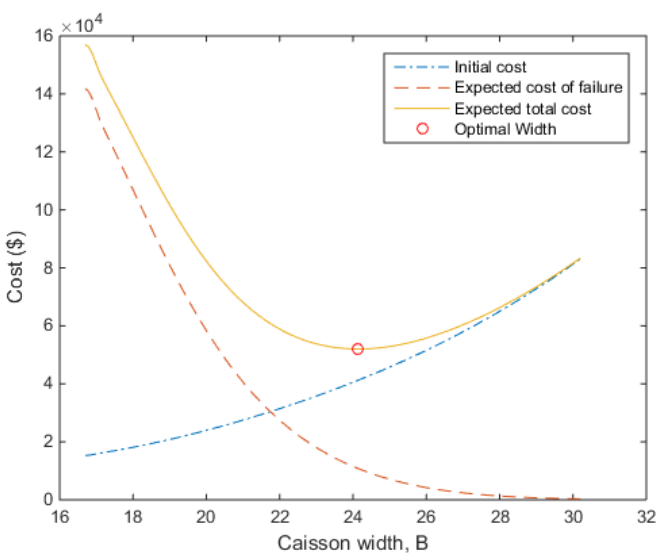

Figure C.1 Expected total lifetime cost for Goda's fictitious composite breakwater

Table C.1 Optimal width, minimal expected total lifetime cost and overall safety factor for **Goda's fictitious composite breakwater**

Trial	1	2	3	4	5
Optimal Width	24.2 m	24.1 m	24.1 m	24.1 m	24.1 m
Minimal Cost	5.23×10^4 \$	5.21×10^4 \$	5.26×10^4 \$	5.23×10^4 \$	5.22×10^4 \$
Overall Safety Factor	1.45	1.44	1.44	1.44	1.44

(2) Section 2 of Shibushi breakwater (Wave Condition: Typhoon 1)

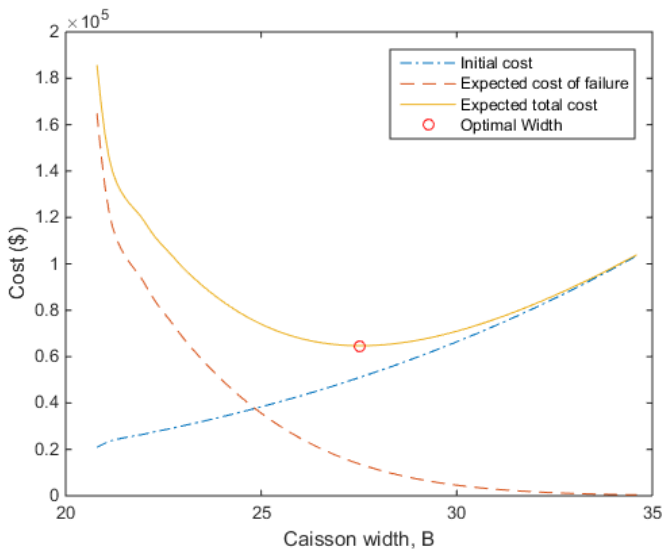

Figure C.2 Expected total lifetime cost at section 2 of Shibushi breakwater when Typhoon 1 condition is used

Table C.2 Optimal width, minimal expected total lifetime cost and overall safety factor at section 2 of Shibushi breakwater (Typhoon 1)

Trial	1	2	3	4	5
Optimal Width	27.4 m	27.5 m	27.4 m	27.5 m	27.4 m
Minimal Cost	6.44×10^4 \$	6.42×10^4 \$	6.38×10^4 \$	6.49×10^4 \$	6.36×10^4 \$
Overall Safety Factor	1.43	1.44	1.44	1.44	1.43

(3) Section 2 of Shibushi breakwater (Wave Condition: Typhoon 2)

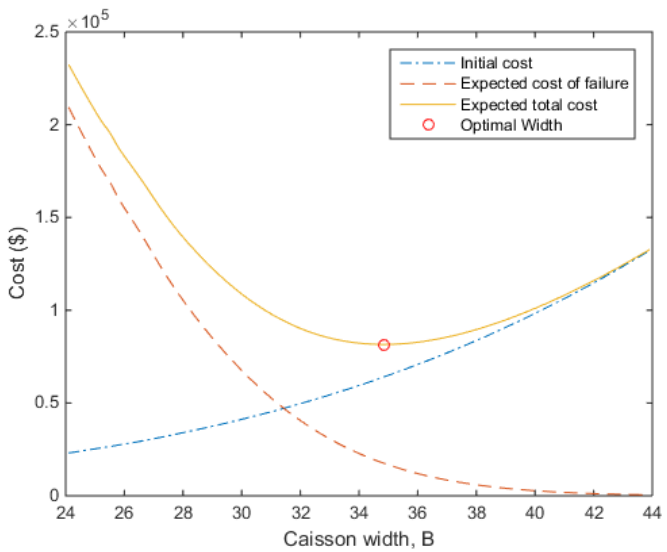

Figure C.3 Expected total lifetime cost at section 2 of Shibushi breakwater when Typhoon 2 condition is used

Table C.3 Optimal width, minimal expected total lifetime cost and overall safety factor at section 2 of Shibushi breakwater (Typhoon 2)

Trial	1	2	3	4	5
Optimal Width	34.8 m	34.8 m	34.8 m	34.9 m	34.7 m
Minimal Cost	8.14×10^4 \$	8.12×10^4 \$	8.20×10^4 \$	8.15×10^4 \$	8.22×10^4 \$
Overall Safety Factor	1.46	1.45	1.45	1.45	1.45

(4) Section 2 of Shibushi breakwater (Wave Condition: Typhoon 3)

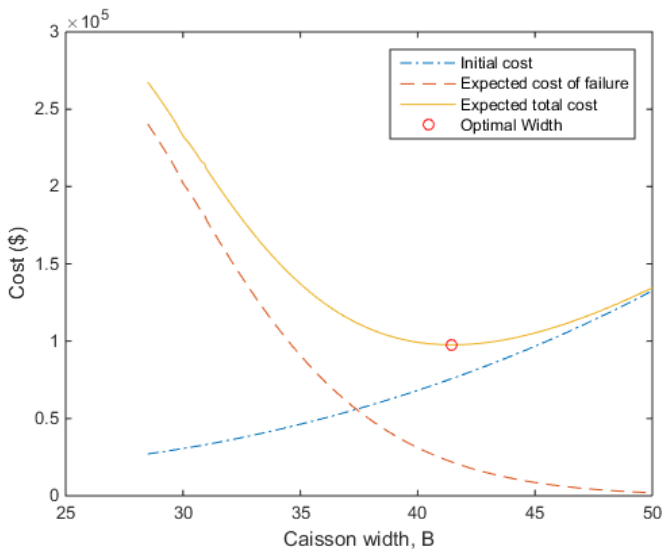

Figure C.4 Expected total lifetime cost at section 2 of Shibushi breakwater when Typhoon 3 condition is used

Table C.4 Optimal width, minimal expected total lifetime cost and overall safety factor at section 2 of Shibushi breakwater (Typhoon 3)

Trial	1	2	3	4	5
Optimal Width	41.6 m	41.5 m	41.4 m	41.5 m	41.3 m
Minimal Cost	9.87×10^4 \$	9.77×10^4 \$	9.82×10^4 \$	9.81×10^4 \$	9.75×10^4 \$
Overall Safety Factor	1.47	1.46	1.46	1.46	1.46

(5) Section 4 of Shibushi breakwater (Wave Condition: Typhoon 1)

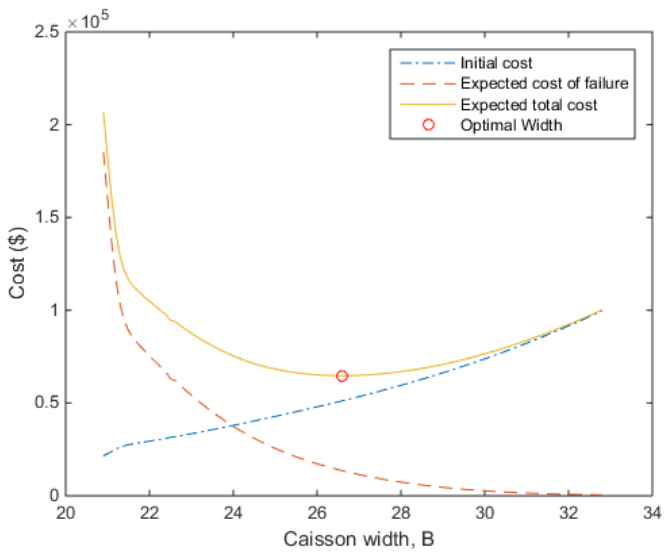

Figure C.5 Expected total lifetime cost at section 4 of Shibushi breakwater when Typhoon 1 condition is used

Table C.5 Optimal width, minimal expected total lifetime cost and overall safety factor at section 4 of Shibushi breakwater (Typhoon 1)

Trial	1	2	3	4	5
Optimal Width	26.7 m	26.7 m	26.7 m	26.5 m	26.6 m
Minimal Cost	6.43×10^4 \$	6.44×10^4 \$	6.48×10^4 \$	6.42×10^4 \$	6.57×10^4 \$
Overall Safety Factor	1.45	1.44	1.45	1.43	1.43

(6) Section 4 of Shibushi breakwater (Wave Condition: Typhoon 2)

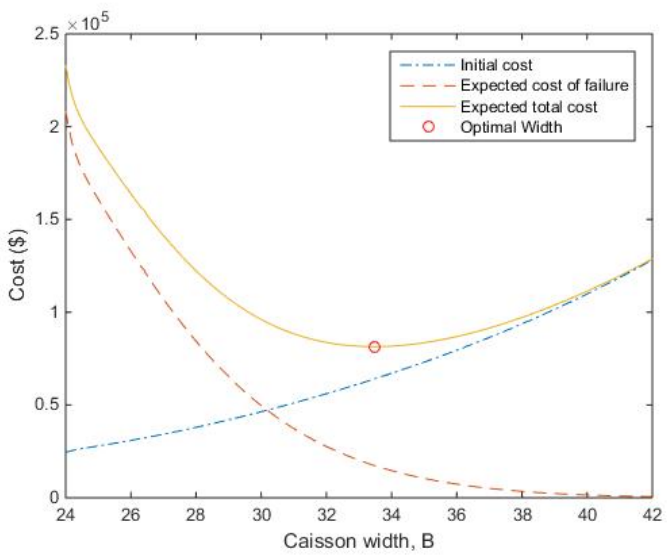

Figure C.6 Expected total lifetime cost at section 4 of Shibushi breakwater when Typhoon 2 condition is used

Table C.6 Optimal width, minimal expected total lifetime cost and overall safety factor at section 4 of Shibushi breakwater (Typhoon 2)

Trial	1	2	3	4	5
Optimal Width	33.5 m	33.3 m	33.3 m	33.3 m	33.4 m
Minimal Cost	8.19×10^4 \$	8.18×10^4 \$	8.09×10^4 \$	8.19×10^4 \$	8.17×10^4 \$
Overall Safety Factor	1.44	1.44	1.45	1.45	1.45

(7) Section 4 of Shibushi breakwater (Wave Condition: Typhoon 3)

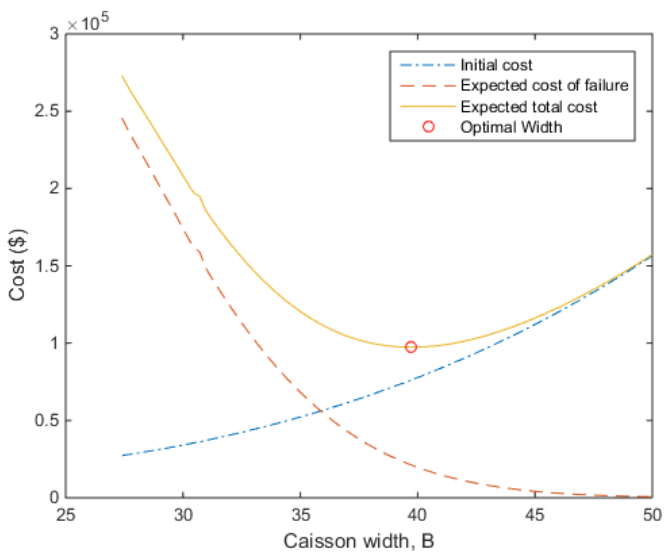

Figure C.7 Expected total lifetime cost at section 4 of Shibushi breakwater when Typhoon 3 condition is used

Table C.7 Optimal width, minimal expected total lifetime cost and overall safety factor at section 4 of Shibushi breakwater (Typhoon 3)

Trial	1	2	3	4	5
Optimal Width	39.8 m	39.9 m	39.9 m	39.6 m	39.7 m
Minimal Cost	9.75×10^4 \$	9.77×10^4 \$	9.75×10^4 \$	9.66×10^4 \$	9.73×10^4 \$
Overall Safety Factor	1.45	1.45	1.45	1.45	1.46

(8) Section 5 of Shibushi breakwater (Wave Condition: Typhoon 1)

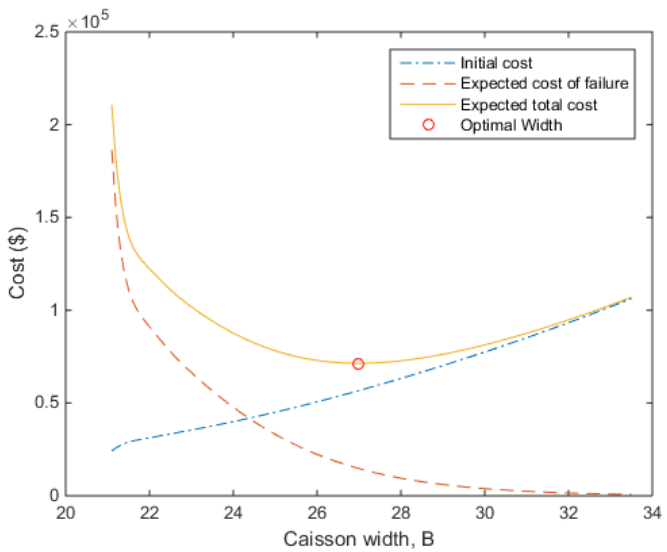

Figure C.8 Expected total lifetime cost at section 5 of Shibushi breakwater when Typhoon 1 condition is used

Table C.8 Optimal width, minimal expected total lifetime cost and overall safety factor at section 5 of Shibushi breakwater (Typhoon 1)

Trial	1	2	3	4	5
Optimal Width	27.0 m	27.0 m	26.9 m	26.9 m	27.0 m
Minimal Cost	7.15×10^4 \$	7.12×10^4 \$	7.13×10^4 \$	7.13×10^4 \$	7.15×10^4 \$
Overall Safety Factor	1.44	1.44	1.44	1.44	1.44

(9) Section 5 of Shibushi breakwater (Wave Condition: Typhoon 2)

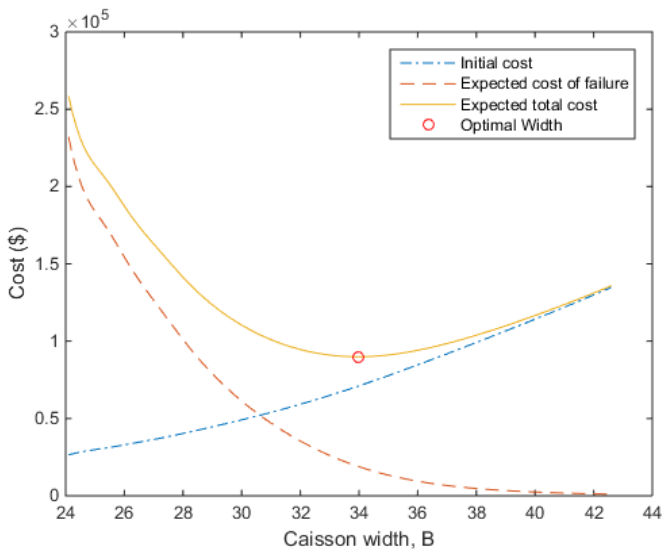

Figure C.9 Expected total lifetime cost at section 5 of Shibushi breakwater when Typhoon 2 condition is used

Table C.9 Optimal width, minimal expected total lifetime cost and overall safety factor at section 5 of Shibushi breakwater (Typhoon 2)

Trial	1	2	3	4	5
Optimal Width	33.8 m	34.0 m	33.9 m	33.9 m	34.0 m
Minimal Cost	8.88×10^4 \$	9.02×10^4 \$	8.91×10^4 \$	8.88×10^4 \$	8.96×10^4 \$
Overall Safety Factor	1.45	1.45	1.46	1.45	1.46

(10) Section 5 of Shibushi breakwater (Wave Condition: Typhoon 3)

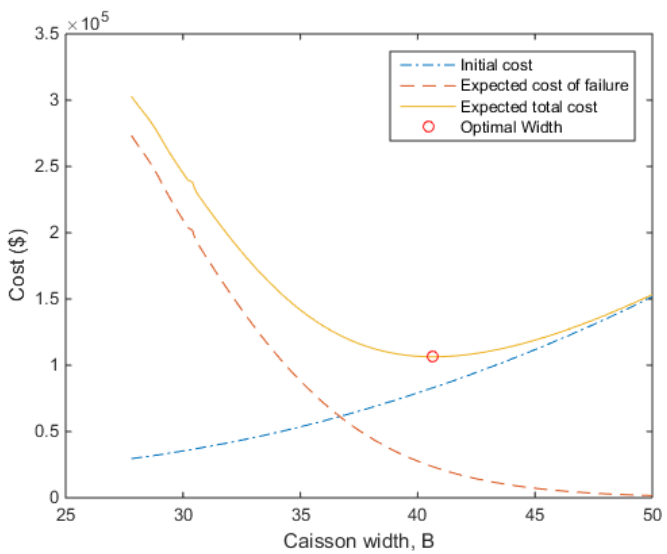

Figure C.10 Expected total lifetime cost at section 5 of Shibushi breakwater when Typhoon 3 condition is used

Table C.10 Optimal width, minimal expected total lifetime cost and overall safety factor at section 5 of Shibushi breakwater (Typhoon 3)

Trial	1	2	3	4	5
Optimal Width	40.6 m	40.6 m	40.6 m	40.7 m	40.5 m
Minimal Cost	10.67×10^4 \$	10.65×10^4 \$	10.75×10^4 \$	10.72×10^4 \$	10.75×10^4 \$
Overall Safety Factor	1.46	1.46	1.46	1.46	1.46

(11) Section 7 of Shibushi breakwater (Wave Condition: Typhoon 1)

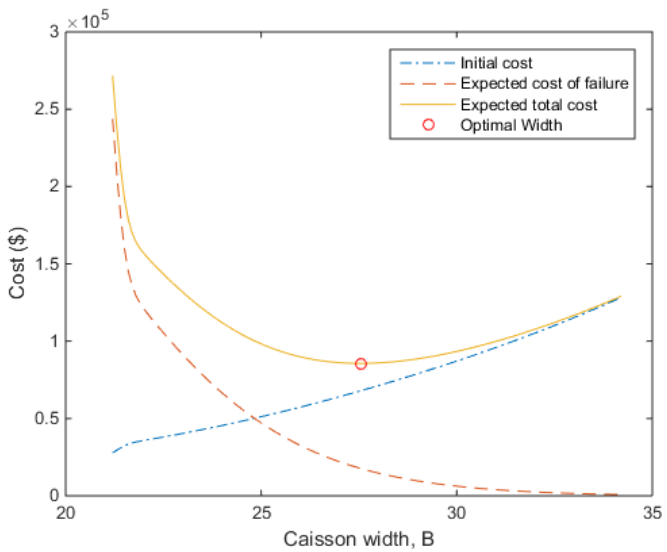

Figure C.11 Expected total lifetime cost at section 7 of Shibushi breakwater when Typhoon 1 condition is used

Table C.11 Optimal width, minimal expected total lifetime cost and overall safety factor at section 7 of Shibushi breakwater (Typhoon 1)

Trial	1	2	3	4	5
Optimal Width	27.6 m	27.6 m	27.6 m	27.7 m	27.8 m
Minimal Cost	8.60×10^4 $	8.62×10^4 $	8.52×10^4 $	8.53×10^4 $	8.63×10^4 $
Overall Safety Factor	1.45	1.44	1.45	1.45	1.45

(12) Section 7 of Shibushi breakwater (Wave Condition: Typhoon 2)

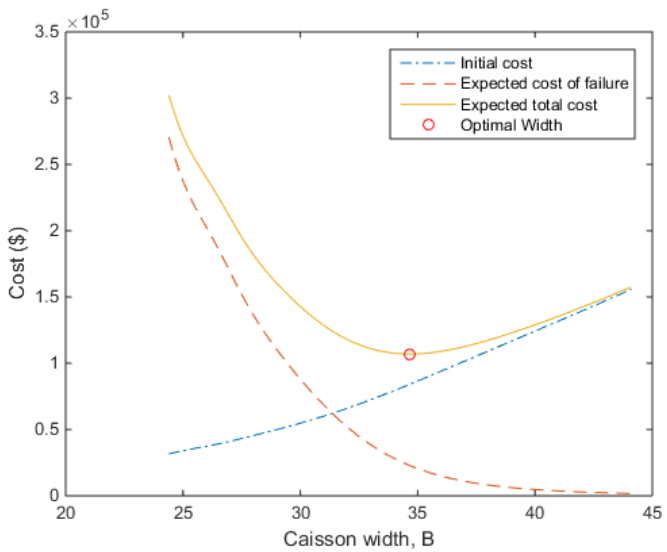

Figure C.12 Expected total lifetime cost at section 7 of Shibushi breakwater when Typhoon 2 condition is used

Table C.12 Optimal width, minimal expected total lifetime cost and overall safety factor at section 7 of Shibushi breakwater (Typhoon 2)

Trial	1	2	3	4	5
Optimal Width	34.8 m	34.7 m	34.8 m	34.8 m	34.8 m
Minimal Cost	10.70×10^4 \$	10.77×10^4 \$	10.77×10^4 \$	10.75×10^4 \$	10.74×10^4 \$
Overall Safety Factor	1.46	1.46	1.46	1.46	1.46

(13) Section 7 of Shibushi breakwater (Wave Condition: Typhoon 3)

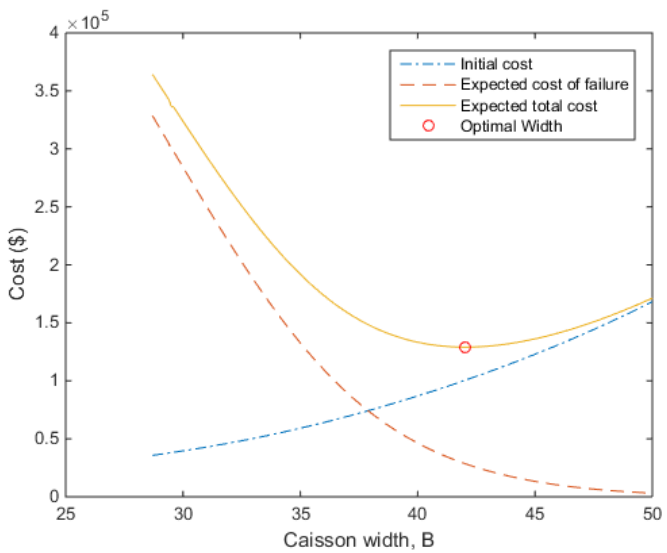

Figure C.13 Expected total lifetime cost at section 7 of Shibushi breakwater when Typhoon 3 condition is used

Table C.13 Optimal width, minimal expected total lifetime cost and overall safety factor at section 7 of Shibushi breakwater (Typhoon 3)

Trial	1	2	3	4	5
Optimal Width	42.1 m	41.9 m	42.0 m	42.0 m	42.1 m
Minimal Cost	12.88×10^4 \$	12.85×10^4 \$	12.94×10^4 \$	12.83×10^4 \$	12.96×10^4 \$
Overall Safety Factor	1.46	1.46	1.47	1.47	1.47

국문초록

신뢰도 기반 설계 최적화를 활용한 방파제 케이슨의 최적 폭 산정

서울대학교 대학원

건설환경공학부

김 택 상

직립 케이슨의 파괴모드는 활동에 의한 파괴, 전도에 의한 파괴, 지반 침하에 의한 파괴 등과 같이 다양하다. 기존에 연구에서는 가장 발생할

확률이 높은 활동에 의한 파괴만을 고려하거나 각각의 파괴를 따로 고려하는 연구가 주로 행해졌다. 본 연구에서는 다양한 파괴 모드를 동시에 고려하기 위해 시스템 신뢰도 방법 중 FORM approximation을 활용하여 직립 케이슨의 파괴 확률을 계산한 후 Harmony Search 최적화 방법을 활용하여 방파제 케이슨의 최적 폭을 산정한다.

설계에 활용하게 되는 방파제의 형상은 총 5가지이며(고다의 가상 방파제: 1, 일본의 Shibushi 방파제: 4) 파랑 조건은 총 4가지(고다의 가상 방파제: 1, 일본의 Shibushi 방파제: 3)이다. 위의 조건과 고다의 파압산정식을 활용하여 총 6개의 랜덤 변수(마찰계수, 수평파압, 부력, 케이슨 중량, 케이슨 순수 모멘트, 케이슨 순중량)가 생성되었으며 랜덤 변수 중 일부는 설계 변수인 케이슨의 폭이 변하게 되면 같이 변하게 된다.

본 연구에서 활용되는 파괴 모드는 활동(Sliding)에 의한 파괴와, 기울어짐(Tilting)에 의한 파괴로써 이 2가지의 파괴모드는 랜덤 변수로 표현된 후, 정규화 된다. FORM approximation에 의해 계산되는 파괴확률은 설계변수인 케이슨의 폭에 따라서 각각 구해지며 이 둘 사이의 관계를 함수식으로 표현하기 위해 비선형 최소제곱법이 활용된다. 그 결과 가우스 함수 4개의 합으로 함수식을 표현할 수 있다.

Lee (2002) 가 제시한 기대 총 건설비 함수는 FORM approximation으로부터 얻어진 파괴확률 함수식을 대입하여 설계 변수인 케이슨의 폭에 관련된 함수로 표현이 가능하다. 케이슨의 최적 폭은 하모니 서치 방법을 통해서 계산된다. 모든 설계 경우에 대해 하모니 서치 방법을 적용하였

고 총 5번의 반복 수행을 통해 결과의 신뢰도를 높인다.

본 연구를 통해서 계산되는 방파제의 최적 폭은 각각의 파괴 모드를 고려한 기존 연구에 비해 현실적이라고 할 수 있으며, 이 방법은 추후 방파제 케이슨 뿐만 아니라 다른 분야에도 적용 가능할 것이다.

keywords: 직립 케이슨, 시스템 신뢰도, FORM Approximation, 가우스 함수, 기대 총 건설비 최소화기법, 하모니 서치

학번: 2015-21285